MINISTRY OF NATURAL RESOURCES AND ENVIRONMENT
VIET NAM INSTITUTE OF METEOROLOGY, HYDROLOGY AND CLIMATE CHANGE

NGUYEN THI TUYET

A STUDY ON CLIMATE CHANGE PROJECTION AND CLIMATE ANALOG IN SOUTHEAST ASIA

PHD THESIS ON CLIMATE CHANGE

Ha Noi - 2020

MINISTRY OF NATURAL RESOURCES AND ENVIRONMENT
VIET NAM INSTITUTE OF METEOROLOGY, HYDROLOGY AND CLIMATE CHANGE

NGUYEN THI TUYET

A STUDY ON CLIMATE CHANGE PROJECTION AND CLIMATE ANALOG IN SOUTHEAST ASIA

Major: Climate Change

Code : 9440221

PHD THESIS ON CLIMATE CHANGE

Thesis Author	Primary Supervisor	Second Supervisor
Nguyen Thi Tuyet	*Assoc. Prof. Dr. Ngo Duc Thanh*	*Prof. Dr. Phan Van Tan*

Ha Noi - 2020

COMMITMENT

I commit that the thesis is my own research. The results shown in the thesis are honest, objective and have not been defended at any degree level.

I commit that all help with completing the thesis is acknowledged, and references in the thesis are fully sourced.

Ha Noi, …… 2020

AUTHOR

Nguyen Thi Tuyet

ACKNOWLEDGEMENT

I would like to send my sincere gratitude to my two supervisors: Assoc. Prof. Dr. Ngo Duc Thanh and Prof. Dr. Phan Van Tan. Without their great guidance and teaching, I could not complete my thesis.

I would also want to send my gratitude to the training institution – Viet Nam Institute of Meteorology, Hydrology and Climate Change (IMHEN) and my workplace – Viet Nam Institute for Development Strategies (VIDS) who have been always to best facilitate my PhD study.

I would be much grateful for the Department of Space and Applications, USTH, which provides the HILO cluster where I could implement the calculations, analysis and visualization of my PhD thesis' results, and for the Research group for Remote sEnsing and MOdeling of Surface and ATmosphere (REMOSAT) lab under the leadership of Assoc. Prof. Ngo Duc Thanh, USTH for facilitating my PhD study.

I would express gratitude to the Southeast Asia Regional Climate Downscaling/ Coordinated Regional Climate Downscaling Experiment – Southeast Asia (SEACLID/CORDEX-SEA) project, of which observed and model data were used in my thesis.

Last but not least, I would like to send my deep thanks to my family and friends who have kept encouraging me as well as facilitating my study.

Ha Noi, …… 2020

AUTHOR

Nguyen Thi Tuyet

CONTENT

LIST OF ABBREVIATIONS

ADB	Asian Development Bank
AOGCMs	Atmosphere – Ocean General Circulation Models
APHRODITE	Asian Precipitation-Highly Resolved Observational Data Integration Towards Evaluation of Water Resources
AR5	The Fifth Assessment Report
BATS	Biosphere-Atmosphere Transfer Scheme
BAU	Business As Usual
CCAFS/ CGIAR	Climate Change, Agriculture and Food Security under the Consultative Group on International Agriculture Research
CCAM	Conformal-Cubic Atmospheric Model
CCRS-MSS	Centre for Climate Research Singapore of the Meteorological Service Singapore
CDO	Climate Data Operators
CFS	Climate Forecast System
CH	Central Highland
CLM	Community Land Model
CMIP5	Coupled Model Intercomparison Project Phase 5
CNRM-CM5	Centre National de Recherches Météorologiques Coupled Global Climate Model, version 5
COP	Conference of the Parties
CORDEX	Coordinated Regional climate Downscaling Experiment
CRU	Climatic Research Unit of the University of East Anglia
CSIRO	Commonwealth Scientific and Industrial Research

	Organization
CSIRO-MK36	CSIRO Mark 36
CTL	Control simulation
DECK	Diagnostic, Evaluation and Characterization of Klima
ECMWF	European Centre for Medium-Range Weather Forecasts
EC-EARTH	European Community Earth system model
ENSO	El Niño Southern Oscillation
ERA40	ECMWF 40-year Re-Analysis
ERA-Interim	ECMWF Interim Reanalysis
ESMs	Earth System Models
ESP	Earth System Physics
GCM	Global Climate/Circulation Model
GDP	Gross domestic products
GFDL-ESM2M	Geophysical Fluid Dynamics Laboratory Earth System Model with MOM, version 4 component
GHG	Green House Gas
GMT	Generic Mapping Tools
HadGEM2	Hadley Centre Global Environment Model, version 2
IAM	Integrated Assessment Model
IC	Initial conditions
ICBC	Initial and boundary conditions
ICTP	International Center for Theoretical Physics
IMHEN	Viet Nam Institute of Meteorology, Hydrology and Climate Change
INDC	Intended National Determined Contribution
IOD	Indian Ocean Dipole

IPCC	International Panel on Climate Change
IPSL-CM 5A-LR	L'Institut Pierre-Simon Laplace Coupled Model, version 5A, low resolution
LBC	Lateral boundary conditions
MIT	Massachusetts Institute of Technology
MOHC	Met Office Hadley Centre
MONRE	Ministry of Natural Resources and Environment
MPI-ESM-MR	Max Planck Institute - Earth System Model – Medium Resolution
MRI	Meteorological Research Institute
MRI/JMA	Meteorological Research Institute of Japan Meterological Agency
MRI-AGCM3.2H	Meteorological Research Institute Atmospheric General Circulation Model, version 3.2 (high resolution)
NOAA	National Oceanic and Atmospheric Administration
NC	North Central
NCO	NetCDF Operators
NE	North East
NW	North West
NCAR	National Center for Atmospheric Research
NCEP	National Centers for Environmental Prediction
NHRCM	Non-hydrostatic regional climate model
NW	North West
PBL	Planetary Boundary Layer
PPE	Perturbed Physics Ensemble
PRECIS	Providing Regional Climates for Impacts Studies

PRUDENCE	Prediction of Regional scenarios and Uncertainties for Defining European Climate change risks and Effects
RCM	Regional Climate Model
RCPs	Representative Concentration Pathways
RegCM	Regional Climate Model (established by the Earth System Physics section of the Abdus Salam International Centre for Theoretical Physics)
RMSD	Root mean square difference
RIHN	Research Institute for Humanity and Nature
RRD	Red River Delta
RSTD	Ratio of standard deviation
SA	South America
SC	South Central
SEA	Southeast Asia
SEACAM	SEA Climate Analysis and Modeling Framework
SEACLID	Southeast Asia Regional Climate Downscaling
SED	Standardized Euclidean Distance
SPI	Standardized Precipitation Index
SRES	Special Report on Emissions Scenarios
SST	Sea Surface Temperature
SV	Southern Viet Nam
T2m	2m mean air temperture
TC	Tropical cyclone
Tn	Minimum air temperture
Tx	Maximum air temperture
TRMM	Tropical Rainfall Measuring Mission

UM	Unified Model
UNDP	United Nations Development Program
UNFCCC	United Nations Framework Convention on Climate Change
UK	The United Kingdom
VnGP	Viet Nam Gridded Precipitation Dataset
WCRP	World Climate Research Programme
WGCM	Working Group on Coupled Modeling
WGI	Working Group I
WGII	Working Group II
WRF	Weather Research & Forecasting

LIST OF TABLES

LIST OF FIGURES

LIST OF ANNEX

INTRODUCTION

Necessity of the chosen thesis topic "A study on climate change projection and climate analog in Southeast Asia"

In the past years, the term 'climate change' has been intensively used in daily life and in research documents. It has been existent and affecting many aspects of human life. As climate change is a global issue, this phenomenon has attracted great concerns from most countries in the world. Therefore, the Conference of the Parties (COP) of the United Nations Framework Convention on Climate Change (UNFCCC) has been periodically organized since 1995 till the present time. The latest COP 25 has just been held in Madrid, Spain in 2019 with certain results. At the Katowice summit in COP 24, the Global Climate Risk Index 2019 was released and indicated that intense cyclones, excessive rainfall and severe floods have caused some countries in South and Southeast Asia (SEA) to be at most risk by climate change (Figure 0.1).

The SEA region is considered to be one of the most vulnerable areas to climate change impacts as most countries in the region has long coastlines, major economic activities concentrated in coastal areas and their citizens' livelihood heavily depend on agriculture, forestry and fisheries and other natural resources [15]. The SEA area has crowded population of over 662 million in mid-2019 [164] with diverse culture and not high living standard (except for Singapore and Brunei). Moreover, SEA is located in an area influenced by the monsoon systems, which are 'large-scale seasonal reversals of the wind regime' [147]. In the recent years, some countries in SEA has suffered natural disasters such as droughts, storms, floods, heavy rains, heat wave, etc. Increasing intensities of rainfall during the monsoons do not only

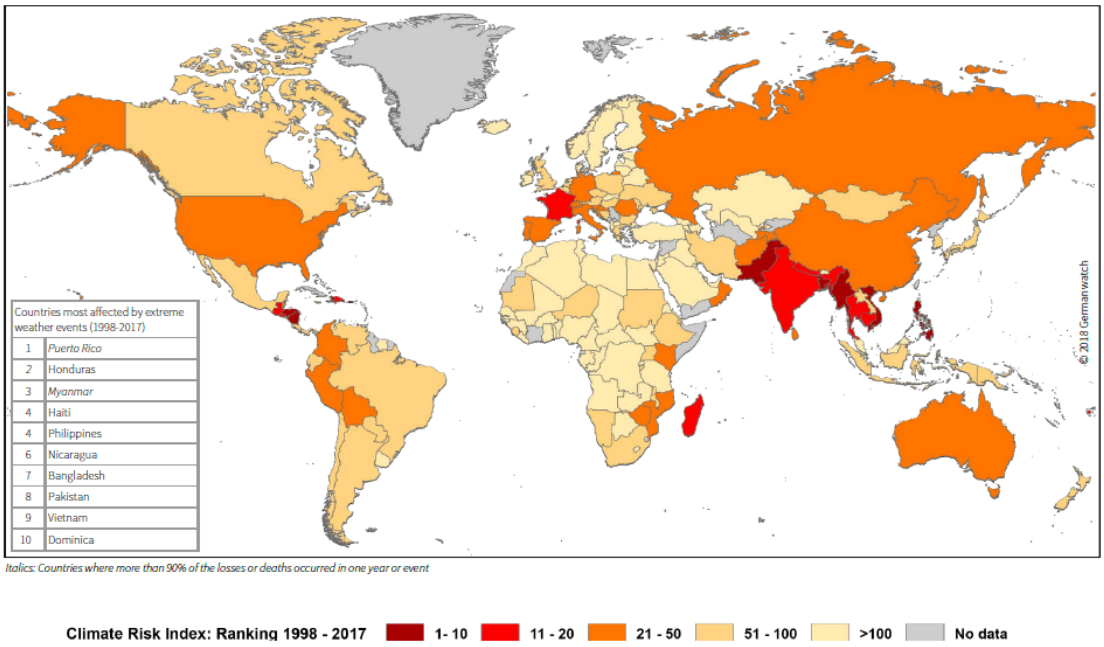

Source: Climate Risk Index 2019, Germanwatch

Figure 0.1. The World Map of Climate Risk Index 2019.

cause major floods but also cause landslide events in Malaysia and some Southeast Asian countries [21]. Indonesia and Thailand experienced a giant tsunami in 2004. Philippines and Viet Nam suffered the super typhoon Haiyan in 2013. In early 2016, Viet Nam experienced a devastating drought. Thailand was one of ten countries, which were badly affected by floods with the monsoon flooding in September - October 1980 and in March - April 2011 that inundated almost southern Thailand [121]. Recently, during June and July 2019, several forest fires have occurred in Central Viet Nam.

In the Fifth Assessment Report (AR5) of the Intergovernmental Panel on Climate Change (IPCC), the Working Group I (WGI) described that the SEA region had already experienced durable changes in its regional climate [29]. Moreover, the IPCC Working Group II (WGII) also underlined that the SEA region obviously had been impacted by regional climate change [71]. However, through a limited number of recent studies, these reports also demonstrated a substantial lack of regional climate change research and its

impact in the SEA region.

In addition, climate analog is used to define locations at which their present climate is similar to the projected future climate of a reference site [57], [100], [107]. It is an interesting tool to study climate in spatio-temporal relationship. The approach is relatively comprehensive compared to the one based on only temperature or precipitation or both, as it helps to realize spatio-temporal climatic vision. It helps to have an 'on the ground' and real-life version of the projected climate in the future, instead of abstract hypothesis projection [57], [102], [171]. Via this approach, the projected future climate, at most of target locations on earth, can be observed at the present, but in another location [18]. In analog analysis, the projected future climate of a site is used to choose a location where the above projected conditions can be found today [100], [141]. In some cases, climate analogs are applied only for explanatory reasons, i.e., the analogous sites are used to illustrate the severity of projected climate change [68], [90]. Climate analogs may also be used as examining grounds for suggested practices [100], [101]. Though climate analogs have been used relatively widely in studies in the world, there is, to date, no study on this analog approach conducted in SEA.

Therefore, the above-mentioned contexts lead to the author's choice of the thesis topic "A study on climate change projection and climate analog in Southeast Asia". Data used in the thesis were the results of the Coordinated Regional climate Downscaling Experiment (CORDEX) of the World Climate Research Programme (WCRP) [62]. It is currently known as the Southeast Asia Regional Climate Downscaling (SEACLID)/ CORDEX-SEA [83], [124].

General objective and specific aims

The general objective of the thesis is to grasp future climate change in

SEA through climate projection and climate analog.

The specific research aims of the thesis include:

1) To project temperature and rainfall and their changes over the SEA region;
2) To define the best climate analog locations of some cities in SEA and Viet Nam and their common moving tendency;
3) To identify locations and land fractions of novel climate and disappearing climate in SEA and Viet Nam.

Research subjects and research scopes

The research subjects and scopes of the thesis are projected climate, climate analog, novel climate and disappearing climate within the research region of SEA and Viet Nam.

The essential climate variables includes atmospheric, oceanic and terrestial variables. In terms of surface-atmosphere variables, they are air temperature, wind speed and direction, water vapor, pressure, precipitation and surface radiation budget [61]. Among the surface-atmosphere variables, the thesis focuses on two variables: 2m temperature and precipitation.

Defending points

The thesis points to be defended consist of:

1. Among 6 global circulation models (GCMs) and 6 regional climate models (RCMs), ensemble mean (ENS) has some advantages in simulating climate over SEA compared to individual experiments;
2. A modified version of an existing formulation to estimate climate distance was appropriate in SEA;
3. Land fraction of novel climate in SEA and disappearing climate in Viet Nam will be defined by climate analog approach at the end of the 21st century.

New contributions

The thesis' new contributions or key findings include:

1. Evaluation on climate simulation in SEA and Viet Nam by 6 CMIP5 GCMs and 6 RCMs, and generally showing ENS's superior role.
2. Identification of a modified version of an existing formulation to estimate climate distance with weighted parameters for temperature and rainfall, and for ENS and analog climate thresholds
3. Distribution of good-analog, poor-analog, and novel climate over SEA and disappearing climate in Viet Nam under the Representative Concentration Pathway 4.5 (RCP4.5) and RCP8.5.

Scientific and practical significance of the PhD thesis

The thesis would provide scientific knowledge on projected temperature and rainfall changes, the appearance of novel climate as well as the disappearance of present climate in the future in the SEA and Viet Nam region.

These results would contribute practical inputs to climate change impact assessment and adaptation studies for scientists and to adaptation planning for policy makers.

Thesis structure

The thesis structure includes:

Introduction

Chapter 1: Literature review on regional climate downscaling and climate analog

Chapter 2: Observed data, numerical experiments and methodology

Chapter 3: Performance of multi-model experiments in Southeast Asia

Chapter 4: Climate change projection and Climate analog in Southeast Asia

Conclusions and Recommendations.

CHAPTER 1 – LITERATURE REVIEW ON REGIONAL CLIMATE DOWNSCALING AND CLIMATE ANALOG

1.1. Related concepts

Greenhouse gas concentration scenarios

Greenhouse gases (GHG) emissions or concentration scenarios were used for driving GCMs to develop climate change scenarios. The first global GHG scenarios were published by the IPCC in 1992. They were named IS92 scenarios [77]. The IS92 scenarios were used as input to climate model runs, impact assessment and mitigation solutions [95]. However, many changes on our knowledge of future GHG emissions and climate change have happened since this time. Thus, a new collection of emissions scenarios was developed by the IPCC in 1996, which was used as input to the IPCC AR3. They were also the input to assessments on climatic and environmental consequences of future GHG emissions and on mitigation and adaptation strategies. These new scenarios were kept updating on economic restructuring and technological changes and expanded the range of economic development pathways. Achieving this was due to the so-called 'open-process', where the broad community of experts' input and feedback were sought for [120]. Therefore, the new scenarios helped to provide useful knowledge on the inter-connections between environmental quality and development choices and were an effective tool for policy-makers and scientists. Thus, the 1996 Panel of the IPCC requested the Special Report on Emission Scenarios (SRES) [120]. SRES contains a large span of the key driving forces of future emissions ranging from demographic to technological and economic developments. All these scenarios exclude future policies explicitly addressing climate change but include many policies of other types. SRES is

based on analysis of considerable literature, six modeling methods and ‘open process’ which solicited large attendance and feedback from the community of scientists. It covers a span of emissions of all related types of GHGs and sulfur and their driving forces.

Future GHG emissions and concentrations are the result of highly complicated dynamic systems and defined by driving forces such as demographic and socio-economic development and technological changes [77]. Scenarios are the different pictures of how the future might happen and are a suitable tool to assess how the driving forces affect future emissions results and evaluate the related uncertainties. They are frequently used in climate change analysis including climate modeling, impact assessment, adaptation and mitigation measures. The probability that any individual emissions path will happen as indicated in scenarios is highly uncertain.

There are three types of uncertainty in scenarios analysis. They are uncertainty in quantities, uncertainty in model structure and uncertainty originated from views of experts [117]. Sources of uncertainties could come from statistical differences, intuitive evaluation (systematic error), incomplete denotation (linguistic inaccuracy), natural variability, differences in experts’ opinions and approximation [117]. According to Funtowicz and Ravetz [60], drivers of uncertainties are "data uncertainties", "modeling uncertainties" and "completeness uncertainties". Data uncertainties stem from the suitability of data used as inputs into models. Modeling uncertainties result from insufficient perception of modeled events or from approximations applied in representation of the processes. Completeness uncertainties relate to all absences ascribed to the shortage of comprehension. These reasons are, in general, non-quantifiable and irreducible.

Scenarios enables the evaluation of future developments in complicated

systems which are either intrinsically unpredictable or contain high scientific uncertainties [120]. Future emissions and the development process of driving forces are encompassed by uncertainties, which is indicated through a large number of future emissions pathways. These uncertainties become worse when developing from emission pathways to climate change, from climate change to possible impacts, and eventually from driving forces to adaptation and mitigation measures and policies. Therefore, the application of alternative scenarios is requisite to describe possible future emissions.

The SRES scenarios identify sources of uncertainties including: 1) selection of storylines (free choice of qualitative scenario parameter combination, such as low population incorporated with high gross domestic products (GDP)); 2) authors' understanding of storylines (different modelers' transformation from narrative scenario storyline text into quantitative scenario drivers); 3) Turning from the comprehension of linkages among driving forces to quantitative inputs to scenario analysis (this turning is often imperfect or qualitative only); 4) Methodology dissimilarity (differences in concept and structure (model approaches) and parameterization of model; assumption on the linkage between scenario drivers and output); 5) Different data; and 6) Inherent uncertainties (rare events occur and bring out results which are basically distinct from those provided by SRES model runs) [120].

Scenarios can be considered to be the connecting tool between qualitative future stories and quantitative formulations based on modeling. Thus, they help us understand how the systems work, behave and progress. Scenarios relate to both quantitative and qualitative parts. They hold a narrative section named storylines and several equivalent quantitative scenarios for every storyline [120]. Figure 1.1 depicts the inter-connected characteristics of these alternative scenario formulations.

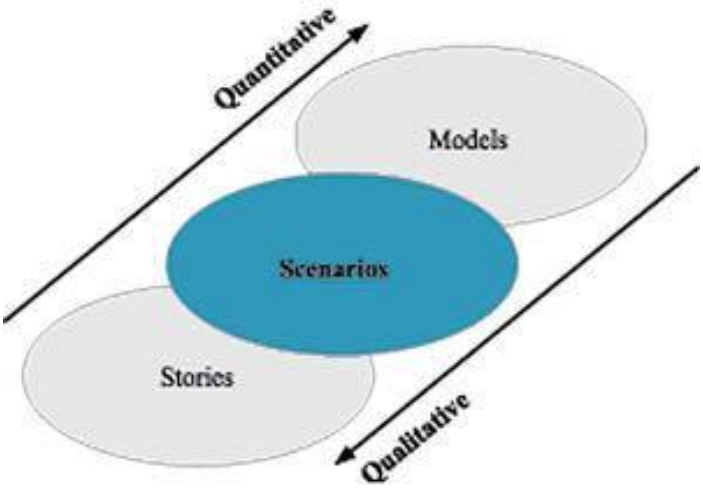

Source: [77]

Figure 1.1. Schematic illustration of alternative scenario formulations, from narrative storylines to quantitative formal models.

In 2000, the IPCC introduced the SRES scenarios with future assumptions of global population growth, technological development, globalization and societal values. The SRES were used in the AR3 (2001) and the AR4 (2007) of the IPCC. After that, the research community at that time needed new scenarios as indicated by Moss et al. [118]. This need induced the IPCC to plead the scientific community for developing a new set of scenarios to promote future assessment on climate change [78]. As a result, the community developed a three phase procedure [118] [168]: 1) Evolution of a scenario set including emission, concentration and land-use routes – referred to as "representative concentration pathways" (RCPs); 2) An evolution phase paralleling with climate model runs and evolution of new socio-economic scenarios. In 2009, the starting of the 'parallel phase' of new scenario process for the IPCC AR5 was initiated by RCPs [118]; and 3) A final phase of incorporation and circulation.

In the AR5 (2013), the SRES were replaced by the RCPs, which is the change in the net, downward minus upward, radiative flux (expressed in Wat-

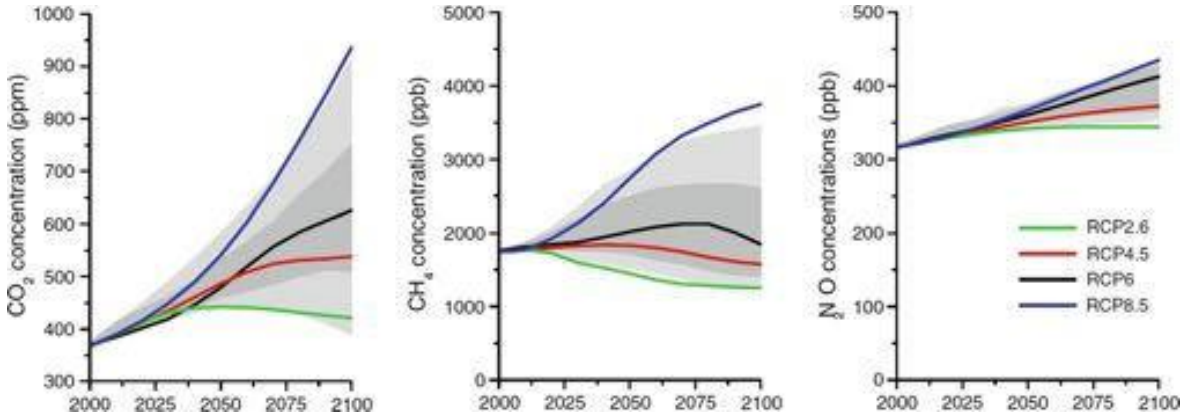

Source: [167]

Figure 1.2. Concentrations of the greenhouse gases carbon dioxide (CO_2), methane (CH_4) and nitrous oxide (N_2O) across the RCPs. The grey area indicates the 98th and 90th percentiles (light/dark grey) of an earlier emission study (EMF-22).

-ts per square metre; Wm^{-2}) at the tropopause or top of the atmosphere due to a change in a driver of climate change, such as a change in the concentration of carbon dioxide (CO_2) or the incoming solar radiation [80]. They cumulatively measure human emissions of GHGs from all sources shown in Wm^{-2}. The RCPs are identifined by their approximate total radiative forcing in the year 2100 relative to 1850. Literature reviews showed that previous scenarios can show a radiative forcing in 2100 from as low as 2.5 Wm^{-2} to between 8 and 9 Wm^{-2} and higher [54] [169]. Thus, the RCPs include the radiative forcing 2.6 Wm^{-2} for RCP2.6, 4.5 Wm^{-2} for RCP4.5, 6.0 Wm^{-2} for RCP6.0, and 8.5 Wm^{-2} for RCP8.5. Figure 1.2 shows the change of concentrations of CO_2, CH_4 and N_2O with the timeline to 2100 and under the various RCPs.

The RCPs have two essential features reflected in their names. The word “representative” means that each of the RCPs is equal to a bigger set of scenarios in the literature. In the context, the RCPs should get on well with

the full range of available emissions scenarios. The word "concentration pathway" signifies that the RCPs are not the final completely integrated scenarios, i.e. they are not a comprehensive combination of socio-economic emissions and climate projections, but are internally uniform series of projections of the components of radiative forcing used in following phases [168].

Global climate models

The CMIP was set up to study and intercompare climate simulations by coupled ocean-atmosphere-cryosphere-land GCMs [111]. Figure 1.3 indicates the relationship of the international organizations related to climate research and the CMIP. The Working Group on Coupled Modeling (WGCM) under the WCRP directly coordinates the activities of the CMIP data archive.

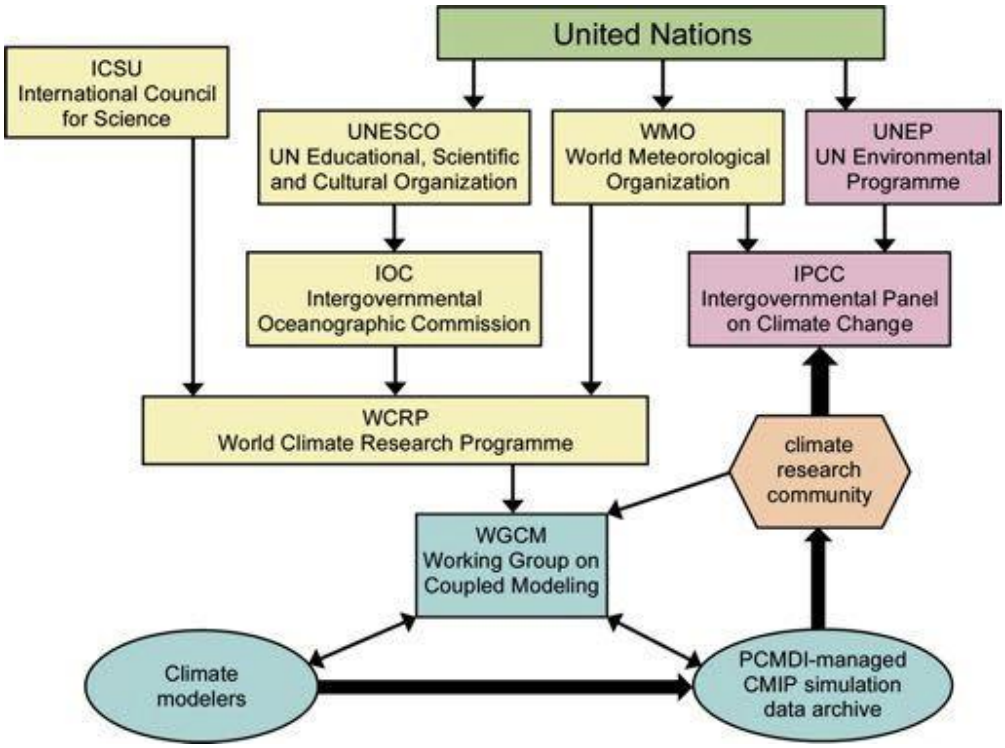

Source: [159]

Figure 1.3. The relationship of the international organizations related to climate research and the CMIP.

The first phase of the project (CMIP1) studied the ability of models in simulating current climate, while the second phase (CMIP2) simulated climate change due to an idealized change in forcing, i.e. a 1% per year CO_2 increase [110]. A subset of model data was then gathered and stored at the Program for Climate Model Diagnosis and Intercomparison (PCMDI) and was accessible to researchers outside the modeling groups. Subsequently an additional phase CMIP2+ was conducted [31] [112]. In late 2003, the WGCM started a process of coordinating a set of experiments including substantial aspects of climate variability and change which could be implemented by many modeling groups. The model data were then gathered and made available for analysis [112] [113]. An important part of this attempt was to store and sort out the data so that they were easily accessible to the international climate science community for analysis. PCMDI consented to take over this substantial challenge, which led to the birth of the third phase of CMIP (CMIP3). The CMIP3 suite of models was used in the AR4 [151] [116]. The fourth phase of CMIP (CMIP4) was intermediate but not widely popular, which humbly added the experiments performed in the CMIP3 with single-forcing experiments [153].

The next main phase was the CMIP5 [160], which based on the CMIP3 and contained more idealized process- and feedback-oriented experiments and results to improve the knowledge of the climate system. It was also tailored to deal with the physical mechanisms through which the climate system responds to changes in external forcing as well as intrinsic climate variability, which considered extreme conditions of the ancient past [24]. New factors in the CMIP5 included an ability to investigate the quick climate responses to perturbed atmospheric CO2 concentrations [160] and the impact of atmospheric chemistry on climate [92], troposphere-stratosphere interactions

[49], and carbon-climate interactions [19] [59] and feedbacks and ideal model configurations used, e.g. in the aquaplanet experiments [152].

In 2014, Meehl et al. [114] made an initial proposal for the design of CMIP6. The CMIP6 design was then finalized by the WGCM and the CMIP Panel at the WGCM 18th session in consultation with the model groups and MIP co-chairs in October 2014 in Grainau, Germany. It includes three main elements: (1) a handful of general experiments, the DECK (Diagnostic, Evaluation and Characterization of Klima) and CMIP historical simulations (1850 – near-present) that will preserve continuity and endorse documentation of principal features of models across different phases of CMIP; (2) general standards, coordination, infrastructure and documentation that will help the distribution of model outputs and the features of the model ensemble; and (3) an ensemble of CMIP-Endorsed Model Intercomparison Projects (MIPs) that will be particular to a definite phase of CMIP (now CMIP6) and that will base on the DECK and CMIP historical simulations to deal with a wide series of particular questions and fill the scientific gaps of the past CMIP phases [50]. CMIP6 data have been released recently. However, not all model groups have released the full database. These initial results are used for the IPCC AR6 that is going to be published in 2021.

GCMs depict physical processes in atmosphere, ocean, cryosphere, and land surface through simulating the response of the global climate system to increasing GHG concentrations (https://www.ipcc-data.org/guidelines/pages/gcm_guide.html). The essential components of climate system (atmosphere, land surface, ocean, and sea ice) are mathematically represented in a GCM. The main issue of long-term climate simulation is the earth's energy balance among these four elements. The key climate system components dealt within a climate model include: 1) Atmosp--

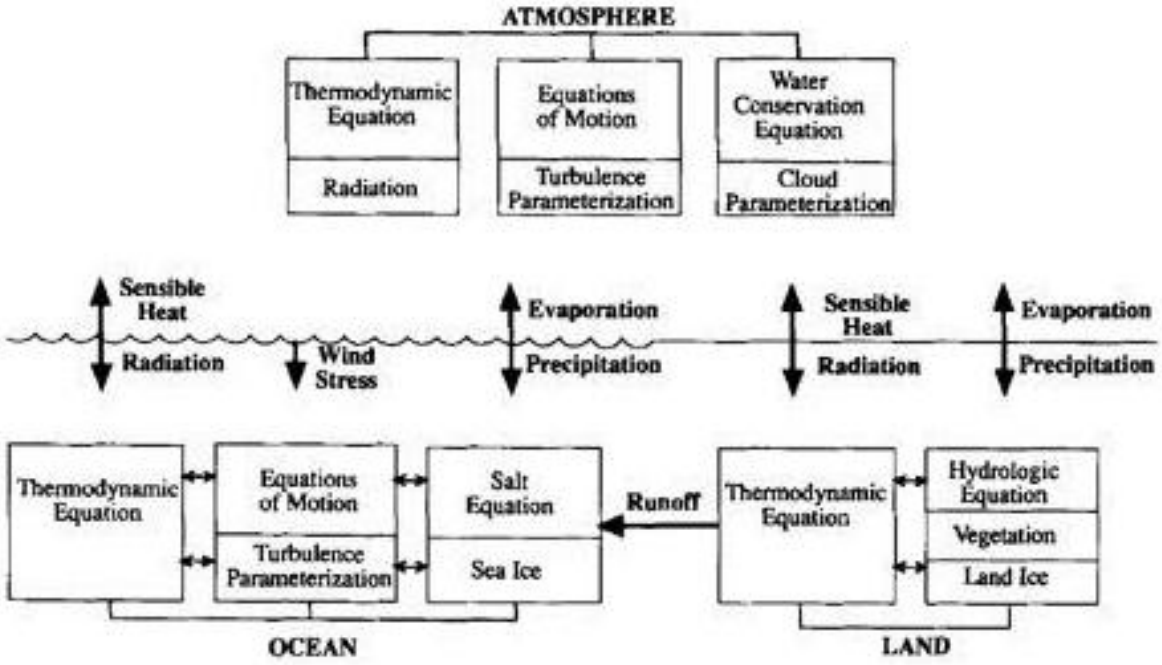

Source: [36]

Figure 1.4. Skematic diagram showing the components of a global climate model.

-heric component (simulating clouds and aerosol, which highly contribute to transportation of heat and water around the earth); 2) Land surface (simulating surface features such as vegetation, snow cover, soil water, rivers and carbon storage); 3) Ocean component (simulating current movement and mixing, and biogeochemistry as the ocean is the main reservoir of heat and carbon in the climate system); and 4) Sea ice component (modulating solar radiation absorption and air-sea heat and water exchanges) (https://www.gfdl.noaa.gov/climate-modeling/) (Figure 1.4).

GCMs use three dimensional grid to describe the globe. The GCMs often have the horizontal resolution of from 100 to 600 km, 10 to 20 vertical layers in the atmosphere and occasionally as many as 30 layers in the oceans (https://www.ipcc-data.org/guidelines/pages/gcm_guide.html).

There are two kinds of processes within climate models that are employed currently: simulation and parameterization. Simulations are

implemented with the grid-size scale or larger, for example large scale flow within a tropical cyclone, and are based on the primitive equation system (e.g. conservation of energy, mass, and momentum). Besides, a large number of physical processes such as those associated with clouds happen in smaller scales. Thus, their known attributes have to be averaged at larger scales using a technique named as parameterization. Parameterizations require more complicated processes of which the scales are smaller than the grid scale. Thus, they cannot be physically represented. Their formulations are directed by both basic physical principles and observational data. The process of representing cloud and aerosol composition is an illustration of the parameterization (https://www.gfdl.noaa.gov/climate-modeling/). Significant processes that are not dealed with grid spacings of climate models must be parameterized. These parameterizations are among the main causes of model errors and uncertainty in future climate projections [37], [47], [69], [133]. Others stem from simulation of diverse feedback mechanisms in models: water vapour and warming, clouds and radiation, ocean circulation and ice and snow albedo. Hence, with the same forcing, GCMs can produce different simulation outcomes due to the way the particular processes and feedbacks are modelled (https://www.ipcc-data.org/guidelines/pages/gcm_guide.html).

GCMs are essential tools that enhance the comprehension and predictability of climate behavior on various time scales. The models permit us to identify the effects of distinctive climate characteristics through evaluating climate sensitivities with experiments that cannot be implemented on the actual earth. By only changing some features in a climate model, one could better understand the impacts of the changes such as warming or cooling of sea surface temperatures on the climate. GCMs also involve diagnosis and prognosis. Detection and attribution are an illustration of a

diagnostic use, which demands first indicating that a detected change is statistically essential, and then attributing this change to unnatural causes such as the role of anthropogenic forcing in the 20th century climate change. Prognosis here denotes future climate prediction, such as global warming trends, employing current or historic data as a basis (https://www.gfdl.noaa.gov/climate-modeling/).

In the thesis, 6 GCMs (shown in Table 2.1) are used as initial and boundary conditions for the downscaling experiments over SEA.

CNRM-CM5 is an earth system model, which is developed jointly by CNRM-GAME (Centre National de Recherches Météorologiques—Groupe d'études de l'Atmosphère Météorologique) and Cerfacs (Centre Européen de Recherche et de Formation Avancée). Components of this model is described in Figure 1.5, which includes the atmospheric model ARPEGE-Climat (v5.2), the ocean model NEMO (v3.2), the land surface scheme ISBA and the sea ice model GELATO (v5) coupled through the OASIS (v3) system [172].

CSIRO-Mk3.6 is a coupled atmosphere-ocean model with dynamic sea ice model. It also has a soil-canopy scheme with prescribed vegetation properties. The ocean, sea-ice and soil-canopy models are unchanged between the version Mk3.5 and Mk3.6 [144].

EC-Earth is an earth system model that belongs to the European community. It helps promote international cooperation and access to a wide range of knowledge and database. Its major aim is to develop and apply an ESM based on the ECMWFs seasonal forecasting system for supplying reliable climate information to climate services and to develop scientific knowledge on the earth system, its variability, predictability and long-term changes deriving from external forcing. EC-Earth has become a notable advanced model among the Earth System Models in Europe, as shown by its -

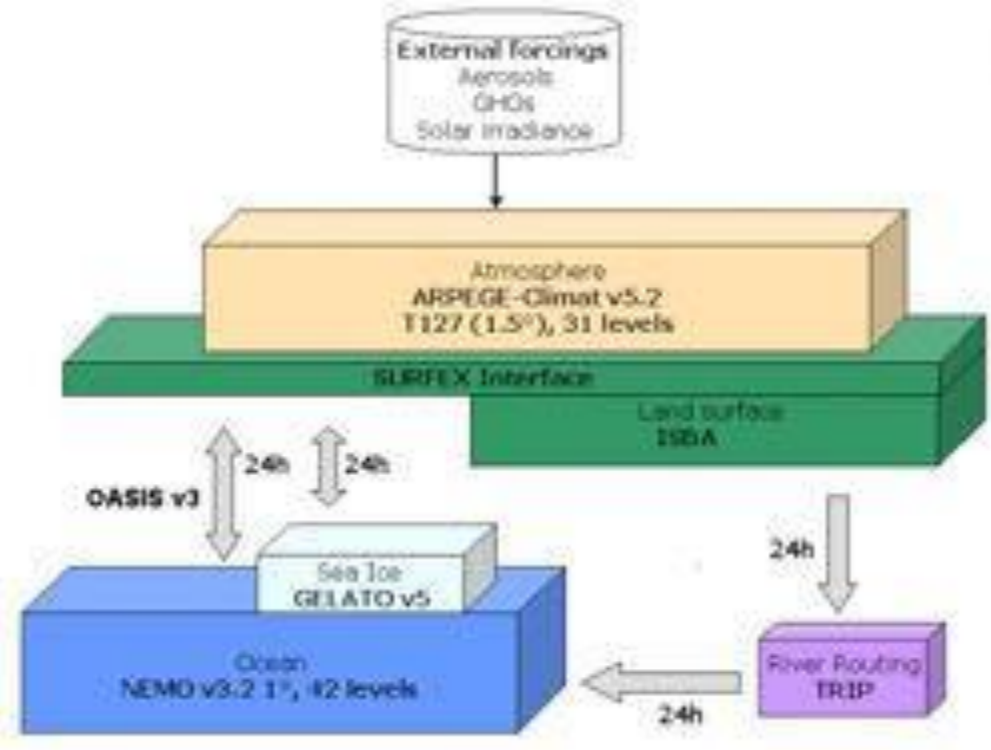

Source: http://www.umr-cnrm.fr/spip.php?article126

Figure 1.5. Schematic discription of GCM CNRM-CM5.

contribution in many European projects, the CMIP5 and CMIP6 (http://www.ec-earth.org).

GFDL is an earth system model developed by the Geophysical Fluid Dynamics Laboratory in the Princeton University. GFDL has designed National Oceanic and Atmospheric Administration (NOAA)'s first ESMs [44], [45]. ESM2M uses pressure-based vertical coordinates along the developmental path of the GFDL Modular Ocean Model version 4.1. It uses a more advanced land model, which is LM3 with a variety of improvements compared to what was available in ESM2.1. Figure 1.6 shows the basic structure of the GFDL ESM.

HadGEM2-ES is a coupled earth system model that was used by the Met Office Hadley Centre for simulations in the CMIP5. HadGEM2 is a configuration of the Met Office Unified Model (UM) developed from the UM

version 6.6. HadGEM2-ES was the first model to include earth system components. The UM is applied by several institutions in the world both for operational weather forecasting and for climate research. The HadGEM2-ES climate model includes: 1) an atmospheric GCM at N96 (horizontal) and L38 (vertical) resolution; and 2) an ocean GCM with a 1-degree horizontal resolution (increasing to 1/3 degree at the equator) and 40 vertical levels. Its components comprise the terrestrial and ocean carbon cycle and tropospheric chemistry (https://portal.enes.org/models/earthsystem-models/metoffice-hadley centre/hadgem2-es).

MPI-ESM is an earth system model developed by the Max Planck Institute. The atmosphere, ocean and land surface in the MPI ESM are combined through the exchange of energy, momentum, water and carbon dioxide. It comprises the components of ECHAM6 for atmosphere and MPIOM for ocean as well as JSBACH for terrestrial biosphere and HAMOCC for the ocean´s biogeochemistry. The separate coupling program OASIS3 is used to split the coupling of atmosphere and land and that of ocean and biogeochemistry (**Figure 1.7**). (https://www.mpimet.mpg.de/en/science/models/mpi-esm/).

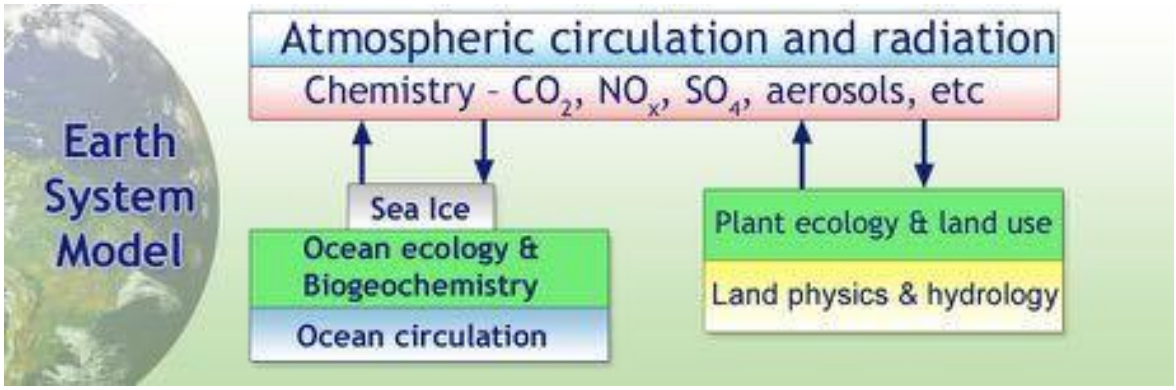

Source: https://www.gfdl.noaa.gov/earth-system-model/

Figure 1.6. Basic structure of the GFDL Earth System Model.

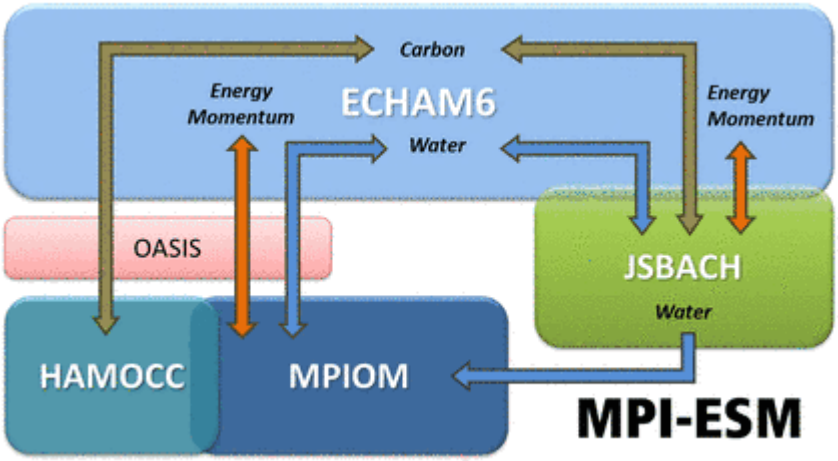

Source: https://www.mpimet.mpg.de/en/science/models/mpi-esm/

Figure 1.7. Basic structure of the MPI ESM.

Downscaling

Downscaling is a general terminology describing a procedure to derive information known at large scales to make predictions at regional to local scales (https://gisclimatechange.ucar.edu/question/63). Figure 1.8 depicts the downscaling of the SEA region from the global scale to the regional and local scale. Generally, more detailed information is obtained after the processes of downscaling.

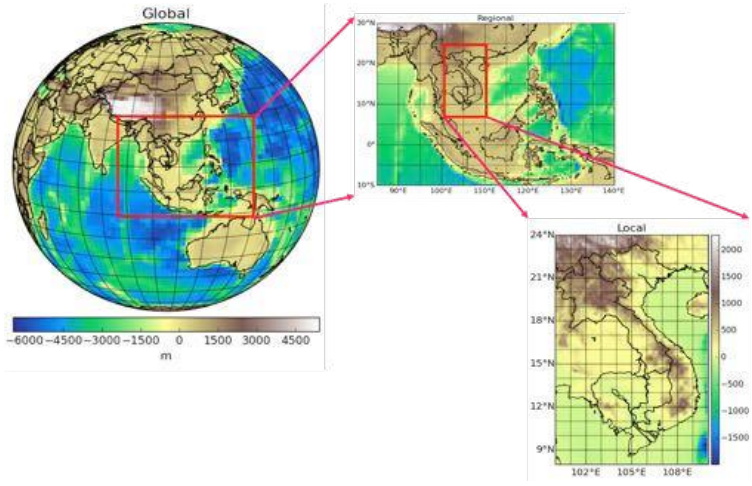

Courtesy of N.D. Thanh

Figure 1.8. Visualizing concept on climate downscaling.

There are two main approaches to downscale climate information, i.e. dynamic and statistical ones. *Dynamic downscaling* produces a high-resolution computation on a local sub-domain with boundary and initial conditions resulted from a coarser-resolution experiment. In dynamical climate downscaling, a limited-area model, regularly called regional climate model (RCM), is used to downscale outputs from a parent/driving GCM.

Regional climate models

A RCM is a numerical climate model forced by initial conditions (IC) and lateral boundary conditions (LBC) from a GCM (one-way nesting [108]) or analysis of observations (perfect LBC) that simulates atmospheric and land surface processes, while providing high-resolution topographical data, land-sea contrasts, surface characteristics, and other parts of the earth system. As RCMs only cover a restricted area, the values at their boundaries must be stated explicitly, known as boundary conditions, by the results from a coarser GCM or reanalysis. RCMs are initialized with the initial conditions and driven along its lateral-atmospheric-boundaries and lower-surface boundaries with time-variable conditions. RCMs thus downscale global reanalysis or GCM runs to simulate climate variability with regional refinements (http://glossary.ametsoc.org/wiki/Regional_climate_model).

RCM is used to develop climate change scenarios at a higher spatial and temporal resolution of about 30-50 km and a time step size of 6 hours for one specific period in the present and future [108]. The ‘nested’ RCM approach was first used in the climate change research by Dickinson et al. in 1989 [38]. Although the one-way nested approach is often used in the climate simulation studies, the two-way nesting that includes feedback from RCM to GCM, is a probable choice [23], [25], [56], [98].

The RCM resolution has increased from around 50 km to around 25 km

and finer since the AR4 [28]. However, long RCM runs at very high resolution are still rather limited [23], [85], [173]. Coupled RCMs with interactive ocean and sea ice have also been in progress [20], [41], [42], [150]. Vegetation dynamics - ecosystem biogeochemistry was added in an RCM by Smith et al. [150].

During the period of the AR4, RCMs were usually applied for time-slice experiments. Since then, multi-decadal and centennial RCM simulations have been implemented with greater quantities [34], [39], [88]. At present, coordinated RCM experiments and ensembles (ENS) have also become much more popular with domains covering Europe [30], [170], North America [64], [95], [109], South America [28], [91], [110], Africa [43], [94], [128], [132], [146], the Arctic [76] and Asian regions [52], [53], [131], [147], [155].

Climate analog

Climate analog is used to define locations at which their present climate is similar to the projected future climate of a reference site [107]. This concept implies the spatio-temporal relationship between the reference site and the analog location (Figure 1.9).

Figure 1.10 illustrates the concept of climate analog through the seasonal cycle of temperature in Ha Noi at the present and in the future and the present cycle at an analog location. The smaller the climate distance between the black line (future projected cycle of Ha Noi) and the red line (present cycle of an analog location) is, the better the climate analog is. When the estimated distance reaches its minimum, the best analog location is found.

Good analog

When the future climate of a reference point is projected to be highly similar to the present climate of a grid point, the reference point is considered as a good analog. The similarity level is subjectively arbitrary (Figure 1.11). -

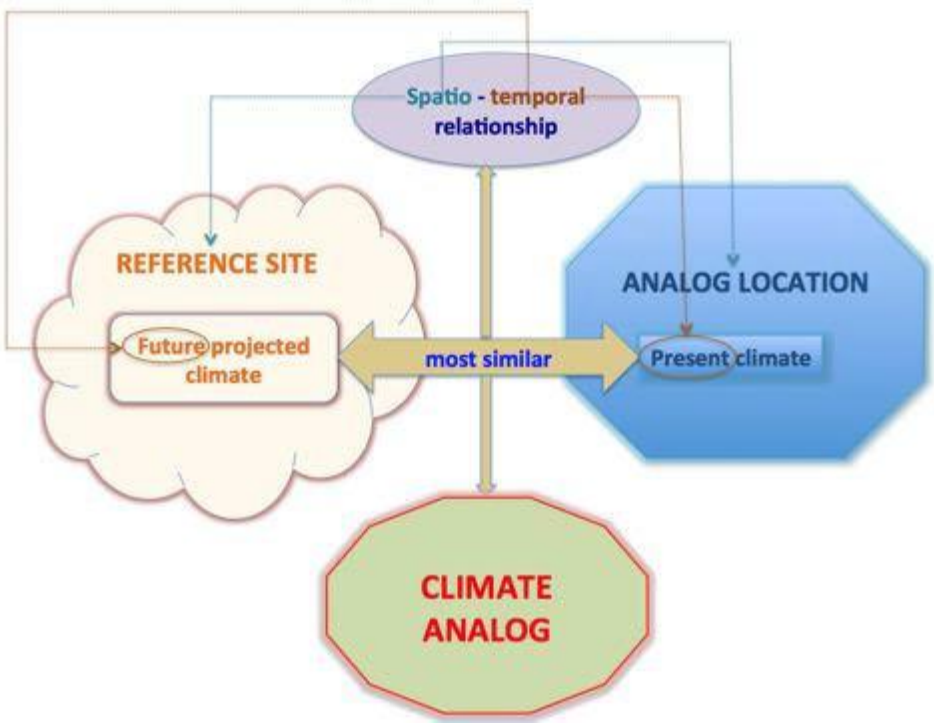

Figure 1.9. Schematic concept of climate analog.

The climate distance illustrated in Figure 1.10 in this case is small.

Poor analog

When the future climate of a reference point is projected to be poorly similar to the present climate of all grid points within the study area, the reference point is considered as poor analog (Figure 1.11). Again, the poor similarity level is subjectively arbitrary. The climate distance illustrated in Figure 1.10 in this case is larger than that of good analog.

Novel climate

When the future climate of a reference grid point is not similar to the present climate of all grid points within the study area, the reference point is considered as novel climate [51] (Figure 1.11). The climate distance illustrated in Figure 1.10 in this case is larger than that of poor analog.

Disappearing climate

When the present climate of a reference grid point is not similar to the future climate of all grid points within the study area, the reference point is d-

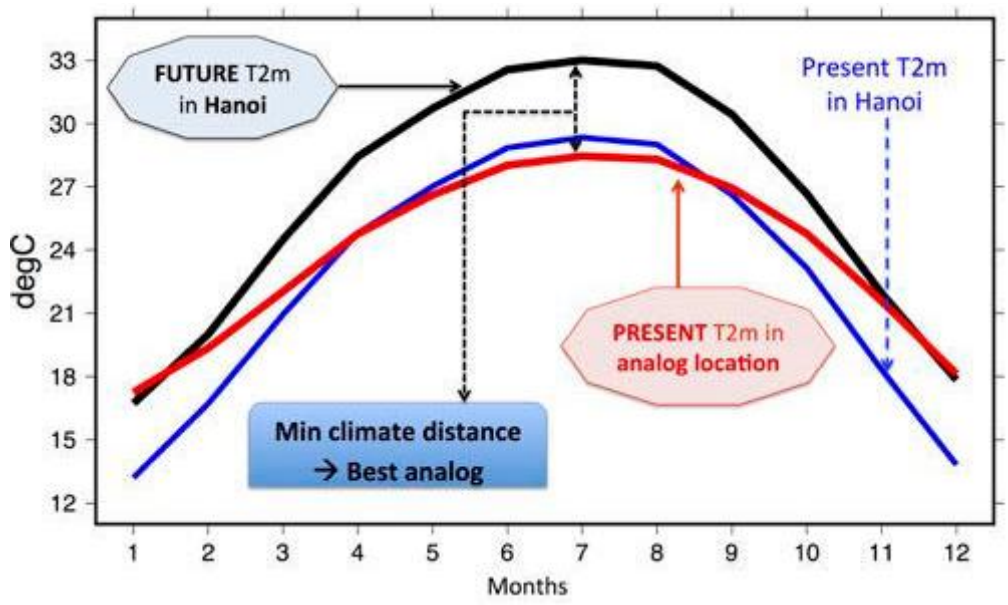

Figure 1.10. Illustration of the climate analog concept via the seasonal cycle of temperature in Ha Noi at the present (blue) and in the future (black) and the present cycle at an analog location (red).

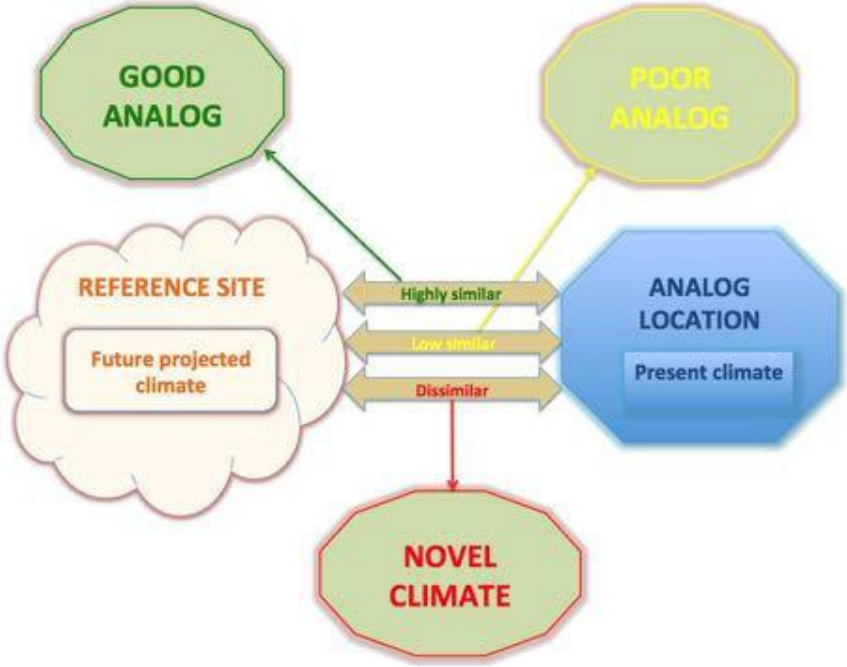

Figure 1.11. Schematic concepts of good analog, poor analog and novel climate.

-efined as disappearing climate [51] (Figure 1.12).

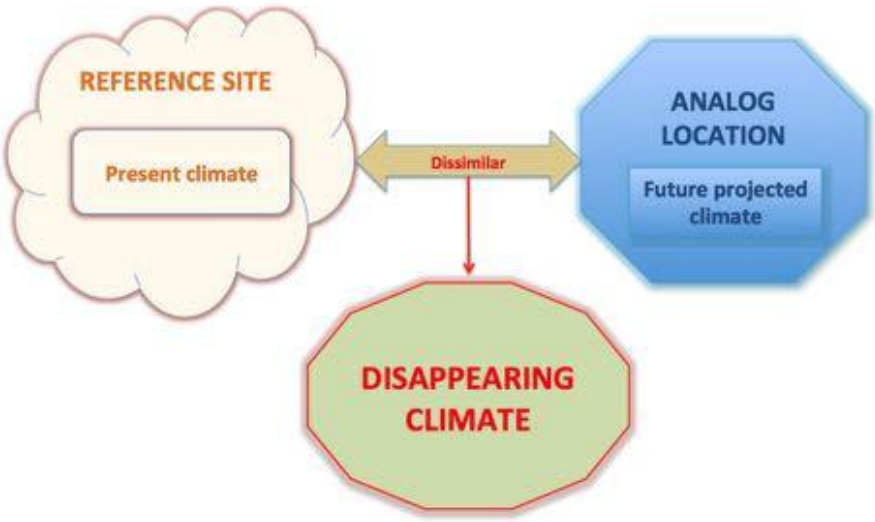

Figure 1.12. Schematic concept of disappearing climate.

1.2. Literature review

In the world

One of the most typical and comprehensive worldwide reference documents on climate simulation and projection is the AR5 contributed by the WGI of the IPCC [79]. Based on plenty of independent scientific analysis from observations on climate system, paleoclimate archives, theoretical research on climatic processes and simulations using climate models, the AR5 described inclusive pictures of Atmosphere – Ocean General Circulation Models (AOGCMs), Earth System Models (ESMs), Regional Climate Models (RCMs), etc. RCMs are regularly utilized to dynamically downscale global climate models (GCMs) for some particular geographical areas to supply more elaborate information [93], [145].

The research on climate change at the regional scale often requires high-resolution data, while state of the art GCMs with rather coarse resolution could rarely provide them. Therefore, a joint initiative on regional climate downscaling for SEA has been set up under the framework of CORDEX of WCRP [62]. It is currently known as SEACLID/ CORDEX-SEA [83], [124].

One of the major purposes of this initiative is to produce high-resolution regional climate change scenarios over the SEA region. The Regional Climate Model version 4.3 (RegCM4.3), established by the Earth System Physics section of the Abdus Salam International Centre for Theoretical Physics (ICTP) [63], was applied to downscale a number of Coupled Model Intercomparison Project Phase 5 (CMIP5) GCMs for the CORDEX-SEA domain by several institutions from the SEA region [83], [124].

Over the last few years, a number of studies using RCMs have been implemented to figure out the characteristics and variability of regional climate as well as to evaluate the models' performance worldwide.

Im et al. [74] investigated the capability of RegCM3 in simulating regional climate over the Korean peninsula and its sensitivity to the two convective schemes, i.e. the Grell scheme (Grell) and the MIT-Emanuel scheme (EMU). The result showed that the EMU better simulated the timing and amplitude of the rain band propagating northward compared to the Grell. The spatial distribution of precipitation was also well reproduced and could capture the localized maxima over Korea. The EMU also showed better performance in simulating the frequency distribution of daily temperature and rainfall compared to the Grell.

An evaluation on ensemble mean of five RCMs from CORDEX East Asia was implemented and the ensemble was used to project future regional climate change in China [65]. The study focused on five subregions in China, including northeastern China, northern China, southern China, northwestern China, and the Tibetan Plateau. The added value was shown due to the better performance of RCMs in representing annual and seasonal mean temperature and precipitation for the period 1980-2005. Persistent warming tendency at around 1^{o}C in the whole domain was shown for the period 2030-2049.

Increased annual precipitation was prominent in most of the region, except for the Tibetan Plateau. The result of average precipitation simulated by the RCM ensemble and the driving GCM was opposite over southern China, northeastern China and the Tibetan Plateau.

Over the Tibetan Plateau, CORDEX regional climate models were evaluated in simulating temperature and precipitation [66]. Identical spatial patterns, but a mean cold bias in the temperature climatology and a wet bias in the precipitation one versus station data were shown by all RCMs used in the study. The RCMs did not succeed in representing the observed spatial patterns of temperature and precipitation trends. Among the five RCMs, RegCM4 was proved to be the best in reproducing simulated trends. There were significant differences in the RCMs' results, which pointed the essential dependency on model in simulating climate over the Tibetan Plateau. The temperature (precipitation) changes in 2016-2035 compared to 1986-2005 were 1.38 ± 0.09 °C ($0.8\% \pm 4.0\%$) and 1.77 ± 0.28 °C ($7.3\% \pm 2.5\%$) under RCP4.5 and RCP8.5, respectively.

The skills of the RCM Consortium for Small-Scale Modeling in Climate Mode (CCLM) in representing present climatic characteristics and their added value were evaluated over the CORDEX-East Asia [96]. The study showed that the simulated summer temperature had smaller bias than that of the winter temperature. This led to the larger added-value areas in simulating temperature in the winter than in the summer as compared to the driving GCMs. Climatological precipitation means and daily precipitation distribution for most areas in the winter were better reproduced by CCLM than GCMs, but this was different in the summer. Moreover, characteristics of consecutive wet days for the tropics and of consecutive dry days for regions to the north of 30^{o}N showed added value of downscaled simulations.

Ensemble mean daily precipitation and near-surface temperatures from RCM simulations over seven CORDEX domains (including CORDEX-South Asia and CORDEX-East Asia) for the winter and summer seasons were analysed [64]. The results showed that model simulations and the Climatic Research Unit (CRU) had a good agreement in representing seasonal cycles. Downscaled ERA-Interim precipitation reproduced better simulations than raw ERA-Interim precipitation. Larger biases occurred in the domains located in the low latitudes and those with high topography, especially precipitation.

Kim et al. [88] evaluated and projected precipitation in CORDEX-East Asia Phase I. The RCMs generally represented identical bias features to the result implemented by the GCM. Mean and extreme precipitation amounts increased over the Korean Peninsula and northern China in the middle of 21st century (2025-2049). The East Asian summer monsoon was increased in mid-latitudes and lasted longer in summer due to the improved western North Pacific Subtropical High. The increase in precipitation in this area can be attributed to the increasing southerly wind from East Asian summer monsoon.

Model errors and projected seasonal mean temperature and precipitation over CORDEX South Asia were evaluated using two climate simulation ensembles, one global and one regional [142]. A RCM – RCA4 was used to downscale ten GCMs. The study showed that RCA4 could represent, lessen or expand large-scale GCM biases. However, precipitation bias pattern in all RCA4 simulations were analogous, regardless of driving GCM. This implied the essential role of RCA4 in simulated precipitation. In terms of projected climate, it was shown that RCA4 could alter the signal projected by the GCM ensemble and its individual members. The results identified that considering only RCMs, regardless of GCMs, could modify the message on future regional climate change.

In Southeast Asia, a number of studies have been conducted at the regional and country level. Aldrian et al. [16] simulated rainfall in Indonesia using the Max Planck Institute regional climate model REMO. Three lateral boundary forcings were used in the study, including reanalyses from the European Centre for Medium-Range Weather Forecasts (ECMWF) ERA15 and National Center for Atmospheric Research (NCAR), the National Centers for Environmental Prediction (NCEP) and NCAR and the simulations from ECHAM4 climate model. The result showed that REMO generally well reproduced the spatial pattern of monthly and seasonal rainfall over land, but overestimated rainfall over the ocean. It was also shown that the quality of driving data could significantly affect the performance of the REMO experiments.

The sensitivity of summer monsoon rainfall over the Philippines to driving lateral boundary conditions (the NCEP reanalysis and the ECMWF 40-year Re-Analysis (ERA40)) and ocean flux schemes (BATS and Zeng) were assessed by Francisco et al. [58]. The result showed that greater precipitation amounts were simulated with the use of the ERA40 lateral boundary fields than with the use of the NCEP ones. The BATS scheme also yielded more precipitation compared to the Zeng scheme. Therefore, it was shown that different combinations of lateral boundary fields and surface ocean flux schemes could well simulate precipitation amounts and spatial structure over the region.

Chotamonsak et al. [27] conducted climate change projection over the SEA region by using the Weather Research and Forecasting (WRF) model to dynamically downscale a GCM product to 60 km horizontal resolution. The result showed a cold bias for maximum temperature and a warm bias for minimum temperature. The projected warming varied from 0.1 to 3ºC

depending on the location and season and was warmer at night than daytime for all seasons. The projected rainfall generally increased but with local decreases in the dry season.

Torsri et al. [161] characterized means and variability of temperature and precipitation for the period 1961–2000 over Thailand using the RegCM3 model. They concluded that the model was appropriate for climate studies in Thailand, and could well simulate seasonal features and tendencies but with a lower level.

Manomaiphiboon et al. [105] projected temperature and rainfall changes in Thailand for the period 2031-2070 under the Special Report on Emissions Scenarios (SRES) [120], using 20-km RegCM3 simulations driven by the ECHAM5/MPI-OM GCM. The temperature in Thailand was projected to increase from 0.4 to 3.3^{o}C under the A2 and A1B scenarios for the summer of the decade 2061-2070 compared to that of the reference period 1961-2000. There were not significant changes in average precipitation in the Central-East, North, and Northeast sub-regions, and less rainfall was projected in Southern Thailand in most seasons.

Rahmat et al. [139] built a technical report, which was the product of the SEA Climate Analysis and Modeling (SEACAM) Framework, initiated by the Centre for Climate Research Singapore of the Meteorological Service Singapore (CCRS-MSS) and in collaboration with the Met Office Hadley Centre (MOHC). The output of 17-member Perturbed Physics Ensemble (PPE) of HadCM3Q global model was downscaled using the Providing Regional Climates for Impacts Studies (PRECIS) RCM to the 25 km resolution under the A1B emission scenario. This report provided a comprehensive climate change evaluation and projection over SEA.

The WRF model's capability in simulating major weather phenomena

(dry conditions, tropical cyclones (TCs) and monsoonal flow) was evaluated over East Asia and SEA by Raktham et al. [140]. Various cumulus and microphysics used together with different placement of lateral boundaries to comprehend and define an appropriate model configuration for weather and climate simulations over the Asian region. It showed a low sensitivity to configuration choices for dry season. For TC cases, it showed a high sensitivity to the cumulus schemes and a low sensitivity to the microphysical schemes. A high sensitivity to the placement of the lateral boundaries was shown with monsoon simulations.

A WRF simulation at the resolution of 25 km was also used by Raghavan et al. [137] to analyze the present day (1961-1990) climate over Vietnam. The model was able to represent the observed spatial patterns of the climate with some biases. It was underlined that improvements in modeling should be implemented to reproduce the realistic patterns of climate at a better spatial resolution before the model information can be applied for impact studies at a local scale.

Juneng et al. [83] analyzed the sensitivity of precipitation and extremes to cumulus and air-sea flux parameterizations using RegCM4. Their results showed dry biases in the equatorial area and rather wet biases in the mainland Indo-China, except for the experiments with the MIT Emanuel cumulus schemes.

Loh et al. [97] projected rainfall and temperature changes in Malaysia by the end of the 21st century using PRECIS RCM and the SRES scenarios. The temperature changes were projected to be from 2.5 to 3.9^{o}C, from 2.7 to 4.2^{o}C and from 1.7 to 3.1^{o}C for the A2, A1B and B2 scenarios, respectively. About 20 to 40% decrease of rainfall in the months of December to May was projected over Peninsular Malaysia and Borneo, especially for the A2 and B2

emission scenarios, while a rainfall increase from ~20 to 40% during the summer months in most Malaysia was shown, particularly for the A2 and A1B scenarios. The spatio-temporal variations in the projected rainfall can be attributed to the weakening monsoon circulations, which in turn change the patterns of regional moisture convergences in Malaysia.

Ratna et al. [143] evaluated the performance of a regional climate model - WRF in simulating the climate variablity in SEA. The model reproduced the mean precipitation climatology and the annual cycle. The study showed an overestimation of boreal summer precipitation in the SEA mainland and an underestimation of boreal winter precipitation in Indonesia. Model biases were related to the bias in simulating the vertically integrated moisture fluxes. At an interannual scale, the model could produce well over the SEA mainland and the Phillipines in all seasons except for the boreal summer. The model well reproduced the weak influence of El Niño/Southern Oscillation (ENSO) on rainfall over mainland SE Asia and the Philippines during June to August (JJA), and the influence of the Indian Ocean Dipole (IOD) in the boreal autumn over the Indonesian region.

Tangang et al. [155] projected changes in annual precipitation extremes over SEA under the global warming of $2^{o}C$ based on the SEACLID/CORDEX-SEA simulations. They considered four indices of extreme precipitation: annual total precipitation (PRCPTOT), consecutive dry days (CDD), frequency of rainfall exceeding 50 mm day^{-1} (R50mm), and intensity of extreme precipitation (RX1day). The 10-member ensemble mean could represent observed characteristics of extreme precipitation during the period 1986-2005. Their study showed significant and robust changes in consecutive dry days (CDD) in Indonesia and in intensity of extreme precipitation (RX1day) in Indochina. The significant and robust changes in

CDD, frequency of rainfall exceeding 50 mm day^{-1} (R50mm) and RX1day were also projected over the northern Myanmar.

Projected changes in precipitation under RCP4.5 and RCP8.5 over Thailand were studied using multi-model experiments of CORDEX-SEA [156]. The study concluded that results simulated by ensemble mean go well with those by observations, especially for Global Precipitation Climatology Center (GPCC) data for the period 1976-2005. For future projections, precipitation was projected to be generally wetter and drier in the northern-central-eastern parts and the southern parts of Thailand, respectively. The magnitude of change can reach 15% of the historical period. These changes were associated with those in regional circulations driven from winter and summer monsoons.

Precipitation extremes at the end of the 21st century (2081-2100) over SEA were projected using the results of CORDEX-SEA under RCP4.5 and RCP8.5 [154], which was different from the study of Tangang et al. [155] projected in 2041 when global mean temperature reaches 2^{o}C. The four similar precipitation indices were used in this study including PRCPTOT, CDD, R50mm and RX1day. Annual PRCPTOT was projected to decrease over most of SEA, except for Myanmar and Northern Thailand, with the highest magnitude of 20% (30%) under RCP4.5 (RCP8.5). The CDD were found to have the most significant and robust changes reaching 30% under RCP4.5 and 60% under RCP8.5, particularly over Maritime Continent. The projected R50mm and RX1 day increased during all seasons with strong signal of RX1 day during JJA and September to November (SON).

Eleven GCMs and seven RCMs were used to project precipitation over SEA based on the outputs of CORDEX-SEA [157]. The ensemble mean represented the mean spatial patterns of precipitation with systematic wet

biases. There was a prominent dry tendency (10-30%) over the Maritime Continent in JJA, particularly in Indonesia by mid and late 21st century.

Climate analog

With regard to climate analog, there have been studies in various places in the world. In 2007, Hallegatte et al. [68] used two models of the Prediction of Regional scenarios and Uncertainties for Defining European Climate change risks and Effects (PRUDENCE) project (HadRM3H and ARPEGE) to find out the cities, which had present climate analogous to future climate of 17 European cities. These analog cities showed the tendency towards the warmer regions. The study used the tool of climate analog to apprehend major characteristics of the adaptation to climate change and then suggested a way of economic assessment of climate change impacts.

Williams et al. [174] projected the distributions of novel and disappearing climates by 2100. They defined dissimilarities between present and future climates by using standardized Euclidean distance (SED) with numerator to be the squared result of the future mean minus the present and denominator to be the squared standard deviation of the interannual variability for 1980-1999. They used a threshold of SED_t=3.22 to define novel climate The results showed the relationship between novel climates and formation of novel species associations and other ecological surprises. Likewise, the disappearance of some existing climates was able to increase the level of extinction for species with narrow geographic or climatic distributions and disruption of existing communities.

Ackerly et al. [14] examined some geographic aspects of climate change and mapped disappearing, reducing, increasing and novel climates. It also showed the velocity and direction of climate change in California and Nevada. The result showed that spatial heterogeneity in climate was an

essential spatial buffer in response to climate change, and thus useful for conservation planning.

Potential climate change orbits for selected sites were explored through climate analogs in the study of Luedeling and Neufeldt in 2012 [100]. Climate analog regions showed an unsure climate trajectory for the Sahel, but the majority of scenarios predicted escalating aridity and decreased appropriateness for parklands.

Veloz et al. [171] used climate analog analyses to define and convey climate change impacts. The study downscaled the outputs of several GCMs over the state of Wisconsin to 0.1^{o} horizontal resolution. The result showed that the present areas in North America were the most similar to the projected future climates in Wisconsin.

Climate analog was also used as an approach to cover all relevant aspects including exposure, sensitivity and adaptive capacity of ecosystems in the study of Luedeling et. al [101]. It was based on a comparison of present ecosystems with those at a different location, where the present climate is analogous to the predicted climate in the target location in the future.

Climate analog analysis was an option for projecting climate change impacts on agroforestry systems in the study of Luedeling et al. in 2014 [102]. This projection depended on a major assumption that observations of present results could be used to instruct estimates of future performance. As the effects of increasing carbon dioxide could not be observed at present, and many areas might undergo novel climates in the future, this approach had some systematic disadvantages that could not easily be overcome.

Climate distance method was used by Nyairo et al. [129] to find out analog areas for Bugabira Commune in Burundi. Climate analog analysis was combined with the interviews conducted in the target and analog communes

to determine the information related to farming systems and adaptation. The study showed that the analog approach exhibited low ability for the farmers in Bugabira to draw out lessons for adaptation planning.

In 2015, in a smallholder farming setting on Mt. Elgon in Kenya, the study of Bos et al. [22] compared yield potentials of maize and coffee among 50 analog sites for various future climate scenarios and models, and compared local ecological knowledge and farm characteristics for one target-analog pair. The result showed that distinction between the target and the analog location was majorly resulted from non-climatic factors. This was not a good indication for applying the analog approach to impact projection and adaptation planning for future climatic conditions with agricultural background.

Arnbjerg-Nielsen et al. [18] used the RCM projections from the ENSEMBLES database to identify climate analogs for precipitation extremes, and showed that the best region to represent future conditions for Denmark was the coastal area of Northern France.

In 2016, Pugh et al. [136] linked the observations of present maximum-attainable yield with climate analogs to give a method of evaluating the effect of climate change on crop yields. The study showed the qualitatively similar results to the previous studies in which climate analogs were applied to assess changes in biodiversity and natural vegetation, which demonstrated poor present-day analogs for end-of-century climates in the tropics with strong climate change.

A non-parametric approach was applied to identify climate analogs for 17 cities in Australia by Nakaegawa et al. [119] with the global research domain in 2017. Among the identified climate analog cities in a global search, ten located within Australia while the other seven were in other continents

(five in Africa, one in Mexico, and one in Argentina).

Fabienne et al. [51] used the climate analog approach to locate novel and disappearing climate across the world in 2017. The climate distance formulation used in the study built on four seasonal variables, which was suitable for temperate zones and high – latitude regions. They did not use weights for temperature and precipitation variable. The threshold 4σ was chosen to define novel and disappearing climate. The study showed that 15%, 21% or more than one third of the global land fractions would experience novel climates at the 1.5^{o}C, 2^{o}C or 4^{o}C global warming levels, respectively. These fractions were similar for the case of disappearing climate.

In 2017, Mahony et al. [104] studied novel climates at continental to landscape scales in the relationship with biology. The study based on the methods SED used by Williamz et al. [175] in 2007 to create an approach called sigma dissimilarity. They made two main modifications to the SED metric: (1) SED was adjusted to Mahalanobis distance and (2) Distances were interpreted into percentiles of the chi distribution. While Williams et al. [175] used a threshold of SED_t=3.22 to define novel climate, the study subjectively identified 2σ analog dissimilarity to be a moderate degree of novelty and 4σ-analog dissimilarity to be extreme novelty. It was shown that novel climate would account for 40% of North American area in RCP8.5.

In 2019, Fitzpatrick and Dunn [55] applied climate analog to identify locations that have present climate most similar to projected future climate in 540 urban areas in the North America. They used the same sigma dissimilarity approach that was previously applied by Mahony et al. [104]. The study showed that climate of most urban areas will shift mainly to the south or will not have modern equivalent.

In Viet Nam

In Viet Nam, a number of climate studies in general and climate change studies in particular have been published to date, such as those of Nguyen Duc Ngu and Nguyen Trong Hieu (1991) [9], (2004) [10], Tran Viet Lien et al. (2007) [8], and Nguyen Duc Ngu (2008) [11].

With regard to greenhouse gas (GHG) inventory, there was a report on national greenhouse gas inventory in the period from 1994 to 1998 led by Nguyen Duc Ngu. The authors built the GHG reduction project in Viet Nam; evaluated climate change impacts on essential socio-economic sectors; and developed climate change scenarios in Viet Nam for the year 2020, 2050 and 2070.

An important legal document submitted to UNFCCC was the Initial National Communication published by the Ministry of Natural Resources and Environment (MONRE) in 2003 [1]. In 2010, the Second National Communication was published with the focus on the national GHG inventory for the year 2010 and the GHG emission projection in the period 2011-2030.

The National Target Program to Respond to Climate Change was adopted by Prime Minister with the Decision number 158/2008/QD–TTg on 02/12/2008. Its strategic goals were to improve the capacity on responding to climate change for each specific period in Viet Nam; to enhance the sustainable development of the country; and to stabilize human life [2].

In 2009, MONRE published the Climate Change and Sea Level Rise Scenarios for Viet Nam. It used the MAGICC/SCENGEN 5.3 software (http://www.cgd.ucar.edu/cas/wigley/magicc/) and statistical downscaling method to provide climate change and sea level rise scenarios for seven climatic sub-regions [3]. In 2012, MONRE updated the climate change scenarios through combining the statistical and dynamical downscaling

results. The dynamical results were from the Providing REgional Climates for Impacts Studies (PRECIS) RCM developed at Hadley Centre, the United Kingdom (UK) and the MRI GCM of the Japanese Meteorological Research Institute [4]. In 2016, the report continued to be updated. An ensemble of RCMs including RegCM, WRF, Conformal-Cubic Atmospheric Model (CCAM), MRI, and PRECIS was used to dynamically downscale a number of CMIP5 GCMs under different Representative Concentration Pathways (RCPs) scenarios [5], [167]. This report has been considered as a reference document for supplying the basis for climate change-related studies in various sectors.

Above are the essential legal documents and reports related to climate change in Viet Nam. The following are researches implemented by individuals or research groups in Viet Nam.

Phan Van et al. [134] studied the seasonal and inter-annual variations of surface climate elements in Vietnam using the RegCM3 model. The observed annual cycle and the inter-annual variability of surface air temperature and precipitation were well reproduced. The model systematically underestimated air temperature over most of seven climatic sub-regions of Vietnam, although the lapse-rate correction for elevation differences between the model grids and the locations of the observed stations was implemented beforehand. The precipitation of rainy and dry seasons were respectively underestimated and overestimated.

Nguyen Van Thang et al. [13] made a comprehensive reportreport on climate change and its impact in Viet Nam. It provided a general picture of basic knowledge, international agreements on climate change, climate change in Viet Nam, climate change scenarios for Viet Nam, its impacts and strategic solutions to respond to climate change in Viet Nam.

Ho et al. [72] also used the RegCM3 to study extreme climatic events in Vietnam. They reported the projected increase of hot summer days and the projected decrease of cold winter nights in the future.

Ngo-Duc et al. [122] evaluated and projected future climate in the Red River Delta (RRD) region. The study showed that temperature patterns could be rather well represented but with systematic cold biases. Precipitation could be also reproduced well during winter – spring but much underestimated during summer-autumn. 2030-2049 projected temperature increased 1.4±0.2^{o}C compared to the baseline period 1980-1999. Precipitation generally decreased for the whole RRD region except the future JJA rainfall projected by the A2 scenario.

Van Khiem et al. [166] evaluated the performance of the PRECIS RCM in simulating seasonal climate in Viet Nam in 2014. It was reported that the model could well simulate the spatial patterns, annual cycles and inter-annual variability of precipitation and temperature.

In 2014, precipitation and temperature variability for the whole Viet Nam and for climate sub-regions were described in the study of Nguyen et al. [126] for the period 1971 - 2010. The result showed that the country's average temperature had increased by 0.26±0.10^{o}C per decade since the 1970s, approximately twice the rate of global warming over the same period. It was shown the linkage between temperature and precipitation variability and El Niño Southern Oscillation at both the national and sub-regional level.

Ngo-Duc et al. [123] used an ensemble of three RCMs to project the climate in Vietnam for the future period 2000-2050 under the A1B scenario. The future temperature was projected to increase significantly and the highest temperature increment of ~0.5^{o}C decade^{-1} was pronounced in summer. The precipitation changes depended on regions and seasons and the most

significant change existed over the coastal plain of Central Vietnam, particularly in the winter monsoon season.

Phan-Van et al. [135] investigated the ability of seasonal climate predictions for Viet Nam using RegCM4.2. The study showed that without any bias correction, the RegCM4.2 forecast had very little or no skill in both tercile and value predictions. With bias correction, model predictions presented improved skill.

The Viet Nam Institute of Meteorology, Hydrology and Climate change (IMHEN) coordinated with the United Nations Development Program (UNDP) published the Viet Nam Special Report on Managing the Risks of Extreme Events and Disasters to Advance Climate Change Adaptation [75]. The report assessed extreme events and their impacts on the natural environment, socio-economic development and sustainable development of Viet Nam, which aimed to promote adaptation to climate change and management of risks of disaters and extreme events in Viet Nam.

In 2016, Ngo-Duc et al. [124] estimated extreme rainfall and temperature indices over the CORDEX-SEA region. In this study, 18 experiments were implemented using various combination of cumulus parameterization and ocean flux schemes. The results showed fairly high similarities among the experiments over mainland Asia compared to those over the Maritime Continent for both seasonal and inter-annual variability. It was also shown that as the MIT-Emanuel convective scheme was combined with the BATS1e ocean flux scheme, the best performance was produced.

Precipitation and tropical cyclone (TC) activity over Viet Nam were studied by Kieu-Thi et al. [87] using the non-hydrostatic RCM (NHRCM). They reported that the projected rainfall in Northwest and Central Viet Nam decreased from June to August, while it increased in Northeast and Central

Viet Nam from September to November in the near and far future. The projected TC quantity and activity area were underestimated in the first half of the TC season, but slightly overestimated in the second half as compared to the best trajectory.

Ngo-Thanh et al. [125] studied the difference between summer rainy season and summer monsoon season over the Central Highlands of Viet Nam. The result showed that there was a close linkage between the year-to-year variations of the onset dates and the rainfall amount within the summer rainy season and summer monsoon season and the preceding winter and spring sea surface temperature in the central-eastern and western Pacific.

In 2019, Trinh-Tuan et al. [162] applied the quantile mapping technique to bias correct the RegCM rainfall in Vietnam. They showed a rainfall decrease with a longer break and shorter consecutive rainfall events over the Northern and Central Vietnam during the wet seasons in the mid-future 2046-2065 under both the RCP4.5 and RCP8.5 scenarios.

In Viet Nam, one of the most comprehensive reference documents on climate change is the Climate Change and Sea Level Rise Scenarios for Viet Nam report [5]. It provides the useful information on climate projection and sea level rise, including detailed information on projection of temperature and rainfall changes in Viet Nam. Figure 1.13 and Figure 1.14 depicted the projected temperature change by the mid-century and the end of the 21st century under the RCP4.5 and RCP8.5 scenario. It showed the increasing tendency of temperature by the end of the century and the higher increment in the northern part compared to the southern one. Projected rainfall changes were shown in Figure 1.15 and Figure 1.16. The tendency of rainfall increment was clearer by the end of the century under both the RCP4.5 and RCP8.5 scenario. The highest rainfall increase was projected in the northern

Viet Nam, Hue, Hoi An, Da Nang and some parts in the southern Viet Nam (Figure 1.16b). This report also projected the changes of extreme rainfall and temperature, climate extremes (tropical depression and typhoon, monsoon, extreme and damaging cold, heat wave and drought) as well as the sea level rise for Viet Nam.

Besides, there have been other climate related studies of Vietnamese authors and institutions conducted or coordinated to conduct to now (e.g. [1], [7], [12], [84]).

1.3. Chapter 1 summary

Chapter 1 introduced the relevant concepts used in the thesis and the overview of literature on regional climate downscaling and climate analog in the world and in Viet Nam.

Although a great effort on conducting researches related to climate simulations and projections using RCMs has been made for the past years, the quantity of studies on these issues over the SEA region is still modest [16], [124], [134], [135].

Previous studies over the SEA region often focused on a particular event and/or using different RCMs, driving data or scenarios. The study of Ratna et al. (2017) [143] investigated the mean precipitation climatology over SEA, but not the mean temperature and the RCM model used was WRF. Extreme rainfall variables were projected over SEA in the study of Tangang et al. [155]. The report of Rahmat et al. [139] provided comprehensive climate evaluation and projection over SEA using PRECIS RCM under the A1B scenario with the driving data of 17-member PPE of HadCM3Q global model.

Through the above-mentioned relevant research in Viet Nam, it is found that there are still a limited number of studies on climate simulation and projection implemented by the Vietnamese authors. The research areas in the-

a) 2046-2065 b) 2080-2099

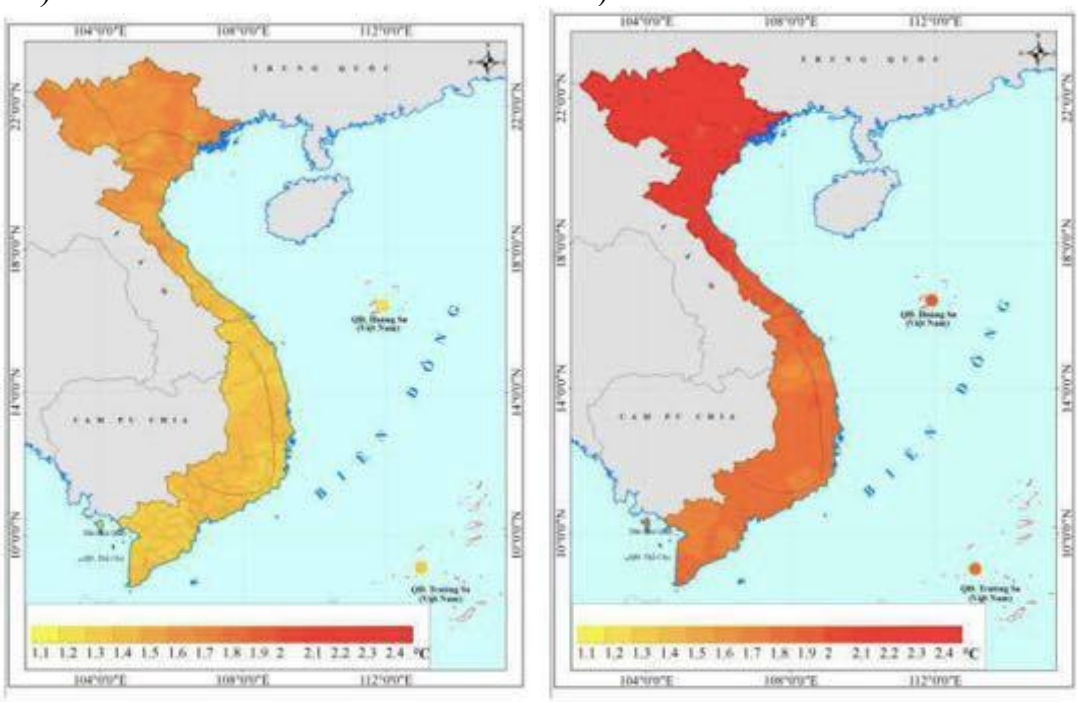

Source: [5]

Figure 1.13. Temperature change projection (deg. C) in Viet Nam under the RCP4.5 for a) the mid-century and b) the end of 21st century.

a) 2046-2065 b) 2080-2099

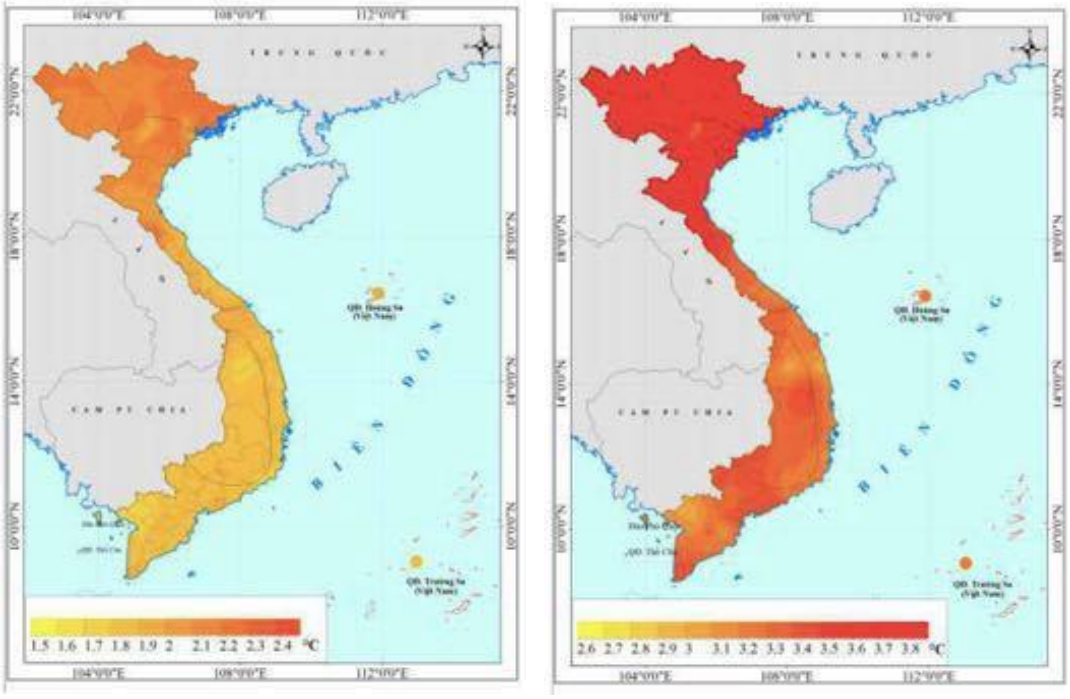

Source: [5]

Figure 1.14. As in **Figure 1.13** but under the RCP8.5.

a) 2046-2065 b) 2080-2099

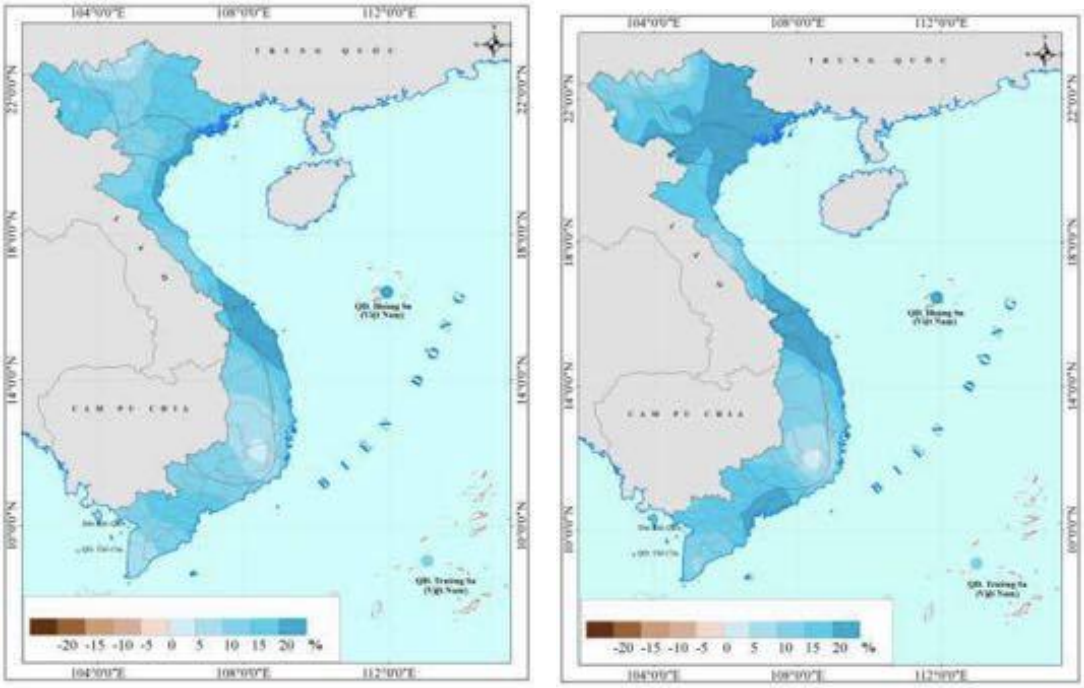

Source: [5]

Figure 1.15. As in **Figure 1.13** but for rainfall change projection (%).

a) 2046-2065 b) 2080-2099

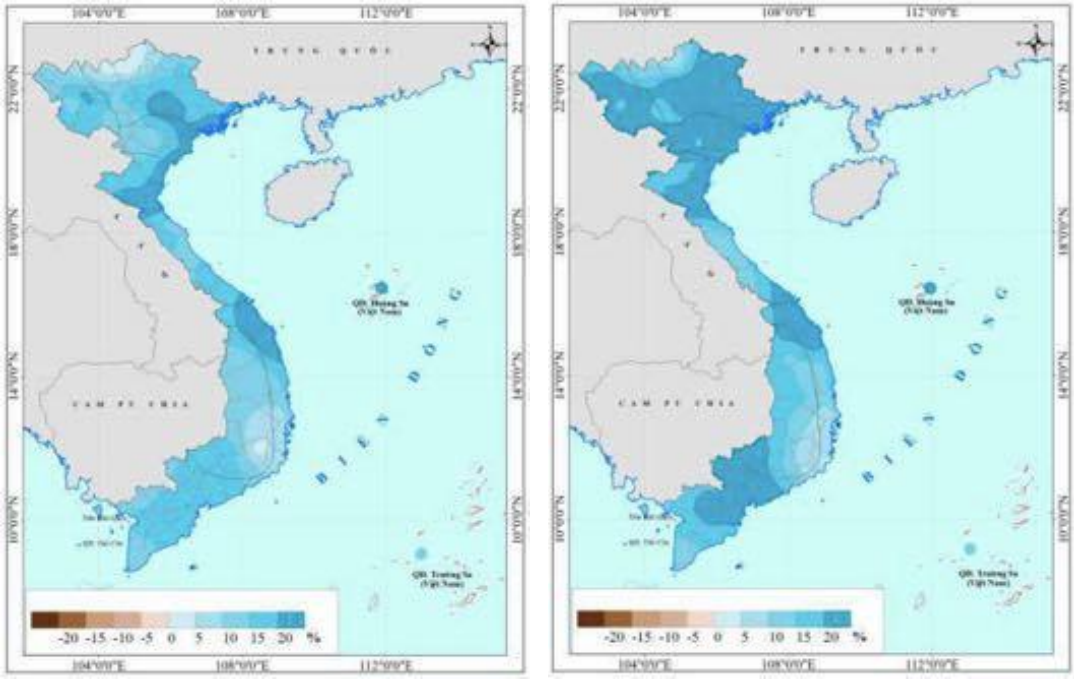

Source: [5]

Figure 1.16. As inin **Figure 1.15** but under the RCP8.5.

-ir studies used to include partly or the whole Viet Nam, except for the study of Ngo-Duc et al. [124] with the study area in the SEA region. However, this study only simulated extreme rainfall and temperature indices, not the 2 m air temperature (T2m) and precipitation (R) of SEA. The climate projection was not also conducted in this study. Trinh-Tuan et al. [162] projected the precipitation changes in Viet Nam by the mid-century (2046-2065) after applying quantile mapping bias-correction.

Thus, the climate evaluation and projection over SEA using RegCM4.3, driving data of 6 CMIP5 GCMs under RCP8.5 and RCP4.5 within the CORDEX-SEA project is quite distinctive from the past studies.

With regard to climate analog, previous studies revealed the tendency for climate analogs to be located in warmer regions. Hallegatte et al. [68] and Kopf et al. [90] used GCMs to determine the best analog locations to the projected climate of 17 and 12 cities in Europe, respectively, and showed the southward pattern of the analog locations from their original ones. Climate analogs for other regions of the world including cities in Japan [81], Australia [119], and Kenya [22], as well as the four cities of Tokyo, Seoul, Moscow and Washington [70] were also concluded to shift equatorward. The analog approach was employed to link climate change with different sectors such as economic hazards in urban areas [68], crop production [99] [136], agricultural impact projection and adaptation [22], species distribution and ecology [40] [171] [174]; and climate change adaptation planning [129] among others.

The studies showed that novel climate existed mostly in tropic and subtropic areas [174] [175]. Williams et al. [175] indicated that 4 - 20% of the global terrestrial surface might experience novel climates by 2100 for the low emission scenario B1 while the percentage for the high emission scenario A2 was 12 – 39%. Fabienne et al. [51] showed that about 15%, 21%, and more

than a third of the global land fraction were projected to experience novel climates at the 1.5°C, 2°C, and 4^{o}C global warming levels, respectively.

To date, future projections from GCMs were often used to study climate analogs at the global scale (e.g. [51], [175]), or at one specific location (e.g. [22], [129]), or in a country (e.g. [81], [119]). Outputs of RCMs could also be used with the advantage of higher spatial resolution to identify climate analogs [18].

As climate analog is linked with a sector, some limitations are shown. The study of Nyairo et al. (2014) [129] reported that the potential of application of the climate analog approach for adaptation planning seemed limited. Among the differences between the target and analog location, none could obviously be ascribed to climatic differences and thus recommended as adaptation strategies for the target site. Although several differences were indicated, they may have resulted from some non-climatic aspects, such as market access, cultural traditions or technological stimulation by government or other development agencies. The study also showed the doubt that in most agricultural structure, climate dissimilarities projected by climate models had a weaker influence on structure properties than dissimilarities resulted from several other factors. Another study also did not bode well for applying the analog method for impact projection and adaptation planning for future climatic conditions in agricultural contexts [22]. The study showed that the climate analog approach was only worthwhile if climate is a ruling element affecting differences between baseline and analog site pairs.

In addition to the studies concerning the linkage between climate analog and other sectors, there were studies on pure climate analog, which was not necessarily linked with any sectors (e.g. [51], [119]).

In spite of a large number of studies on climate analog implemented in

the world, there has been no specific study about climate analog or novel climate in SEA to date.

In order to fill in the above-mentioned research gaps, the thesis identifies the research aims of the thesis as follows: 1) To project temperature and rainfall and their changes over the SEA region; and 2) To study climate analog in SEA.

To achieve those research objectives, the thesis includes two main contents: 1) Performance of multi-model experiments in simulating temperature and precipitation in SEA; and 2) Temperature and rainfall change projection, and climate analog in SEA.

To implement the above-mentioned research contents, the main research methodologies used in the thesis include regional climate downscaling and climate distance formulation, which are thoroughly described in the next chapter.

CHAPTER 2 – OBSERVED DATA, NUMERICAL EXPERIMENTS AND METHODOLOGY

2.1. Data

2.1.1. Observation data

There are different kinds of data used in climate-related studies. They can be classified into the following types: in-situ observations, gridded observation data, model data (including reanalysis) and satellite data.

Two kinds of data are used in the thesis: observation data and model data.

In-situ observations are the observations/measurements obtained at the location of the instrument [46]. Many in-situ observations come from hydrological-meteorological station networks such as air temperature, atmospheric pressure, precipitation, wind speed and direction, humidity, cloud height, visibility, and river discharge. They can be used to better understand climate characteristics or/and to validate various satellite data and model data in climate researches.

In the thesis, daily observation data of rainfall and temperature (mean daily temperature, T2m) were obtained from 365 meteorological stations within the SEA region (Figure 2.1) for the period 1986 - 2005, including 118 stations in Thailand, 70 stations in Viet Nam, 32 stations in the Philippines, 33 stations in Malaysia, 88 stations in Indonesia, 23 stations in Myanmar and one station in Laos. The observation data provided by Vietnam, the Philippines, Indonesia, Malaysia and Thailand are within the SEACLID/CORDEX-SEA project. These observation data were quality checked by each of the five countries before sharing to the CORDEX-SEA members. Data from a part of Thai stations and one station in Laos are obtained from National Centers for Environmental Information (NCDC),

NOAA (ftp://ftp.ncdc.noaa.gov/pub/data). Data from the stations in Myanmar are downloaded from Myanmar Climate Data Portal (http://dmh-cdp.wowspace.org/team/homex.php). The stations in Myanmar are got from Myanmar Climate Data Portal (http://dmh-cdp.wowspace.org/team/homex.php). The detailed list of these stations with their names and coordinates in SEA is shown in Annex 1. Over the Philippines and Myanmar, as the observed T2m data could not be collected, the average of maximum daily temperature (Tx) and minimum daily temperature (Tn) was used to represent T2m instead. As there is only one station in Laos, analysis for Laos is not implemented in Chapter 3 and Chapter 4.

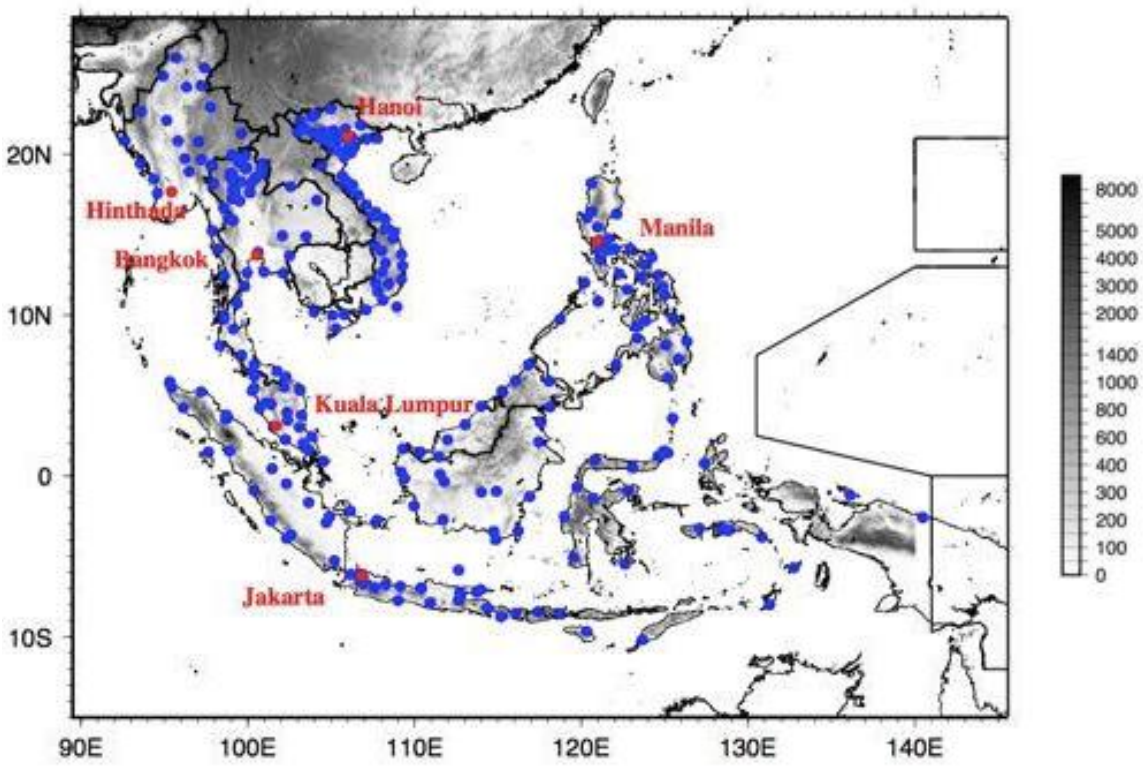

Figure 2.1. The SEA domain with 365 circles showing the station locations in Thailand, Viet Nam, Philippines, Malaysia, Indonesia, Myanmar and Laos where data are used for the analysis in this study. Topography over SEA (shaded, unit is in *m*) is obtained from the Global 30 Arc-Second Elevation (GTOPO30) data set.

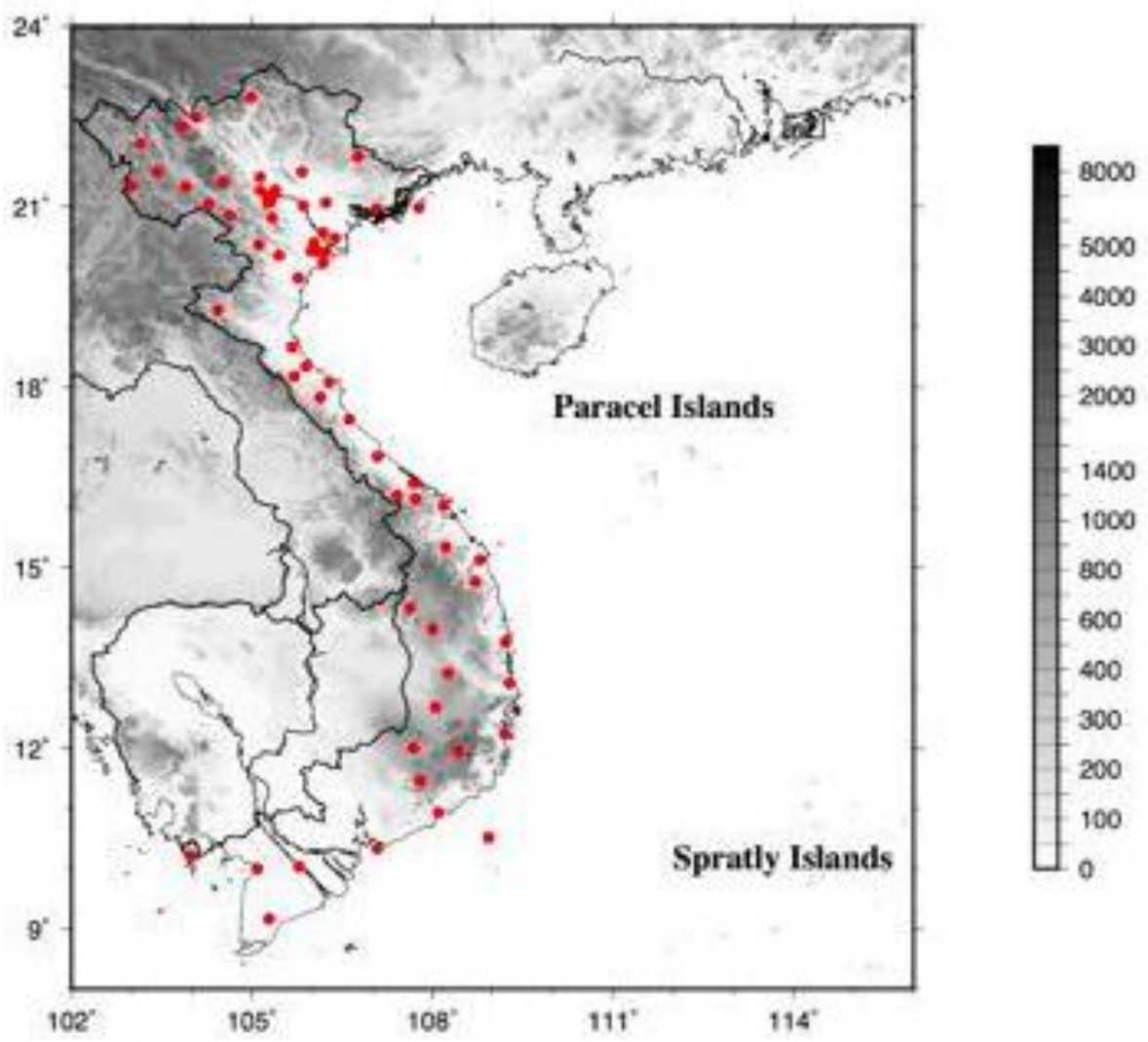

Figure 2.2. The Viet Nam domain with 66 circles showing the locations of the meteorological stations used in this study. Topography over Viet Nam is obtained from the Global 30 Arc-Second Elevation (GTOPO30) dataset (gray shading, in m)

Observed daily rainfall and 2-m temperature data for the period 1986 – 2005 from 66 meteorological stations over seven climatic sub-regions of Viet Nam were also used to evaluate the model performance in Viet Nam. It is noted that in the evaluation section in SEA, 70 stations were chosen while 66 stations were used in the evaluation in Vietnam. The remaining four stations locating in the islands were excluded in this section as the analysis was only

for the mainland of Vietnam. The period 1986 – 2005 was chosen, as this period was usually served as the reference one in the AR5 of the IPCC. The 66 stations belong to the meteorological station network of the Vietnam Meteorological and Hydrological Administration. Their data were quality-checked by using the 3-sigma and 5-sigma rules for identifying the outlier values of temperature and precipitation, respectively. Among the 66 stations, there are six stations located in Northwest (NW), 13 stations in Northeast (NE), 13 stations in RRD 11 stations in North Central (NC), nine stations in South Central (SC), seven stations in Central Highlands (CH) and seven stations in the Southern region of Viet Nam (SV) (Figure 2.2).

2.1.2. Numerical experiments

Temperature and precipitation data used in the thesis are obtained from the regional climate downscaling experiments of the SEACLID/CORDEX-SEA project and from the six respective driving GCMs of the Coupled Model Intercomparison Project Phase 5 (CMIP5). Under the framework of SEACLID/CORDEX-SEA, the Regional Climate Model version 4.3 (RegCM4.3) [63] was used to dynamically downscale a number of CMIP5 GCMs for the historical period and for the RCP8.5 and RCP4.5 [167]. Due to litmited computational resources, the two RCPs were selected. The one is the medium range emission scenario (RCP4.5) suggested by MONRE (2009) [3] while the other is the high range emission scenario (RCP8.5), which is applied for climate change adaptation and mitigation. The RegCM was developed and maintained in the Earth System Physics section of the Abdus Salam International Centre for Theoretical Physics (ICTP), Italy. The model is flexible, portable and can be applied to any region of the world and for a wide range of studies. As the IPCC GCMs have various skills in capturing climate in specific regions, not all GCMs could show good performances in t-

Table 2.1. Six driving GCMs and their short forms and abbreviations of the RCM experiments.

No.	Driving GCMs	Abbreviation for GCMs	Abbreviation for RCMs
1	Centre National de Recherches Météorologiques (CNRM-CM5)	G_CNRM	R_CNRM
2	Commonwealth Scientific and Industrial Research Organization Atmospheric Research Mark 36 (CSIRO-MK36)	G_CSIRO	R_CSIRO
3	Earth Consortium and its Earth system model (EC-EARTH)	G_ECEA	R_ECEA
4	Geophysical Fluid Dynamics Laboratory (GFDL-ESM2M)	G_GFDL	R_GFDL
5	Met Office Hadley Centre (HadGEM2)	G_HADG	R_HADG
6	Max Planck Institute for Meteorology (MPI-ESM-MR)	G_MPI	R_MPI

-he SEA region [149]. The selection of GCMs for the initial and boundary conditions for the CORDEX-SEA experiments is based on assessments on GCMs' simulation capability over SEA and their availability of formatted data. Thus, only eight GCMs were chosen within the CORDEX-SEA project. At the time when analysis in the thesis was done, only six downscaling products from six CMIP5 GCMs were available. Thus, six CMIP5 GCMs and their respective downscaling products using RegCM4.3 are used in the thesis. Both GCM and RCM data chosen to analyse in the thesis target facilitating general assessment and comparison between these two kinds of models' performance.

It is noteworthy to mention that the performance of five GCMs among

the six GCMs used in our studies was previously evaluated for the SEA region [85] [149]. The EC-EARTH model was not included because its data were not available at the time of these studies. Siew et al. [149] showed that the GCMs could simulate the relationship between the regional rainfall and circulation associated with El Niño–Southern Oscillation (ENSO). Katzfey et al. [85] ranked 24 available CMIP5 GCMs at the time of their study based on two criteria: 1) ability to simulate atmospheric variables such as precipitation, temperature, mean sea level pressure; and 2) ability to represent oceanic features such as ENSO. They showed that the five GCMs used in the present study were among the best models. In Chapter 3, the remaining EC-EARTH GCM is shown to rank first among the six GCMs for temperature and second for precipitation representations. These results ensure that the selection of the six GCMs in this study is appropriate.

The detailed names and short forms of these experiments and GCMs are shown in **Table 2.1**. The model output covers the SEA domain of 15S – 27N, 89.5E – 146.5E at 25 km grid resolution. The configuration of RegCM4.3 was determined in an earlier sensitivity experiment of CORDEX-SEA [32], [83], [124]. It was shown that the downscaled products could better represent climate mean and extreme features compare to the driving GCMs over the SEA domain [32], [83], [124], [155], [162].

The 20 – year baseline period is 1986 – 2005 and the future periods to be analyzed is 2046 – 2065 (mid-century) and 2080 – 2099 (far-century) under the RCP4.5 and RCP8.5 scenarios. The GCM outputs were bi-linearly interpolated to the RCM resolution of 25 km. Monthly data from the RCM and GCM experiments were averaged to create ensemble inputs, hereafter referred to as R_ENS and G_ENS experiments, respectively. Modeled data at observation stations are calculated by using values at the the grid points with

coordinates closest to the coordinates of the observation stations.

2.2. Methodology

2.2.1. Evaluation on performance of multi-model experiments

To evaluate performance of multi-model experiments, seasonal climatological cycles of temperature and precipitation over six cities in SEA (Bangkok, Ha Noi, Jakarta, Kuala Lumpur, Manila and Hinthada) simulated by GCMs and RCMs were compared to the observed data.

Another way to evaluate their performance was that data were averaged at each station for the reference period 1986 – 2005. Model data were then compared to observed data at each station.

Taylor diagram [158] was also used to compare the performance of the simulation experiments versus the observed data using climatological monthly time series of temperature or precipitation. Twelve values corresponding to twelve months averaged for the period 1986-2005 are merged in all stations in each country to make create climatological monthly time series of temperature or precipitation. The Taylor diagram indicates the correlation, *rstd,* and *rmsd* between model data and the observations. The observation is shown by the black point on the horizontal axis at unit distance from the origin. One experiment is considered to have a better performance than another if its symbol is closer to the observation point, i.e. its *rmsd* is smaller.

With the aim to define the best experiment, ranking scores of the experiments on their ability to represent observed temperature and precipitation based on the *rmsd* values were applied. In each country and for each variable (temperature or precipitation), the experiments were ranked with scores from 0 to 13, where the one with the smallest *rmsd* was given the

highest score of 13, and the experiment with the highest *rmsd* was given the lowest score of 0.

Besides, daily mean temperature and rainfall data obtained from the Asian Precipitation – Highly Resolved Observational Data Integration Towards Evaluation of the Water Resources (APHRODITE) project [176] at 0.25°x 0.25° resolution were also used in the thesis to evaluate the performance of models. These datasets were created mainly with data obtained from a rain-gauge-observation network in Asia. This project has been conducted by the Research Institute for Humanity and Nature (RIHN) and the Meteorological Research Institute of Japan Meterological Agency (MRI/JMA) since 2006.

In order to calculate simulated/model data at observation stations, the values of grid points having the closest coordinates to the coordinates of observation stations are used.

2.2.2. Projection on temperature and precipitation change

The RegCM4.3 was used to downscale projected data from the CMIP5 GCMs. Thus, RCM projected temperature and precipitation originated from CMIP5 GCMs under two GHG scenarios, i.e. RCP4.5 and RCP8.5.

In the thesis, the absolute change of projected T2m (Δ_{T2m}) and the relative change of R (Δ_{R}) are defined as following:

$$\Delta_{\mathrm{T2m}} = \mathrm{T2m}_{\mathrm{future}} - \mathrm{T2m}_{\mathrm{baseline}} \quad \text{(deg. C)} \quad \text{(Eq. 2.1)}$$

$$\Delta_{\mathrm{R}} = \frac{\mathrm{R}_{\mathrm{future}} - \mathrm{R}_{\mathrm{baseline}}}{\mathrm{R}_{\mathrm{baseline}}} \times 100 \quad (\%) \quad \text{(Eq. 2.2)}$$

The baseline period used in the study is the 20-year period 1986-2005.

Another way to project climate change was that longitudinally averaged temperature/precipitation and temperature/precipitation changes for each

latitude in the SEA region in the mid- and far- future periods under the two scenarios were implemented.

2.2.3. Significance test

In order to determine if there is a significant difference between two independent sample means which are future projected data and baseline data, a t-test is applied. The general test statistic is a function of a comparison of the two sample means, and the real observed difference will be usually some number (not zero). The null hypothesis is often that the actual difference is zero. The alternative hypothesis is that: (1) the true difference is not zero, or (2) one of the two means is bigger than the other [33].

In the t-test, *t- score* is used, which is a ratio between the difference between two groups (projected data and baseline data) and the difference within the groups. A large *t-score* means that the groups are different while a small *t-score* shows that the groups are similar.

The two datasets used in the thesis (future projected data and baseline data) are two independent samples. Thus, the formula to identify *t-score* for independent samples is as following:

$$\boldsymbol{t-score} = \frac{\bar{x}_f - \bar{x}_p}{\sqrt{\left[\frac{(n_f-1)s_f^2+(n_p-1)s_p^2}{n_f+n_p-2}\right]\cdot\left[\frac{1}{n_f}+\frac{1}{n_p}\right]}} \qquad \text{(Eq. 2.3)}$$

in which,

$\bar{x}_f$: Mean of future projected dataset.

$\bar{x}_p$: Mean of baseline/present dataset.

F: future projected data values.

P: baseline data values.

s_f^2: variance of future projected dataset.

s_p^2: variance of baseline dataset.

n_f: number of projected years.

n_p: number of baseline years

Every *t-value* (value of *t-score*) accompanies with a *p-value*, which is the probability that the results from the two datasets occurred by chance. In the thesis, the *p-value* of 5% is applied, which means that only 5% probability that the results from the two datasets happened by chance.

One more factor used in t-test is the degree of freedom (*df*), which is the number of independent data items that are used to define *t-value*. It is not totally the same as the number of items in the sample. The *df* is equal to the number of items subtracted 1. In the thesis, the number of data items for the baseline period is 20 (20 years for the period 1986-2005) and that for the future period is 20 (20 years for the period 2046-2065 or 2080-2099). Thus, the *df* (denominator of Eq. 2.3) used in the thesis is (20 + 20 – 2) = 38. Based on the *df* = 38, *p-value* = 5%, the *t-value* is defined to be 2.024. The *t-score* calculated based on E.q. 2.3 is then compared to that *t-value*. If the *t-score* is greater than the *t-value* with the *p-value* 5%, it is concluded that there is difference between means of future and baseline data. These grid points satisfying the difference at 5% significance level under the *t-test* are calculated to define the percentage with significant differences in the SEA region in Section 4.1.

2.2.4. Climate distance formulation

Climate analog is used to define locations at which their present climate is similar to the projected future climate of a reference site [107]. A climate analog is often defined by climate distance estimated by various methods with different climate variables. Most studies on climate analog were based on the daily [100], [129] or monthly [22], [68], [90] temperature and precipitation.

However in regions with clear seasonality, seasonal variables were also used to define climate distance [51], [119], [175]. In near – equatorial areas, the seasonal cycle is less clear (e.g. Kuala Lumpur in Figure 3.1); thus the use of monthly data, which contains more information than seasonal means, better depicts the climatology of a location.

For each numerical experiment, the dissimilarity (*dis*) between the future climate variable at a reference grid point *f* and the present condition at any grid point *p* in the research area is calculated as follows:

$$\mathbf{A_{dis}} = \frac{\mathbf{1}}{\mathbf{12}} \sum_{\mathbf{n=1}}^{\mathbf{n=12}} \sqrt{\frac{(\mathbf{A_{f,n}} - \mathbf{A_{p,n}})^{\mathbf{2}}}{\boldsymbol{\sigma}_{\mathbf{f,n}}{}^{\mathbf{2}} + \boldsymbol{\sigma}_{\mathbf{p,n}}{}^{\mathbf{2}}}} \qquad \text{(Eq. 2.4)}$$

where A is the 20-year monthly mean temperature (T_{dis}) or precipitation (P_{dis}) for month n (from January to December), and σ is the internal variability derived from the standard deviation of the monthly values within the 20-year present or future period. Fabienne et al. (2017) [51] also used a similar formula but for the four seasons of the year.

Outputs from the GCMs and RCMs are used to compute Eq. 2.4. It should be noted that no bias adjustment has been applied to the products of the GCMs and RCMs in this study. If there is any mean systematic biases in the models, these could be somehow canceled out via the formulation (i.e. via the term $(A_f - A_p)^2$ in Eq. 2.4). However, the biases in variability are not corrected via Eq. 2.4; thus, they could always exist and should be considered in future studies.

One can note that this study investigates the changes in mean temperature and precipitation under the two RCP scenarios according to Eq. 2.4. The changes in climate variability are not considered in terms of climate analog. As the internal climate variability occurs in the denominator of Eq.

2.4, the dissimilarity A_{dis} would consequently decrease with the increase in climate variability. Hence, it is possible that the climate variabilities between two locations are different from each other but a similar climate between them is detected due to their small dissimilarity. Eq. 2.4 is thus a measure of the dissimilarity in the mean climate rather than in the climate variabilities.

For each reference grid point, assuming that there are k land grid points in the research area, k values of T_{dis} or P_{dis} are computed based on Eq. 2.4. Those k values of T_{dis} or P_{dis} are averaged again to define the means of T_{dis} and P_{dis} for each reference grid point. This calculating process is repeated for all k reference grid points, producing k mean values of T_{dis} or P_{dis}. The k mean values are averaged again to obtain the mean T_{dis} or P_{dis} for the whole research area.

Table 2 shows that the mean $\boldsymbol{T_{dis}}$ is 3.5 to 4.9 times higher than the mean $\boldsymbol{P_{dis}}$, depending on the RCM experiments and scenarios. The similar ratio for the GCM experiments varies from 2.5 to 4.2. The full table of all mean $\boldsymbol{T_{dis}}$ and $\boldsymbol{P_{dis}}$ for both the scenarios, RCMs and GCMs and two periods (2046-2065, 2080-2099) is shown in Annex 2. $\boldsymbol{\alpha}$ is defined to be the ratio between mean T_{dis} and mean P_{dis}:

$$\alpha = \frac{\overline{T_{dis}}}{\overline{P_{dis}}} \qquad \text{(Eq. 2.5)}$$

As the mean $\boldsymbol{T_{dis}}$ is always much higher than mean $\boldsymbol{P_{dis}}$, so $\boldsymbol{\alpha}$ is defined as the weighting factor between temperature dissimilarities and precipitation dissimilarities to balance between these two means.

Based on Table 2, the mean dissimilarities estimated with ENS are significantly higher than those estimated with the six RCM experiments, which can be explained by the smaller variances obtained with the temperature and precipitation values of ENS. If x_{ij} indicates a variable x at a

time step *j* of a model *i*, σ_i^2 is the variance of that variable for the model *i* with *n* is the number of time steps (*n* = 12 in this study). The ensemble mean a_j for the time step *j* of *m* model experiments (*m*=6 in this study) as well as the mean ($\bar{a}$) and variance (σ_a^2) of the ensemble can be written as:

$$\mathbf{a_j} = \frac{\mathbf{1}}{\mathbf{m}} \sum_{\mathbf{i=1}}^{\mathbf{m}} \mathbf{x_{ij}} \qquad \text{(Eq. 2.6)}$$

$$\bar{\mathbf{a}} = \frac{\mathbf{1}}{\mathbf{n}} \sum_{\mathbf{j=1}}^{\mathbf{n}} \mathbf{a_j} \qquad \text{(Eq. 2. 7)}$$

$$\boldsymbol{\sigma}_{\mathbf{a}}^{\mathbf{2}} = \frac{\mathbf{1}}{\mathbf{n}} \sum_{\mathbf{j=1}}^{\mathbf{n}} (\mathbf{a_j} - \bar{\mathbf{a}})^{\mathbf{2}} \qquad \text{(Eq. 2. 8)}$$

In a perfect condition where all ensemble members produce the same value series, $\boldsymbol{\sigma_a^2} = \frac{\mathbf{1}}{\boldsymbol{m}} \sum_{\boldsymbol{i=1}}^{\boldsymbol{m}} \boldsymbol{\sigma_i^2}$. In general, $\boldsymbol{\sigma_a^2}$ is smaller than $\frac{\mathbf{1}}{\boldsymbol{m}} \sum_{\boldsymbol{i=1}}^{\boldsymbol{m}} \boldsymbol{\sigma_i^2}$, leading to larger ENS dissimilarities as shown in Table 2.2. Thus, a multiplicative factor $\boldsymbol{\beta}$, which is the ratio between the mean $\boldsymbol{T_{dis}}$ of the ENS experiment ($\overline{\boldsymbol{T_{dis,ENS}}}$) and the average values of the mean $\boldsymbol{T_{dis}}$ of the six RCM experiments ($\overline{\boldsymbol{T_{dis,\iota}}}$), is defined as follows:

$$\beta = \frac{\overline{T_{dis,ENS}}}{\frac{1}{m}\sum_{i=1}^{m} \overline{T_{dis,\iota}}} \qquad \text{(Eq. 2.9)}$$

Therefore, $\boldsymbol{\beta}$ takes a role of weighting factor between $\overline{T_{dis,ENS}}$ and the average values of the mean T_{dis} of the six RCM experiments ($\overline{T_{dis,\iota}}$) due to the much higher values of $\overline{T_{dis,ENS}}$ compared to the mean $\boldsymbol{T_{dis}}$ value of each model.

From Table 2.2, $\beta = 2.0$ under the RCP4.5 for both R_ENS and G_ENS. Under the RCP8.5, $\beta = 1.8\ and\ 1.9$ for R_ENS and G_ENS, respectively (see Annex 2).

Next, we define a temperature climate distance (*ClimD_T)* and a precipitation climate distance (*ClimD_P*) between a reference grid point *f* (for

Table 2.2. Mean dissimilarities of temperature (T_{dis}) and precipitation (P_{dis}) over all reference grid points computed with six GCMs and six RCMs and their ensemble (ENS) values for the RCP4.5 and the RCP8.5.

Model	RCP4.5						Model	RCP8.5					
	RCM			GCM				RCM			GCM		
	Mean T_{dis}	Mean P_{dis}	α	Mean T_{dis}	Mean P_{dis}	α		Mean T_{dis}	Mean P_{dis}	α	Mean T_{dis}	Mean P_{dis}	α
CNRM	5.4	1.4	**3.9**	4.2	1.1	**3.8**	CNRM	5.9	1.4	**4.2**	4.8	1.1	**4.2**
CSIRO	6.1	1.4	**4.2**	4.6	1.5	**3.1**	CSIRO	6.4	1.4	**4.6**	5.3	1.5	**3.6**
ECEA	6.1	1.5	**4.1**	4.5	1.5	**2.9**	ECEA	6.1	1.4	**4.3**	5.2	1.4	**3.6**
GFDL	4.3	1.2	**3.5**	2.8	1.1	**2.5**	GFDL	4.7	1.3	**3.6**	3.7	1.2	**3.1**
HADG	6.7	1.5	**4.3**	5.1	1.8	**2.9**	HADG	7.7	1.6	**4.9**	6.3	1.7	**3.8**
MPI	5.0	1.3	**3.7**	3.2	1.2	**2.7**	MPI	5.4	1.4	**4.0**	4.0	1.2	**3.4**
ENS	11.2	2.9	**3.8**	8.1	2.7	**3.0**	**ENS**	11.0	2.9	**3.8**	9.1	2.8	**3.3**

future climate) and a grid point *p* (for present climate), taking into account both temperature and precipitation dissimilarities estimated in Eq. 2.4 as follows:

For each RCM or GCM:

$$\mathbf{ClimD\_T} = \mathbf{T_{dis}} \qquad \text{(Eq. 2.10)}$$

$$\mathbf{ClimD\_P} = \boldsymbol{\alpha} \times \mathbf{P_{dis}} \qquad \text{(Eq. 2. 11)}$$

As we defined $\boldsymbol{\beta}$ for the relationship between the ensemble experiment and six experiments, the formulation for the ENS experiment was defined as following:

$$\mathbf{ClimD\_T} = \frac{\mathbf{1}}{\boldsymbol{\beta}} \times \mathbf{T_{dis}} \qquad \text{(Eq. 2.12)}$$

$$\mathbf{ClimD\_P} = \frac{\mathbf{1}}{\boldsymbol{\beta}} \times \boldsymbol{\alpha}_{\mathbf{ENS}} \times \mathbf{P_{dis}} \qquad \text{(Eq. 2.13)}$$

where α is the ratio between the mean T_{dis} and P_{dis} for each experiment, shown in Table 2.2; β is the multiplicative factor defined above. In previous studies [22], [100], [129], more emphasis (generally a double weight) was placed on precipitation than on temperature in their climate distance formula,

but the choice was arbitrary.

The climate distance (*ClimD*) between the reference grid point *f* and the grid point *p* is given by:

$$\mathbf{ClimD} = \frac{\mathbf{1}}{\mathbf{2}} \times (\mathbf{ClimD\_T} + \mathbf{ClimD\_P}) \qquad \text{(Eq. 2.14)}$$

Best analog criteria

The best analog location of the reference point *f* is the point at which *ClimD* is the minimum. Based on this, we identify the best analog locations of six cities in SEA including Bangkok, Ha Noi, Jakarta, Kuala Lumpur, Manila and Hinthada and of 78 cities in Viet Nam which is further discussed in Section 4.2 and Section 4.4, respectively.

Criteria for good-analog, poor-analog and novel climate

Unlike in Figure 4.6 where six reference points are identified to define their best analog locations (i.e. one grid point with the minimum *ClimD*), in Figure 4.9 - Figure 4.11 the dissimilarity between the future period at a reference point and the present period of all grid points in the SEA domain is computed, and repeated for all other grid points as reference points in the SEA domain. For each reference point, three grid points with the minimum $ClimD$ are marked out as the best analogs (hereinafter *TP-analogs*) to address the issue of good, poor or no-analog for a specific reference point *f*. These three best *TP-analogs* are averaged to identify a standard value S_{TP} for the point *f*. The choice of three best analogs makes the analysis robust and less susceptible to that of one particular grid point [51]. Similarly, we also define S_T (S_P) from the averaging of three grid points with minimum *ClimD_T* (*ClimD_P*), respectively.

In the thesis, a reference point *f* is subjectively considered to have a good analog, poor analog, or no-analog if $S_{TP} \leq 1$, $1 < S_{TP} \leq 2$, or $S_{TP} > 2$, respectively. The threshold value of 2 for detecting no-analog matched up

with 95% confidence interval if only temperature for a single month, an analog point and a climate model are considered. $S_{TP} \leq 1$ indicates that the present climate of the best analog points well fits the future projected climate of the reference point; thus the future climate of the reference point can be found somewhere today. On the other hand, $S_{TP} > 2$ means that there is no location at which the present climate is similar to that of the reference point in the future, i.e. the reference point is considered to face a novel climate in the projected future. For the poor analog case (i.e. $1 < S_{TP} \leq 2$), the future projected climate of the reference point is somehow similar to the present climate of the poor analog point, but with a lower similarity level compared to the case of good analog. It should be noted that Fabienne et al. [51] subjectively used threshold values of 2 and 4 for detecting good-analog and no-analog, respectively, in their seasonal climate distance formula. Mahony et al. [104] also subjectively used a threshold of 2 with their climate distance for a moderate degree of novelty. Similarly, a reference point is considered to have a T-good analog, T-poor analog, or T-novel climate (P-good analog, P-poor analog, or P-novel climate) if $S_T \leq 1$, $1 < S_T \leq 2$, or $S_T > 2$ ($S_P \leq 1$, $1 < S_P \leq 2$, or $S_P > 2$), respectively.

When the present climate of a target grid point is not able to find the similar future climate in any grid point, it is defined as disappearing climate [51]. Thus, the formulation of calculating disappearing climate is the dissimilarity between the present climate variable at a target grid point and the future one at any grid point in the research area. The threshold to define disappearing climate is similar to that of novel climate, i.e. the S_{TP}, S_T, or $S_P > 2$.

To calculate percentage of climate analog types, area of each grid square defined to be what type was summed up, then this sum was divided by

the total area of SEA (excluding sea area).

Mean climate change versus variability

To examine whether the mean state change or the variance change contributes more to the change in dissimilarity for novel climate areas, based on Eq.2.4, we compute the average square of mean state change of temperature or precipitation (hereinafter called A_m) and their variabilities (hereinafter called A_v) for the novel areas and for the whole SEA domain. A_m and A_v for the novel areas are computed as follows:

$$A_{m,novel} = \frac{1}{N_{novel}} \sum_{\forall f \in G_{novel}} \frac{1}{3} \sum_{p \in G_{3f}} \frac{1}{12} \sum_{n=1}^{12} (A_{f,n} - A_{p,n})^2 \quad \text{(Eq. 2.15)}$$

$$A_{v,novel} = \frac{1}{N_{novel}} \sum_{\forall f \in G_{novel}} \frac{1}{3} \sum_{p \in G_{3f}} \frac{1}{12} \sum_{n=1}^{12} ({\sigma_{f,n}}^2 + {\sigma_{p,n}}^2) \quad \text{(Eq. 2.16)}$$

where $A_f, A_p, \sigma_f, \sigma_p$ and n were already defined in Eq.1. G_{novel} includes all the land grid points defined as novel climate. The size of G_{novel}, i.e. the number of novel grid points, is N_{novel}. G_{3f} includes the 3 best *TP-analog* points for each reference point *f*.

Similarly, we compute A_m and A_v for the whole SEA region:

$$A_{m,SEA} = \frac{1}{N_{SEA}} \sum_{\forall f \in G_{SEA}} \frac{1}{3} \sum_{p \in G_{3f}} \frac{1}{12} \sum_{n=1}^{12} (A_{f,n} - A_{p,n})^2 \quad \text{(Eq. 2.17)}$$

$$A_{v,SEA} = \frac{1}{N_{SEA}} \sum_{\forall f \in G_{SEA}} \frac{1}{3} \sum_{p \in G_{3f}} \frac{1}{12} \sum_{n=1}^{12} ({\sigma_{f,n}}^2 + {\sigma_{p,n}}^2) \quad \text{(Eq. 2.18)}$$

where G_{SEA} includes all the land grid points (N_{SEA} points) in the SEA region.

The ratios $A_{m,novel}/A_{m,SEA}$ and $A_{v,novel}/A_{v,SEA}$ are then computed. Those quantities will be used later to better investigate the contribution of the mean state change and the change in variability to the climate distance. It should be noted that since extreme information is not used for estimating the

dissimilarity, the change in extreme values is not considered in the present study.

2.3. Chapter 2 summary

Chapter 2 introduced the data used in the thesis, including the observation data and model data resulted from six regional climate models of the SEACLID/CORDEX-SEA project in SEA. The thesis used the RegCM4.3 to downscale six CMIP5 GCMs. The model and observation data were then processed by the tools such as climate data operators (CDO), NetCDF Operators (NCO), Generic Mapping Tools (GMT), Ferret, and Fortran 90 to calculate, analyze and visualize the results.

The formula of climate distance/ dissimilarity was formulated to define climate analog, good analog, poor analog, novel climate and disappearing climate in SEA and Viet Nam. This formula was based on the 20-year monthly mean T2m and R for the period 1986-2005 and 2080-2099 under the RCP4.5 and RCP8.5. The weighting factors α were applied for the variable R, which depended on the experiment, the scenario and the regional or global climate model. The multiplicative factor β was also used to rationalize the difference between the variance of ENS and those of individual experiments.

CHAPTER 3 – PERFORMANCE OF MULTI-MODEL EXPERIMENTS IN SOUTHEAST ASIA

This chapter investigates the performance of the six regional climate downscaling experiments, 6 GCMs and their ensemble average (ENS) in simulating rainfall and temperature for the reference period 1986 – 2005 over SEA and seven climatic sub-regions in Viet Nam. The best experiments were then chosen to project climate change in the Chapter 4.

3.1. Performance of downscaling experiments in SEA

Before using the outputs of the numerical experiments for projecting changes of temperature and rainfall and implementing climate analog and novel climate analysis, it is crucial to examine their performance in representing the climate over the SEA domain. Figure 3.1 and Figure 3.2 display the seasonal climatological cycles of temperature and precipitation over six cities in SEA: Bangkok, Ha Noi, Jakarta, Kuala Lumpur, Manila and Hinthada. T2m has a relatively strong seasonal cycle over Ha Noi, followed by Bangkok, Hinthada and Manila. Over Kuala Lumpur and Jakarta, which are near the equator, there is a small difference of less than 1.5ºC in temperature between the hottest and the coldest months. Generally, both GCMs and RCMs well represent the seasonal cycles of temperature in the six cities. There is a systematic cold bias for almost all RCM experiments over the cities, particularly over Bangkok and Hinthada. The well-known cold bias characteristics of the RegCM experiments were found and discussed in previous studies [32], [74], [130], which showed that the degree of cold biases was much dependent on the choice of physical parameterization schemes. The GCM outputs also have a cold bias tendency over the cities, except for Ha Noi, Hinthada and Kuala Lumpur in springtime.

Although there is a large variability among the experiments (Figure 3.2), the GCM and RCM outputs can somehow capture the rainfall seasonal variations. Both GCMs and RCMs can represent the summer monsoon rainfall characteristics over Bangkok, Ha Noi, Hinthada and Manila. The winter monsoon rainfall peaks over Jakarta and Kuala Lumpur are also captured by the models. Although the general rainfall cycles can be simulated, the absolute values of monthly rainfall vary significantly among the experiments. Some experiments can reasonably represent the seasonal cycle but their absolute biases compared to the observation are larger than those of some other experiments (e.g. R_GFDL over Kuala Lumpur). This assessment on the seasonal climatological cycles of temperature and precipitation over six cities in SEA represents neither the results of six nations nor the whole SEA region.

In the Indochina peninsular, Hanoi is strongly influenced by winter monsoon while Bangkok and Hinthada are greatly affected by summer monsoon and tropical monsoon, respectively. Manila locates in the Phillipine archipelago in the northern hemisphere while Jakarta is in about 6^{o}S in the southern hemisphere. Kuala Lumpur is about 3^{o}N distant from the equator. Mechanism of precipitation and temperature in various regions are relatively distinctive, which leads to different simulation capabilities of models in various regions ([32], [82], [124]). This explains various biases of models in simulating temperature and precipitation in these cities in Figure 3.1 and Figure 3.2.

In order to have a more robust assessment over the entire SEA domain, Figure 3.3 and **Figure 3.4** show the Taylor diagram [157], which indicates the performance of the simulation experiments versus the observed data. Each symbol corresponds to the quality of one experiment in representing

climatological monthly time series of temperature or precipitation over the stations in consideration (i.e. 118 stations in Thailand, 70 stations in Viet Nam, 32 stations in the Philippines, 33 stations in Malaysia and 88 stations in Indonesia, 23 stations in Myanmar). The Taylor diagram indicates the correlation, the ratio of the standard deviation (*rstd*), and the centered root mean square difference (*rmsd*) between model data and the observations. The observation is shown by the black point on the horizontal axis at unit distance from the origin. One experiment is considered to have a better performance than another if its symbol is closer to the observation point, i.e. its *rmsd* is smaller.

The RCM experiments show a remarkably better performance compared to the GCMs in representing temperature over Indonesia, Malaysia, the Philippines and Myanmar (Figure 3.3). Better correlations and *rmsd* for RCMs are also observed over Viet Nam and for the whole SEA, except for Thailand, where the GCMs slightly have better correlations compared to the RCMs. Generally, the RCM outputs have larger temperature variability (i.e. *rstd* >1) compared to the observations, except for the stations in Malaysia.

The better performance of the RCM experiments in simulating temperature compared to the GCMs' results is not observed for precipitation. The correlations are generally low (less than 0.5) for both RCMs and GCMs except higher correlations up to ~0.7 can be found over Viet Nam. GCM precipitation tends to have a lower variability compared to the observation, while RCM precipitation has a much larger variability except for certain experiments over Viet Nam (Figure 3.4). The low variability in the GCMs could be attributed to their coarse resolutions that smooth out the signal, while the large variability in the RCMs could be associated with the choice of the cumulus scheme ([32], [83], [124]). This assessment method can represent the result of the whole SEA due to the relatively wide coverage of 364 stations in

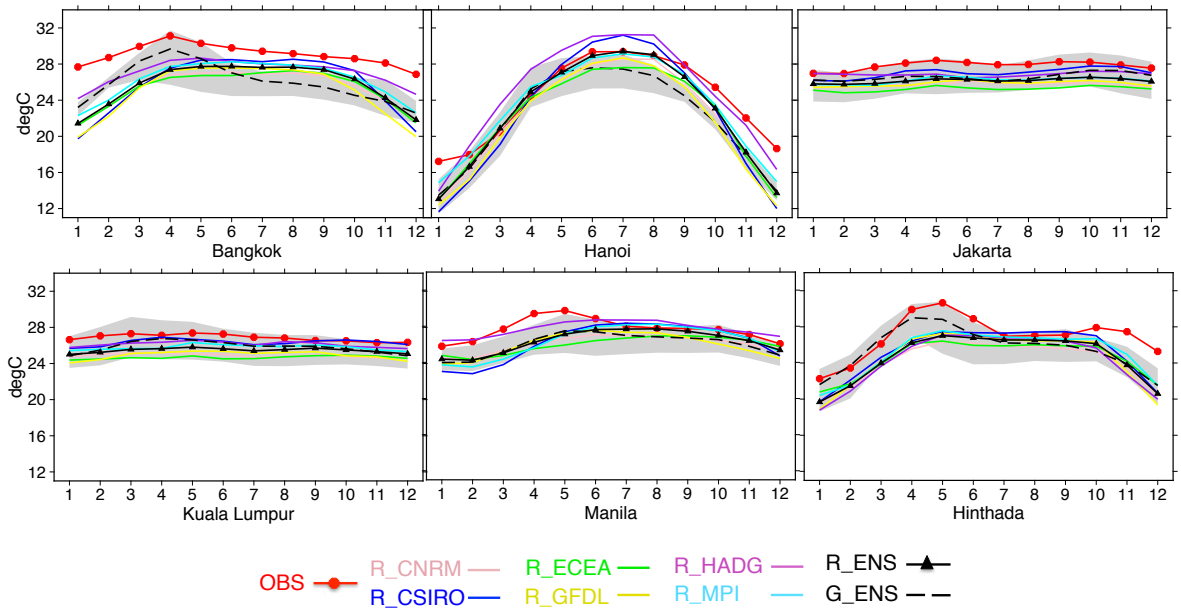

Figure 3.1. Seasonal climatological cycles of T2m at six stations located in six cities in SEA for the baseline period (1986 – 2005). Observation (red octagol symboled lines) and the RCM outputs are denoted by colored lines. The range of the GCM outputs is shaded in light gray. RCM and GCM ensemble experiments are shown by the solid triangle-symboled black (R_ENS) and dashed – black (G_ENS) lines, respectively.

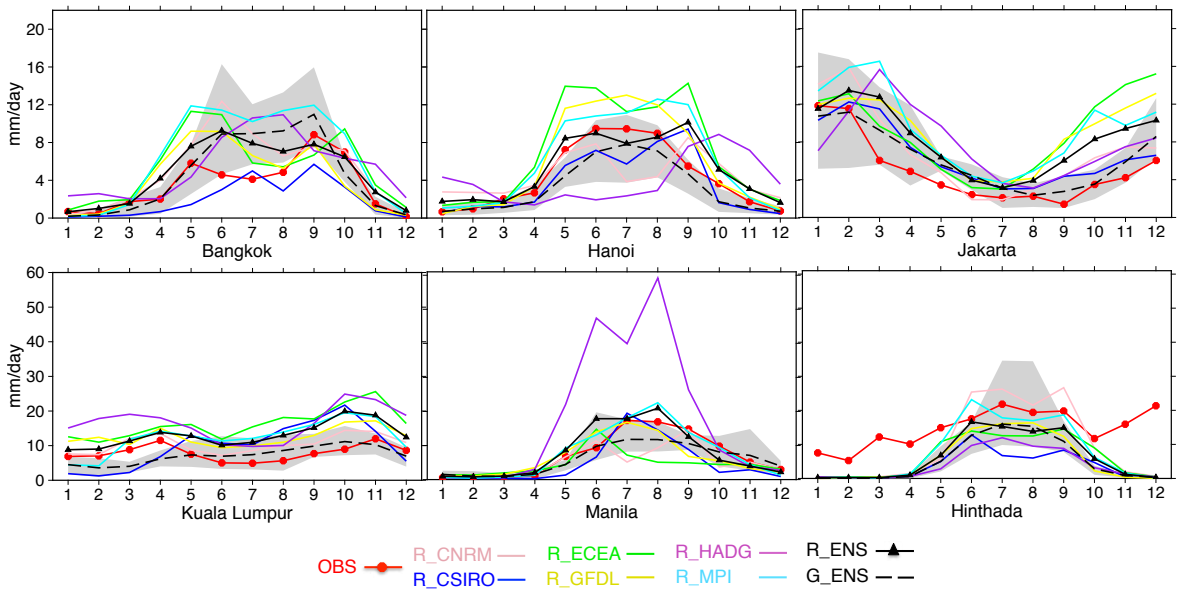

Figure 3.2. Similar as **Figure 3.1** but for precipitation.

six countries.

Figure 3.5 shows the ranking scores of the experiments on their ability to represent observed temperature (Figure 3.5a) and precipitation (Figure 3.5b) based on the *rmsd* values. In each country and for each variable, the experiments were ranked with scores from 0 to 13, where the one with the smallest *rmsd* was given the highest score of 13, and the experiment with the highest *rmsd* was given the lowest score of 0. For temperature, the RCM experiments generally had higher rank than the GCMs, especially for Viet Nam, the Philippines, Myanmar and Malaysia. Among the RCM experiments, the ensemble R_ENS gave the highest-ranking result with the highest score (59). Among the GCM experiments, the ensemble G_ENS with the score 43 -

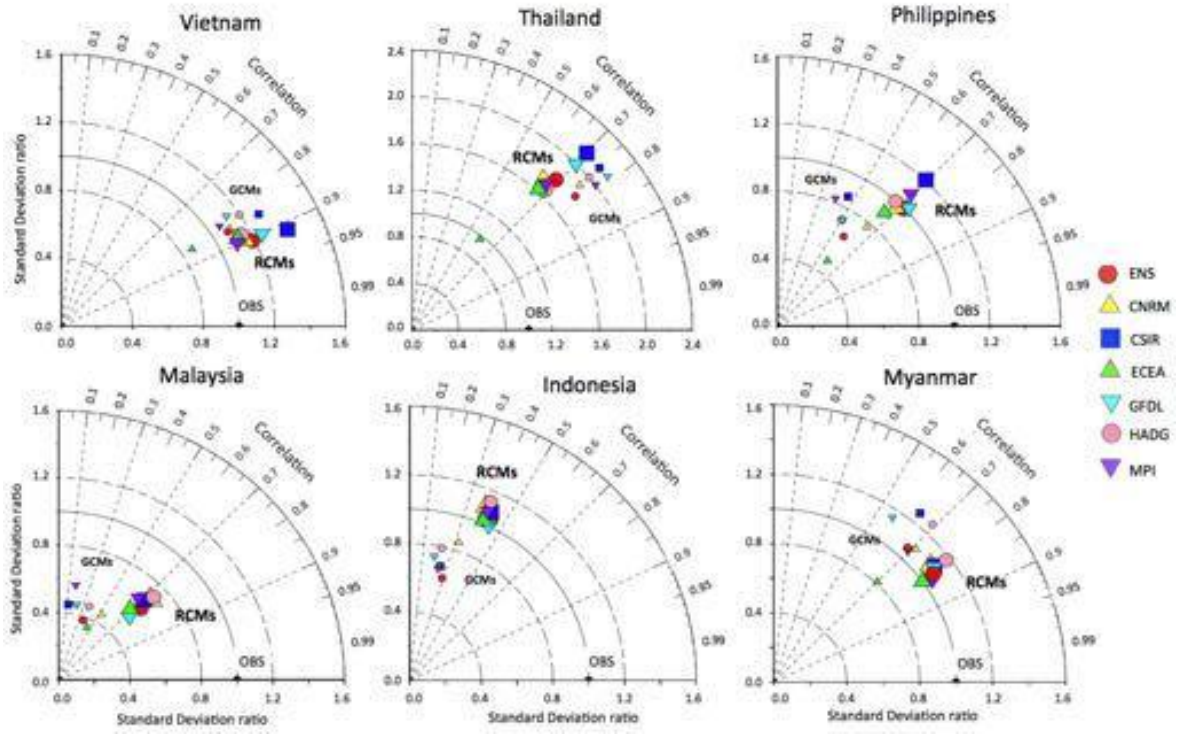

Figure 3.3. Taylor diagram for 1986 – 2005 climatological monthly time series of temperature over the stations of Indonesia, Malaysia, Philippines, Thailand, Viet Nam and Myanmar. Bigger symbols are used for RCMs while smaller ones denote GCMs.

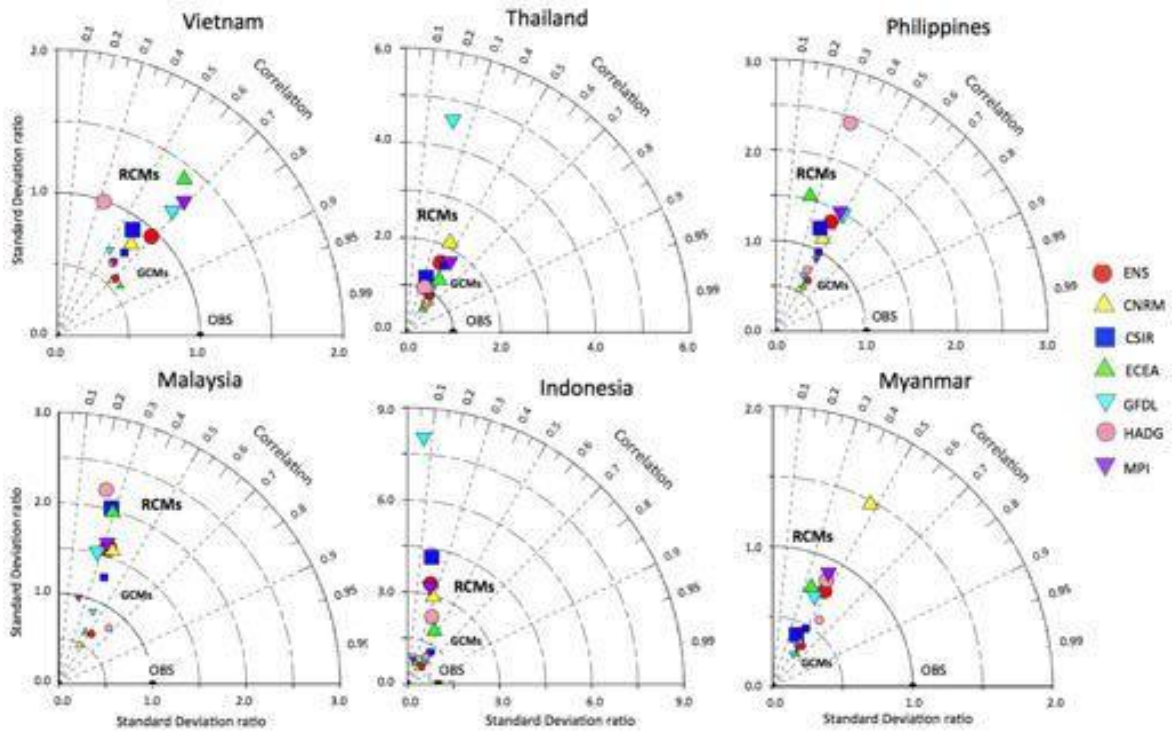

Figure 3.4. Taylor diagram for 1986 – 2005 climatological monthly time series of precipitation over the stations of Indonesia, Malaysia, Philippines, Thailand, Viet Nam and Myanmar. Bigger symbols are used for RCMs while smaller ones denote GCMs.

also outperformed most models, except for the G_ECEA (score 52). Thus, Figure 3.5a shows that regional downscaling allows a more accurate representation of temperature over SEA, and also displays the relatively better performance of the ensemble mean compared to each individual experiment.

For precipitation (Figure 3.5b), the ensemble mean still outperformed the individual experiments. Both the R_ENS and G_ENS got the best ranking score in all 14 experiments, which are 28 and 72, respectively. Figure 3.5b also shows that the GCM experiments ranked higher than the RCM ones. The reason can be seen from the Taylor diagrams (Figure 3.4) when the variability of simulated rainfall from the RCM experiments is much larger than that of the observation. In other words, the *rstd* is often several times greater than 1

leading to the high value of the *rmsd*. Meanwhile, the variability of simulated rainfall from the GCMs is often lower than that of the observation, leading to the smaller *rmsd* values of the GCMs compared to those of the RCMs, thereby deducing the higher ranking scores of the GCMs.

The high degree of variability of the RCM experiments when simulating rainfall in the SEA region was mentioned in previous studies. Juneng et al. [83] indicated the high variability of simulated precipitation with different selections of convective schemes. Ngo-Duc et al. [124] pointed out that precipitation simulated by RegCM is particularly sensitive to convective schemes over the Maritime Continent. The RCM experiments in this study used the MIT-Emanuel convective scheme [48] according to previous sensitivity studies of the SEACLID/CORDEX-SEA project [32], [83], [124].

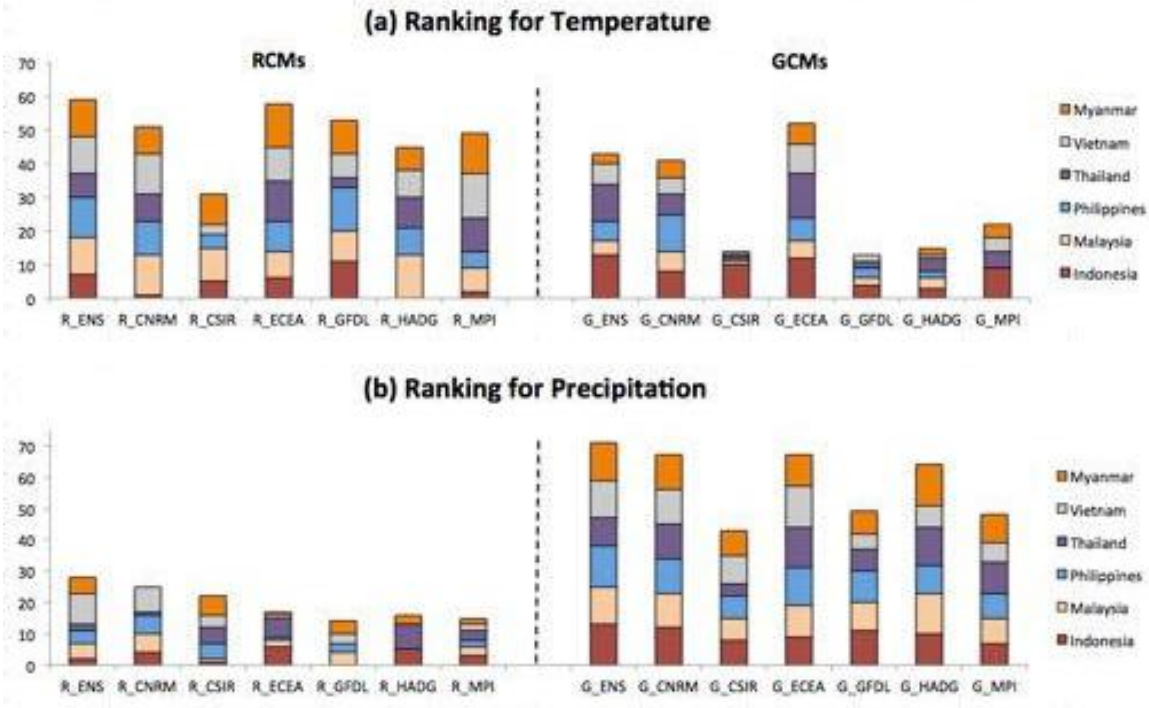

Figure 3.5. The ranking scores of the 7 GCM and 7 RCM experiments based on the centered root mean square difference (*rmsd*) with the observation over the stations of Indonesia, Malaysia, Philippines, Thailand, Viet Nam and Myanmar for (a) temperature and (b) precipitation.

It was shown that the experiments with the MIT-Emanuel convective scheme and with ERA-Interim [35] initial and boundary conditions also resulted in a much higher simulated rainfall variability than the observed one [83]. Moreover, Tangang et al. [157] indicated that rainfall intensity in RCM was higher than GCM.

As the ensemble mean experiments were shown to have clear advantages compared to the individual experiments in representing past climate over SEA, hereafter results with the ENS experiments will be mainly displayed to avoid repetitive and lengthy presentations, and associated uncertainties given by the whole set of models will be discussed when necessary. The comparison of results between GCMs and RCMs will be also discussed due to their differences in representing temperature and precipitation.

From the analysis shown in Figure 3.5, the RCM performance in representing precipitaiton is lower compared to that of the GCM, showing the high uncertainty level of the RCM precipitation results. Thus, the information on future precipitation projected by the RCMs should be assessed with some caution about uncertainty. This result is presented in the study of Nguyen-Thi et al. [127]

Evaluation on performance of R_ENS via APHRODITE

In order to evaluate the performance of the ensemble (R_ENS), average temperature and precipitation in SEA for the period 1986-2005 are compared to those by APHRODITE.

Figure 3.6 depicts the average temperature in SEA for the period 1986-2005 represented by APHRODITE and the ENS. In general, the ENS can reproduce the patterns of T2m in SEA with prominent cold biases in all regions within SEA. These cold biases were already mentioned in previous studies (e.g. [32], [134]). Assuming that the cold biases are from the intrinsic

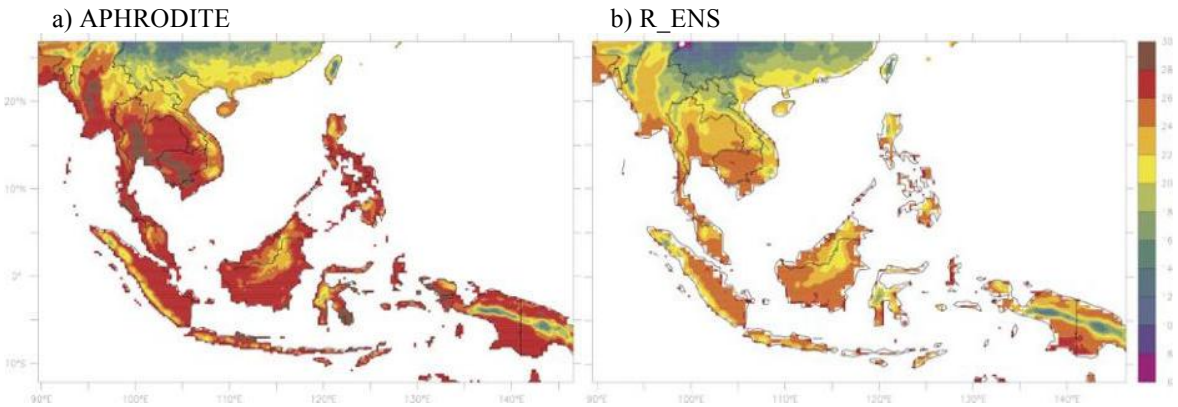

Figure 3.6. Average temperature (ºC) for the period 1986-2005 in SEA by a) APHRODITE and b) the R_ENS.

systematic errors of the used RCMs and still remain for the future period, the projected T2m changes Δ_{T2m} thus cancel out the biases.

Figure 3.7 depicts the simulated rainfall based on APHRODITE and ENS in the period 1986-2005 in SEA. Similar to the case of T2m, the ENS can reproduce the patterns of APHRODITE with wet biases in the whole SEA. Juneng et al. [83] also showed the wet bias in the Indochina region. These wet biases are also assumed to exist in the future projections and the rainfall changes $\Delta_{R\%}$ thus can remove them.

Regarding the quality of APHRODITE data, Chinn et al. [26] affirmed that APHRODITE was appropriate dataset for the climate study over the Indochina region due to its better precipitation simulation compared to other gridded datasets. Lower precipitation was depicted in the equatorial regions, especially over the high orographic areas [83]; in almost SEA [165]. Lower temperature was shown in most areas in SEA, except for a large part of Sumatra [165].

In terms of model uncertainties, there might be several reasons that are (1) a proper choice of GCM could play a significant role in enhancing the downscaling products [124]; and (2) the uncertainty can also come from the insufficient representation of the initial and boundary conditions, such as SST.

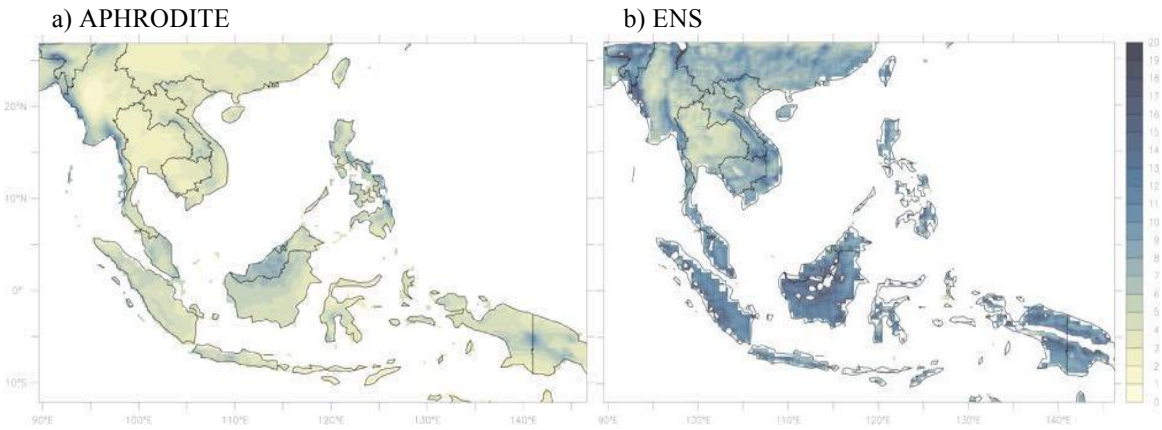

Figure 3.7. Average rainfall (mm day^{-1}) for the period 1986-2005 in SEA by a) APHRODITE, b) the ENS.

For example, a colder SST can result in weaker convective activities, which tends to decrease evaporation over the open ocean, leading to less moisure advected to the mainland, partly explaining the large underestimation of the precipitation in the RCMs [124].

3.2. Performance of downscaling experiments in Viet Nam

The experiments analysed in this section are the outputs of downscaling experiments in Viet Nam.

Figure 3.8 shows the seasonal variability of the monthly means of temperature averaged over the seven climatic sub-regions for the period 1986 – 2005. In general, all experiments underestimate T2m. The underestimation of temperature is prominent in the regions NW and SC in the late winter and in CH and SV in spring. The ENS is in a good agreement with the observation, especially in NE, RRD, NC and CH. HADG and CSIRO show a better performance in NW and HADG is better in SC than the other models (Figure 3.8). It should be noted that Phan-Van et al. [134] also reported the cold bias characteristic of the RegCM model in simulating temperature over the climatic sub-regions of Viet Nam.

Simulated rainfall was not represented as well as temperature due to the

high spatial and temporal variability of rainfall (Figure 3.9). It is generally overestimated by the experiments, e.g. ECEA, MPI, GFDL and ENS. CSIRO seems to perform the best in representing the observed seasonal variations and amplitude of rainfall in all regions in Viet Nam. The wettest bias is obtained with ECEA and MPI in all seven regions while GFDL also largely overestimates rainfall in NW, NE, RRD and NC. Conversely, HADG shows a dry bias in late winter, spring and summer in those four regions. In SC, all models overestimate rainfall from January to September and underestimate rainfall in the rest of year.

The relationships between the observed temperature and the simulations are described in Figure 3.10. Data were averaged at each station f-

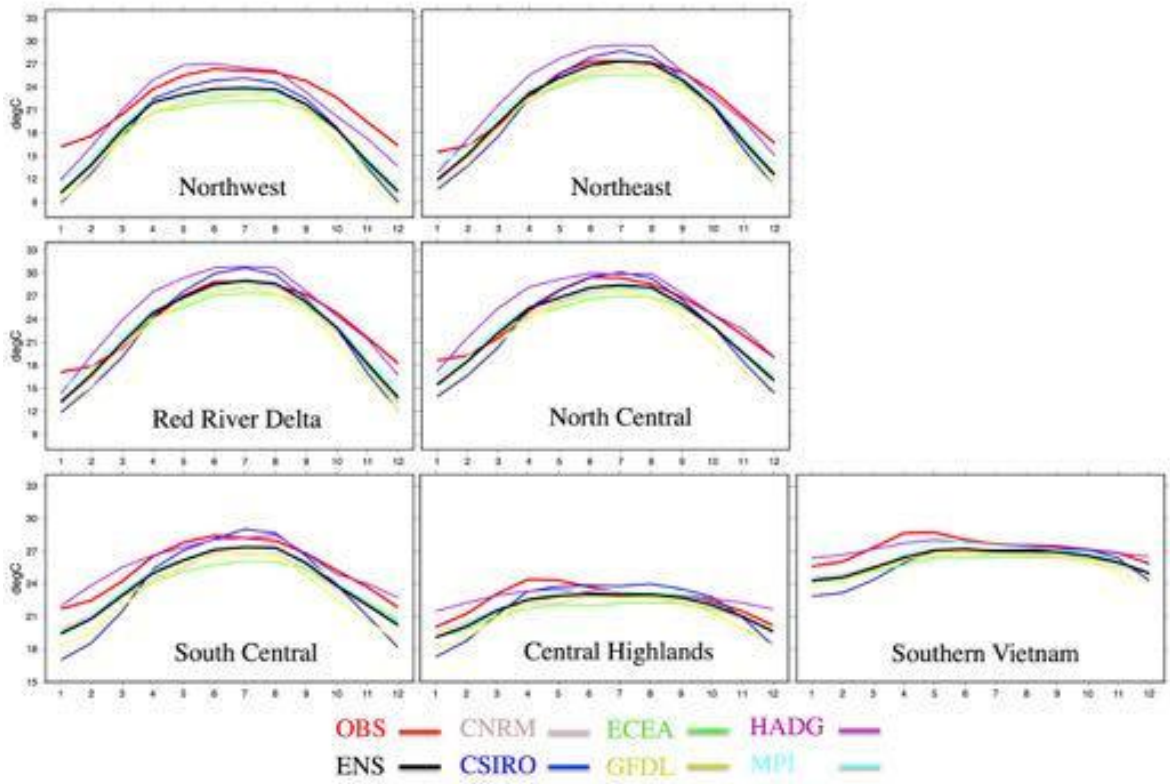

Figure 3.8. Seasonal cycles of T2m observation data and model data. The data are monthly averaged for the period 1986 – 2005 over the stations in seven climatic sub-regions of Viet Nam.

-or the reference period 1986 – 2005. The area between two grey lines denotes the place where the model data are within +/- 2^{o}C from the observation. When the model data at one station is found within this area, that station is considered as a "good" station [122]. In general, the experiments show high percentages of "good" stations in SV and CH with the range of 86 – 100% and 71 – 86%, respectively (Figure 3.10, Table 3.1). However, only 17% of the stations in NW (except for HADG – 50%) are qualified as "good" ones. Among seven regions, HADG shows the highest percentage of good stations, while GFDL shows the lowest one. Most of experiments lie in the right half of the diagonal line in all regions (except for NE), which indicates the cold bias characteristics of the RegCM model shown in Figure 3.8.

Rainfall stations are identified to be "good" if they lie in the area defin-

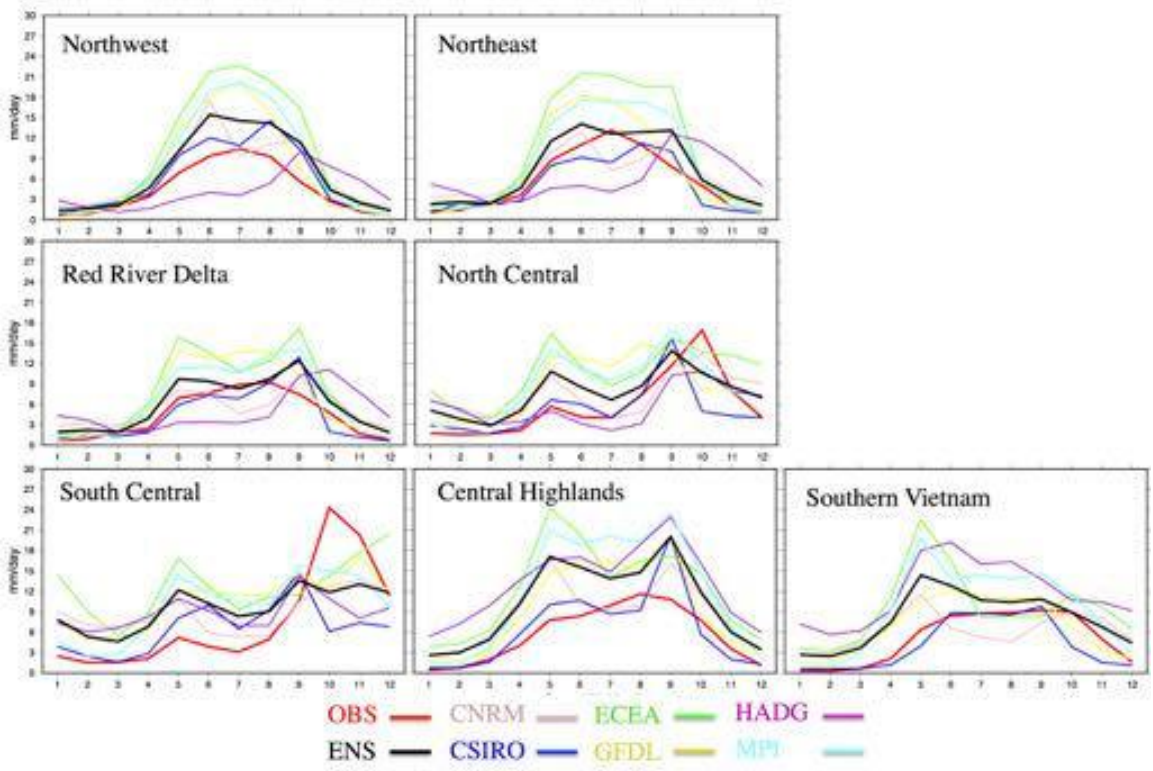

Figure 3.9. Seasonal cycles of precipitation observation data and model data. The data are monthly averaged for the period 1986 – 2005 over the stations in seven climatic sub-regions of Viet Nam.

-ed by two grey lines where their values are within +/- 30% from the observation one. Wet biases are found in all regions as more stations lie in the left half of the diagonal black line. The number of "good" rainfall stations is generally small and lower than that of temperature (Table 3.1). HADG shows the best results in NW and NC with the percentage of good stations to be 83% and 91%, respectively. In RRD and CH, CSIRO well simulates precipitation with 92% and 71% of stations being "good", respectively. ECEA contrastly shows a poor performance with 0% good stations in NW, RRD, NC, CH and SV. In CH, good stations of five experiments only account for 0%. This reveals that simulating precipitation in CH is challenging (Figure 3.11).

The absolute T2m biases were estimated for the period 1986 – 2005 at

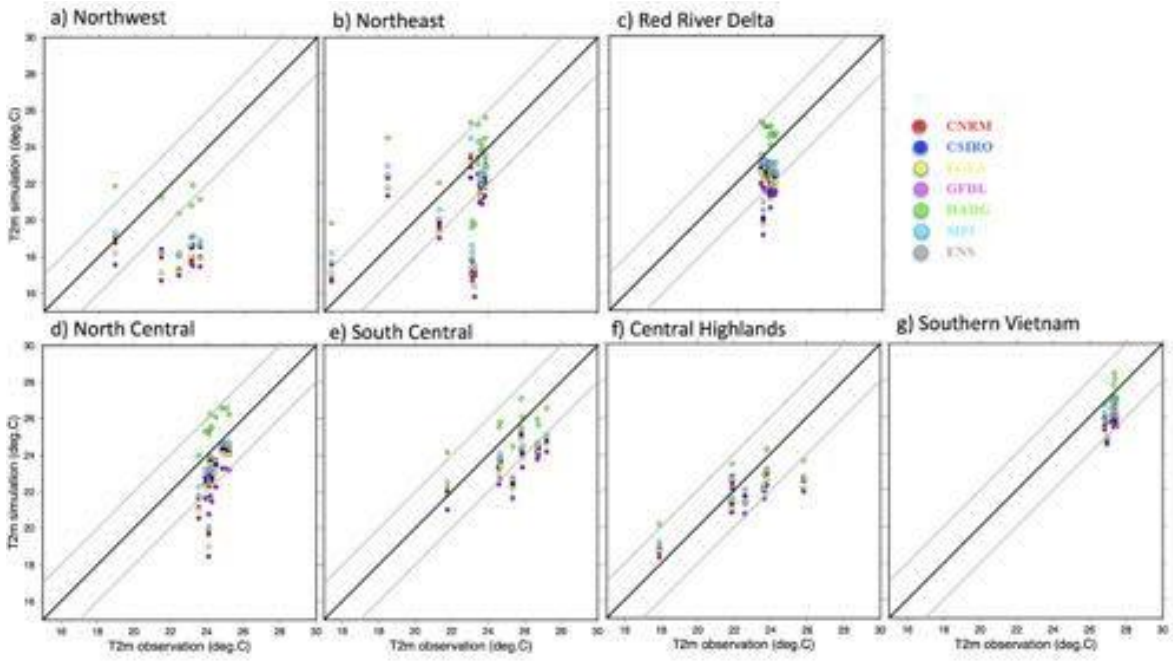

Figure 3.10. Relationship between 1986 – 2005 observed 2m-temperature and different model outputs. The dots indicate the stations located in seven sub-regions in Viet Nam. Black line denotes the ideal case in which the simulated value is equal to the observed one. Two grey lines define the area where simulated values are within +/- 2^{o}C from the observed ones.

each station (Figure 3.12). Cold biases (0 – 4^{o}C) are prominent in mostly Viet Nam (except for HADG), which agrees with the results shown in Figure 3.8 and Figure 3.10. Several stations in NW and CH display warm biases (0 to 2^{o}C) in all experiments. In general, there is a high agreement among the experiments (excluding HADG) in simulating T2m.

Dry biases are found with CSIRO and HADG in simulating rainfall in NW, RRD and NC. Conversely, ECEA and MPI display wet biases (Figure 3.13). For the whole Viet Nam, wet biases (10 – 90%) are popular among the experiments, which is also consistent with the results shown in Figure 3.9 and Figure 3.11.

Figure 3.14 shows the relationship between the monthly simulated T2m and the monthly observation by using Taylor diagrams [157]. In a Taylor diagram, the radius distance represents the ratio of standard deviation (RSTD) of the simulated data to that of observation, while the polar angle expresses the correlation (CORR) between them. The point OBS on the horizontal axis displays the observation where the CORR and RSTD values equal to one. The linear distances between the simulated points and the OBS point are proportional to the centered root mean square difference (RMSD) between thesimulated and observation data. In NW, the experiments show high CORRs (over 0.85) and RSTDs of around 1.2. Among them, ECEA and MPI display the best performance. SV shows the lowest CORRs while the highest are in RRD, NC and SC. HADG and ECEA in SV and ENS and MPI in SC have the best RSTD and RMSD. Among the regions, SC generally displays the best performance.

Table 3.1. The number and percentage of "good" T2m and R stations of six experiments and their ENS in seven regions in Viet Nam.

Model		CNRM		CSIRO		ECEA		GFDL		HADG		MPI		ENS	
Region (No. of stations)	**Var**	**No. of good stations**	**%**	**No. of good stations**	**%**	**No. of good stations**	**%**	**No. of good stations**	**%**	**No. of good stations**	**%**	**No. of good stations**	**%**	**No. of good stations**	**%**
NW (6)	T2m	1	17	1	17	1	17	1	17	3	50	1	17	1	17
	R	1	17	2	33	0	0	1	17	5	83	1	17	1	17
NE (13)	T2m	6	46	8	62	6	46	4	31	7	54	8	62	8	62
	R	7	54	6	46	3	23	5	38	6	46	3	23	6	46
RRD (13)	T2m	9	69	11	85	9	69	4	31	13	100	12	92	11	85
	R	11	85	12	92	0	0	1	8	11	85	1	8	6	46
NC (11)	T2m	9	82	10	91	8	73	3	27	10	91	10	91	10	91
	R	6	55	9	82	0	0	2	18	10	91	2	18	7	64
SC (9)	T2m	5	56	5	56	4	44	3	33	8	89	5	56	5	56
	R	5	56	5	56	1	11	4	44	5	56	5	56	5	56
CH (7)	T2m	6	86	6	86	5	71	5	71	5	71	6	86	6	86
	R	2	29	5	71	0	0	0	0	0	0	0	0	0	0
SV (7)	T2m	6	86	6	86	6	86	6	86	7	100	6	86	6	86
	R	5	71	2	29	0	0	3	43	0	0	1	14	1	14

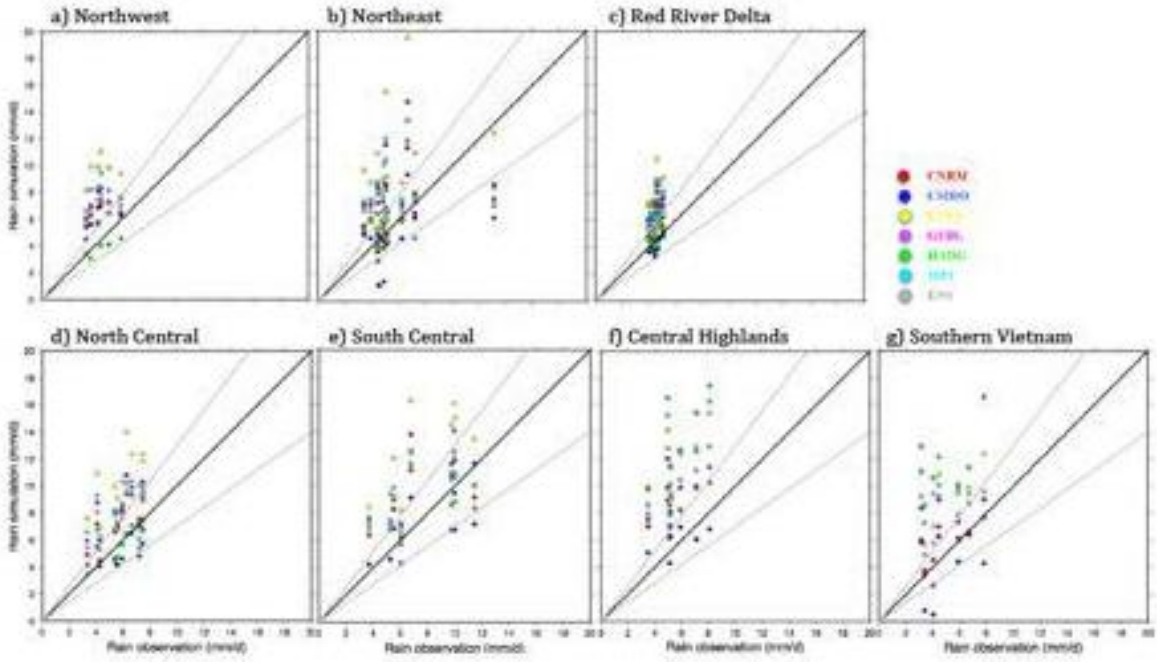

Figure 3.11. Similar as **Figure 3.10** but for precipitation.

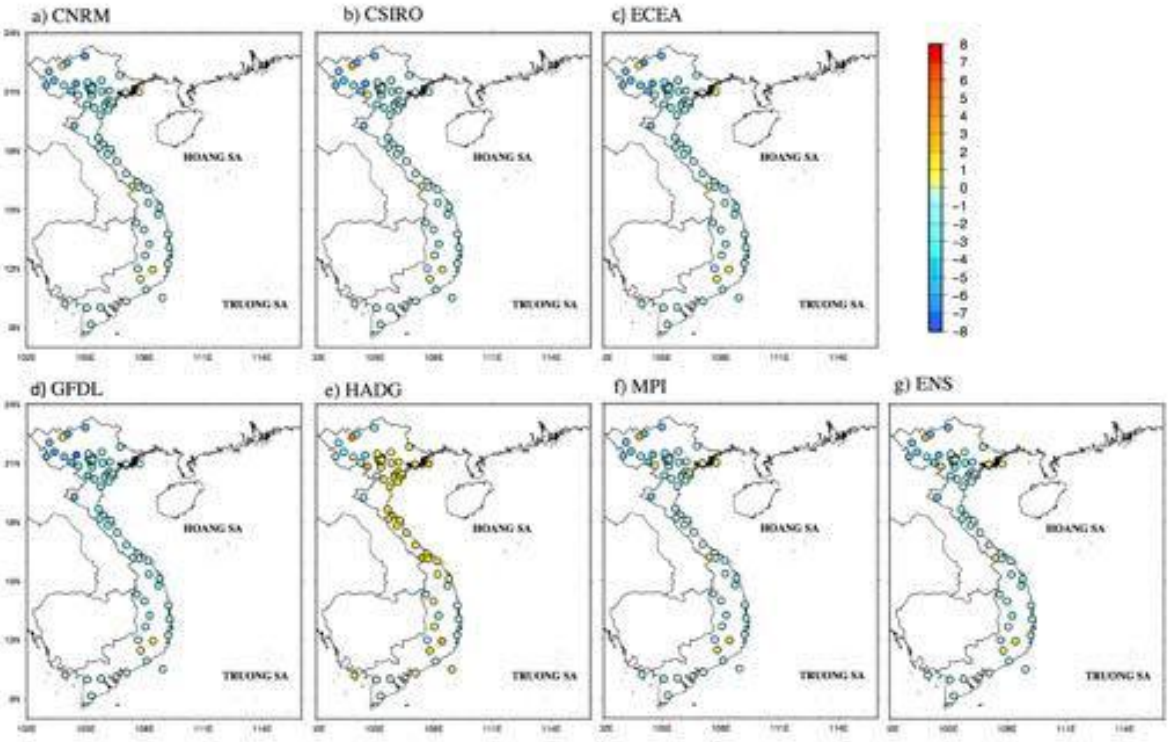

Figure 3.12. T2m biases (ºC) simulated by seven experiments for the period 1986 – 2005 in Viet Nam. Warm (cold) biases are represented by warm (cold) colored circles.

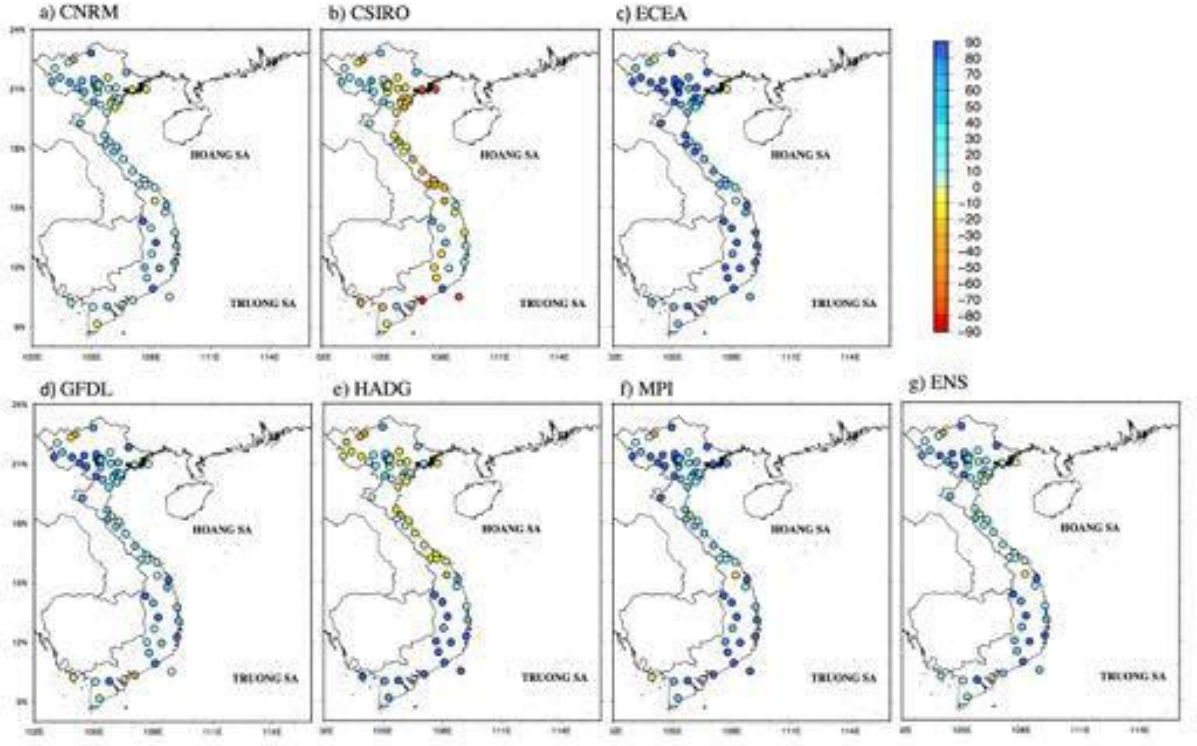

Figure 3.13. Similar as **Figure 3.12** but for rainfall. Wet (dry) biases are represented by cold (warm) colored circles.

The performance of simulated precipitation is not as good as that of temperature (Figure 3.15). This can attribute to the high variability of precipitation simulated by RCMs [82]. While SC shows the best result with simulated temperature, it is the worst for simulated rainfall with low CORRs (0.3 – 0.7) and low RSTDs (0.5 – 0.7). In NE and RRD, HADG displays the lowest CORR (~ 0.1). ENS shows a relatively better performance in NE, RRD and SV.

The above-mentioned different evaluation methods showed that the performance of the experiments depends on the climate variables analyzed, the climatic sub-regions studied, and the evaluation matrix used. It is not obvious to conclude which experiment is the best in all cases.

In order to obtain an objective ranking of the overall performance of the experiments, the following method is implemented based on four criteria:-

(1) minimum absolute bias, (2) minimum RMSD, (3) maximum CORR and (4) RSTD closest to 1. For each criteria, the experiment performing the best gets the score of 6, the second best gets the score of 5 and so on. The worst experiment gets the score of 0. The final score of each region is the average of the temperature score and the precipitation one. Figure 3.16 shows the sum of the scores over seven sub-regions for each experiment. It can be noted that E--

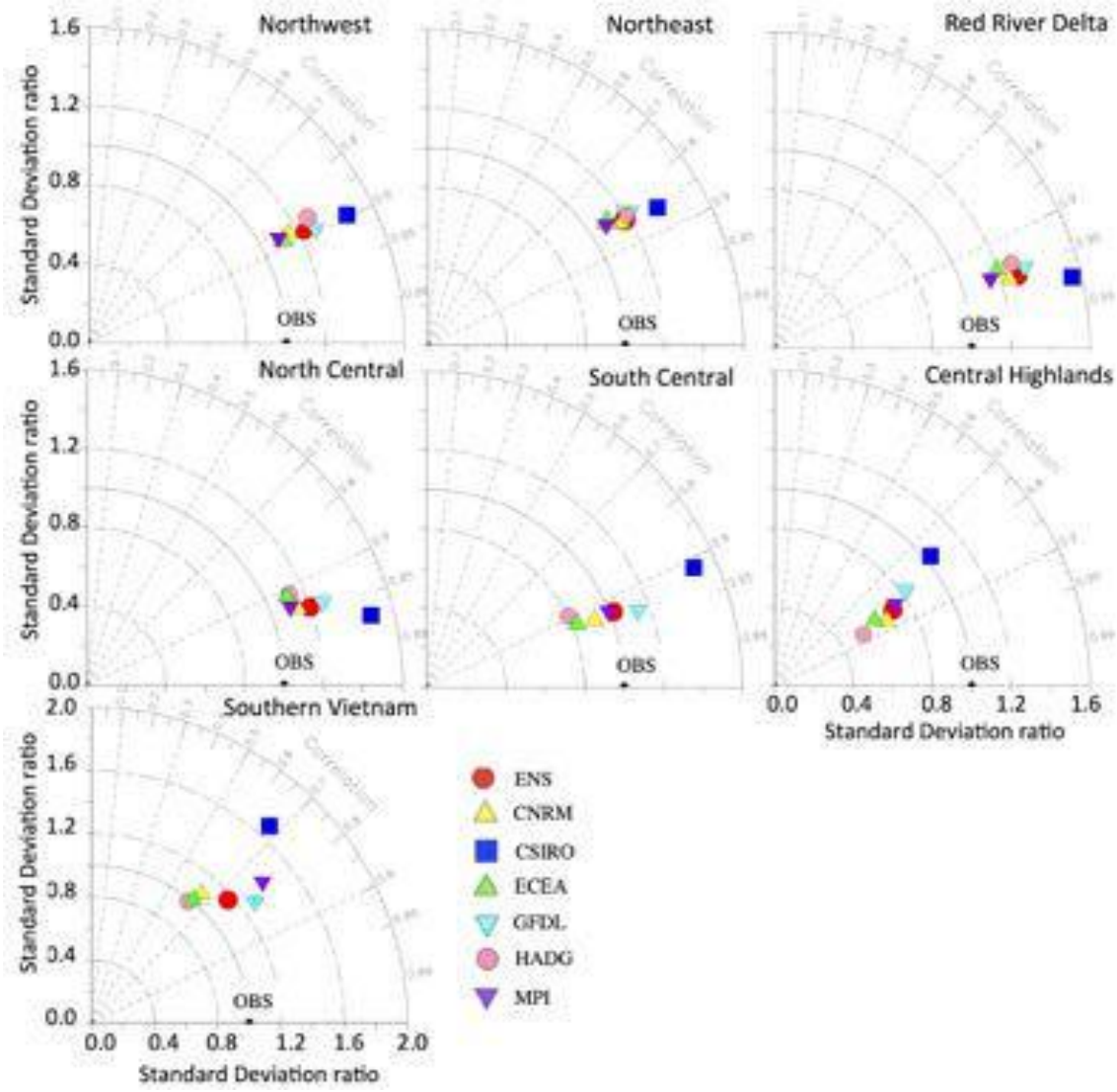

Figure 3.14. Taylor diagram for 1986 – 2005 climatological monthly time series of temperature over the stations of seven regions in Viet Nam with six regional experiments and their ENS.

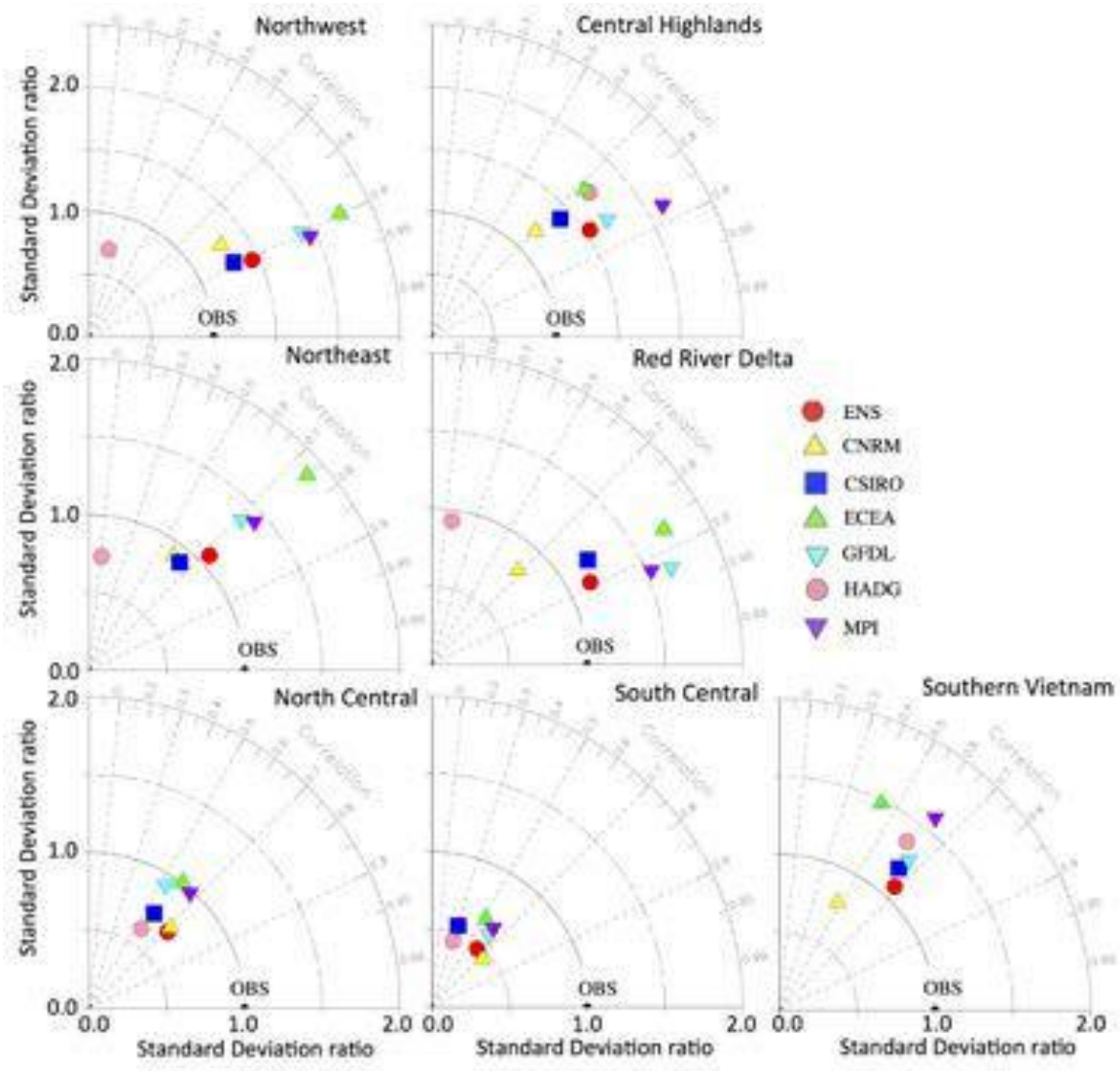

Figure 3.15. Taylor diagram for 1986 – 2005 climatological monthly time series of precipitation over the stations of seven regions in Viet Nam with six regional experiments and their ENS.

-NS has the highest score, followed by CNRM and MPI. Thus, the ensemble mean ENS outperforms each individual experiment in representing temperature and rainfall in seven sub-regions of Viet Nam.

Viet Nam is a nation with complex spatial climate classification due to interaction between monsoon circulation and topography, leading to different rainfall and temperature generating mechanisms among climatic regions and

various times in a year [134]. In summer, the Northeast region, for example, is directly influenced by tropical cyclones while the Northwest is majorly affected by southwest monsoon; in winter, the Northeast region is often influenced by cold fronts while the Northwest is not, although temperature in both the regions decreases due to effect of cold air masses. The southwest summer monsoon was attributed to much rainfall in the Northern, Central Highland and the Southern Viet Nam in summer [106]. The different rainfall and temperature generating mechanisms among regions and various times result in numerous performances of model simulations in climatic regions and various times in a year [124], [134], [162]. Moreover, simulation skills of models are various due to different global boundary conditions in spite of using the same RCM (RegCM4.3).

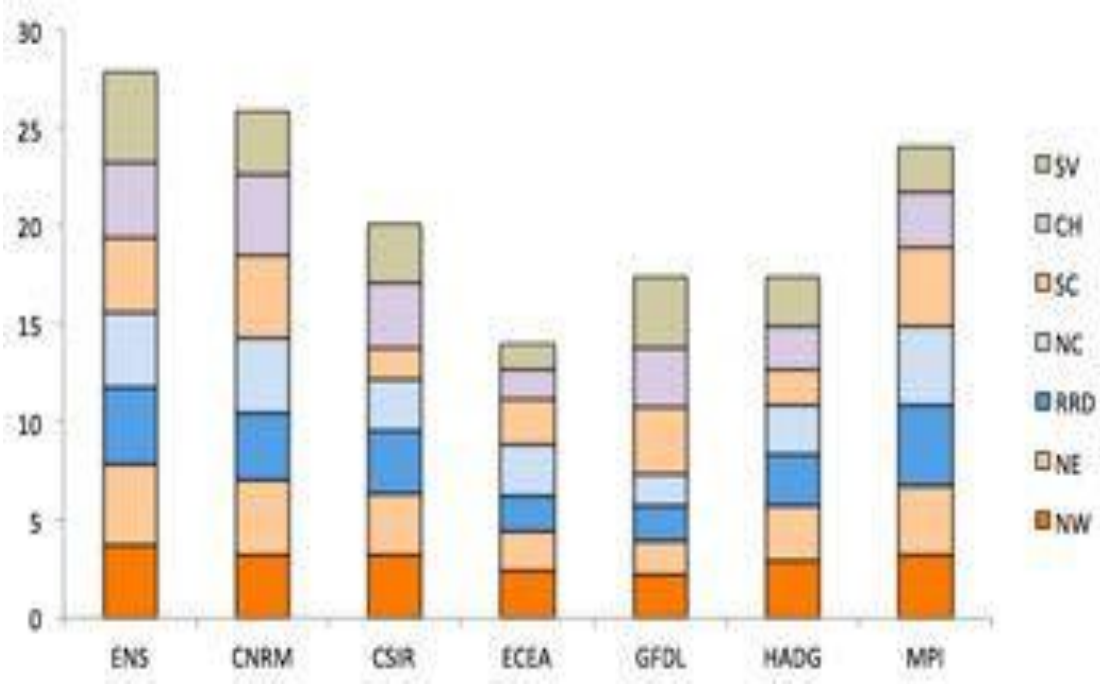

Figure 3.16. The ranking scores of the seven experiments based on the statistic values of (1) absolute bias, (2) CORR, (3) RMSD and (4) RSTD between monthly model and observation values in seven sub-regions of Viet Nam.

3.3. Chapter 3 summary

Chapter 3 evaluated the performance of six regional and global climate models in SEA. When comparing the model outputs with the station data over the six countries in SEA, including Indonesia, Malaysia, the Philippines, Thailand, Vietnam and Myanmar, it was shown that regional downscaling allowed a more accurate representation of temperature but displayed a higher variability of rainfall over SEA compared to the results of the GCMs. The ensemble mean experiment had a relatively better performance compared to each individual model in representing the monthly time series of temperature and precipitation.

Chapter 3 also evaluated the performance of six SEACLID/CORDEX-SEA regional downscaling experiments for the period 1986 – 2005 in Viet Nam. It was shown that there was a systematic cold bias in simulated temperature. ENS exhibited the best in simulating temperature in NE, RRD, NC and CH. For precipitation, the experiments showed a wet bias tendency and CSIRO exhibited the best. The number of "good" stations varied with the experiments and with the variables. CH had a high percentage of "good" T2m stations but a very low percentage of "good" precipitation ones. HADG well exhibited in NW and NC, CSIRO well performed in RRD and CH while ECEA showed the poorest performance in NW, RRD, NC, CH and SV. Finally, a scoring system was elaborated to objectively rank the performance of the experiments. ENS had the highest score, followed by CNRM and MPI. Different climatic regions with typical characteristics on topoghraphy, solar radiation, geographical locations, etc. are partly the reason why various projected results are obtained by the RCM experiments at different time periods. Moreover, distinctive features of model configuration, physical processes, parameterization and feedback mechanisms also contribute to the

diversity of projected results. The results suggested that the ensemble mean of the multi-model SEACLID/CORDEX-SEA experiments could be an appropriate and useful data source for assessing future climate scenarios of Vietnam.

CHAPTER 4 – CLIMATE CHANGE PROJECTION AND CLIMATE ANALOG IN SOUTHEAST ASIA

This chapter investigates the projected changes of temperature and rainfall in SEA and Viet Nam. Those results in Vietnam were compared to the results of the Climate Change and Sea Level Rise Scenario for Viet Nam report by MONRE, 2016 [5] (hereinafter referred to as the CC Scenario). Climate analog, novel climate and disappearing climate are also analysed in this chapter.

4.1. Projected changes of temperature and rainfall in SEA

Figure 4.1 shows that temperature increases by 1-2.2^{o}C (1.3-2.8^{o}C) and 1-2.5^{o}C (2.5-4.6^{o}C) under the RCP4.5 (RCP8.5) for the period 2046-2065 and 2080-2099, respectively. The areas with lower temperature (above the latitude 15N) have higher temperature changes, up to 3.7-4.6^{o}C under the RCP8.5. Difference at 5% significance level under t-test are indicated by diagonal lines and the number in the upper-right corner of each panel shows the percentage of grid points with significant differences. Under two RCPs and for both periods (mid- and far-future), the differences at 5% significance level under t-test are all 100%. This shows that the difference between the means of baseline and future temperature data at 5% significance level under t-test are present in all the land areas in SEA. These results comply with the apparent temperature changes over the time.

Figure 4.2 displays the longitudinally averaged temperature and the temperature changes for each latitude in the SEA region in the mid- and far-future periods under the two scenarios. Higher T2m is in the Southern Hemisphere and around 10N. T2m gradually decreases from 11N to higher northern latitudes. The projected changes of T2m agree with the results shown in Figure 4.1, with higher increases of temperature in the northern part of the

SEA region. The changes between the mid- and far- future periods under the RCP4.5 (~0.2°C) are smaller than those under the RCP8.5 (around 2°C). The projected T2m under the RCP4.5 for both the periods ranges from 17.5°C to over 28°C while that under the RCP8.5 ranges from 18 to 28.5°C (mid-future) and from 20 to 30°C (far-future).

The rainfall changes for both the periods under the RCP4.5 and for the period 2046-2065 under the RCP8.5 are relatively similar (-25 to 30%) (Figure 4.3). The rainfall considerably decreases in most of the SEA region --

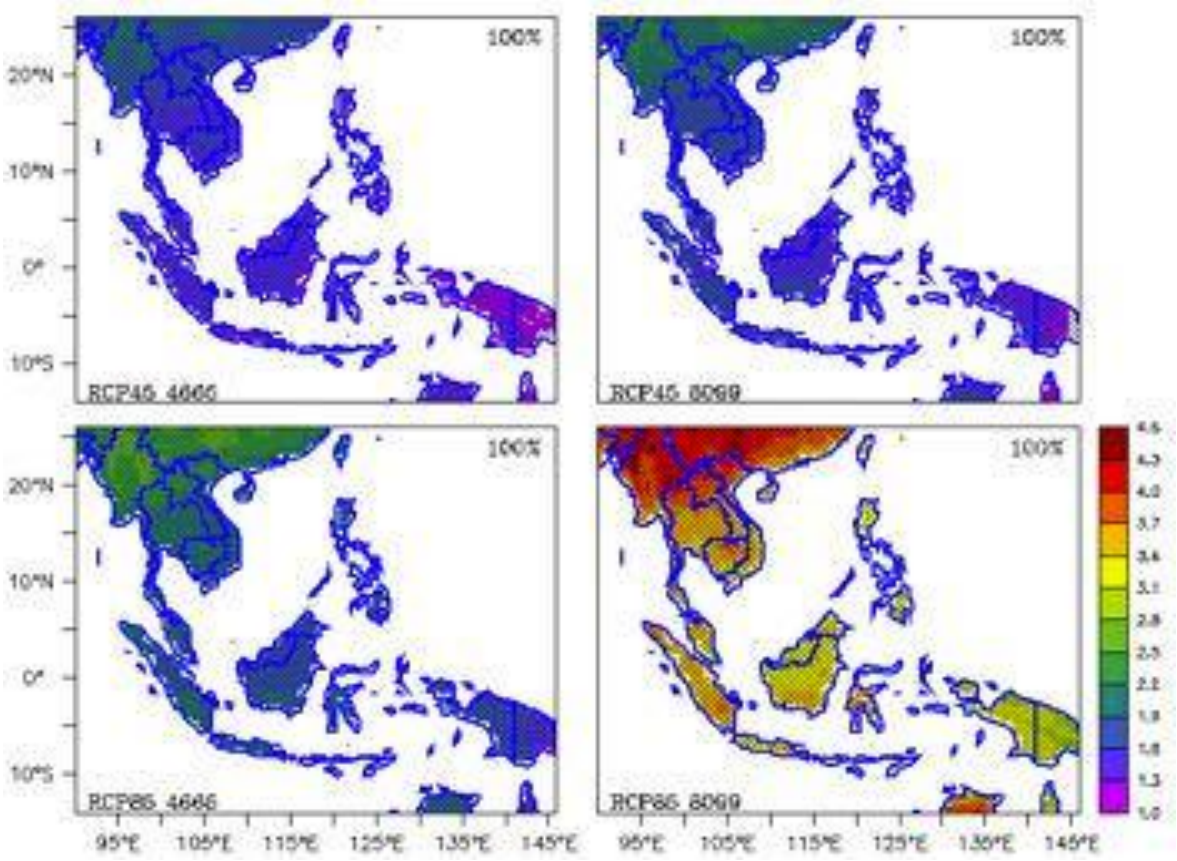

Figure 4.1. Absolute temperature change (ºC) in SEA under the RCP4.5 and RCP8.5 scenarios for the period 2046-2065 and 2080-2099 compared to the baseline 1986-2005. Difference at 5% significance level under t-test indicated by diagonal lines and the number in the upper-right corner of each panel shows the percentage of grid points with significant differences.

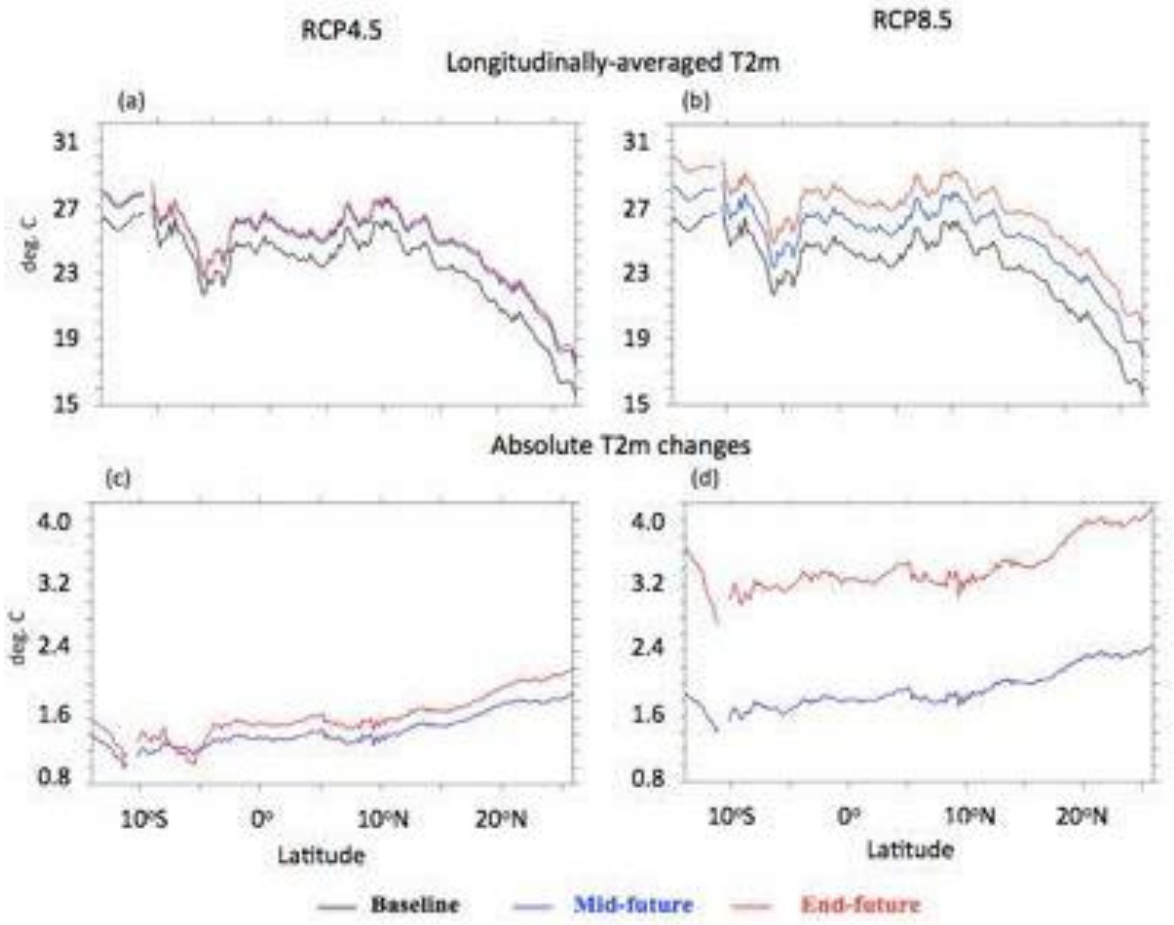

Figure 4.2. Longitudinally averaged temperature (a, b) and T2m change (c, d) for each latitude in the SEA region for the baseline period (black line), the mid-future (blue) and the far-future (red) under the RCP4.5 (left column) and the RCP8.5 (right column).

(-30 to 0%) under the RCP8.5 for the period 2080-2099, except for some parts of Thailand, Myanmar and East Malaysia. Precipitation exhibits high variability on spatial scales, especially over the SEA region ([83], 124]). Models' capability in rainfall simulation is also various in different regions due to regional climatic features, model uncertainties originating from global boundary conditions, GHG scenarios, physical parameterization schemes as well as the RegCM algorithms ([83], [124], [162]). Thus, there are differences in simulating rainfall among regions and GHG scenarios.

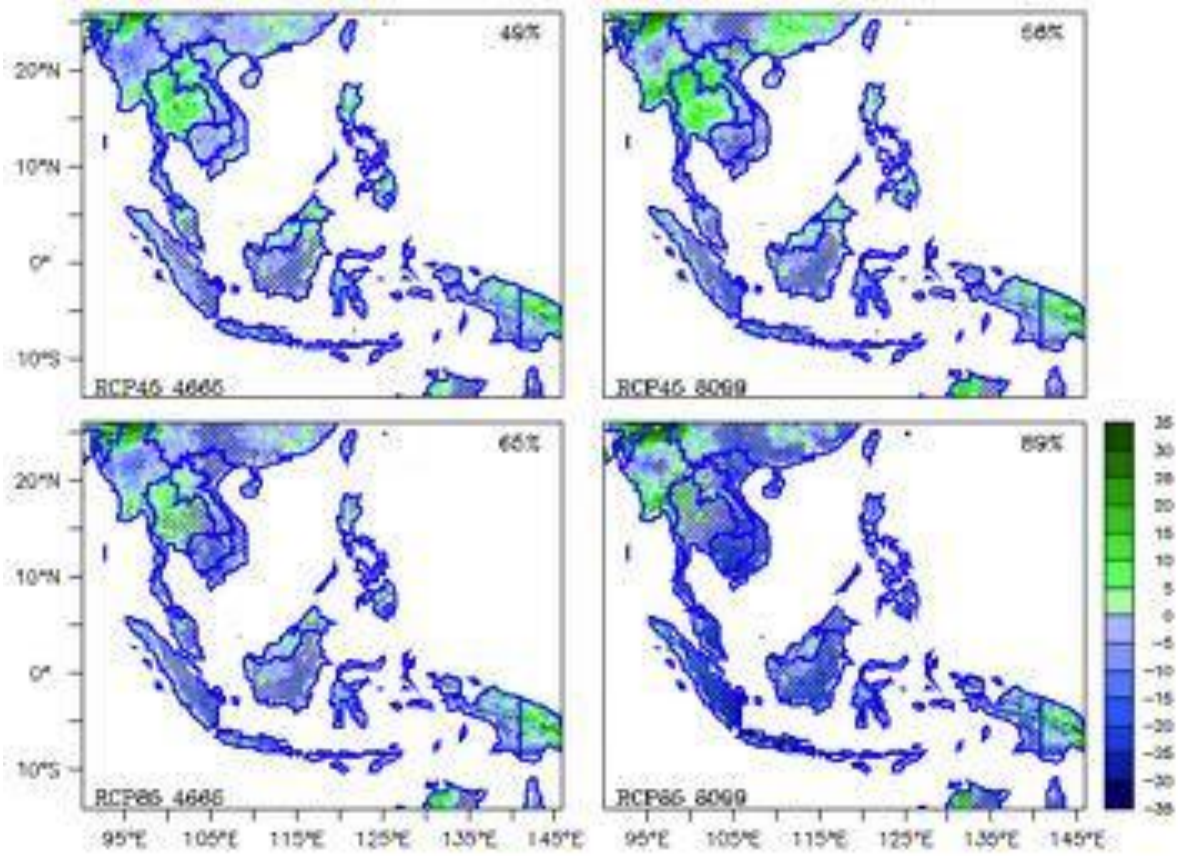

Figure 4.3. Relative rainfall change (%) simulated by ENS in SEA under the RCP4.5 and RCP8.5 scenarios for the period 2046-2065 and 2080-2099 compared to the baseline 1986-2005. Difference at 5% significance level under t-test indicated by diagonal lines and the number in the upper-right corner of each panel shows the percentage of grid points with significant differences.

The difference between the means of future precipitation and baseline one at 5% significance level under t-test are 49% and 56% of the SEA land area under RCP4.5 respectively for the period 2046-2065 and 2080-2099. Under RCP8.5, the difference is 65% and 89% of the SEA land area respectively for the mid- and far-future (areas with diagonal lines in Figure 4.3). At the end of century (2080-2099) under RCP8.5, 89% of the SEA land has significant rainfall difference at 95% confidence level compared to the

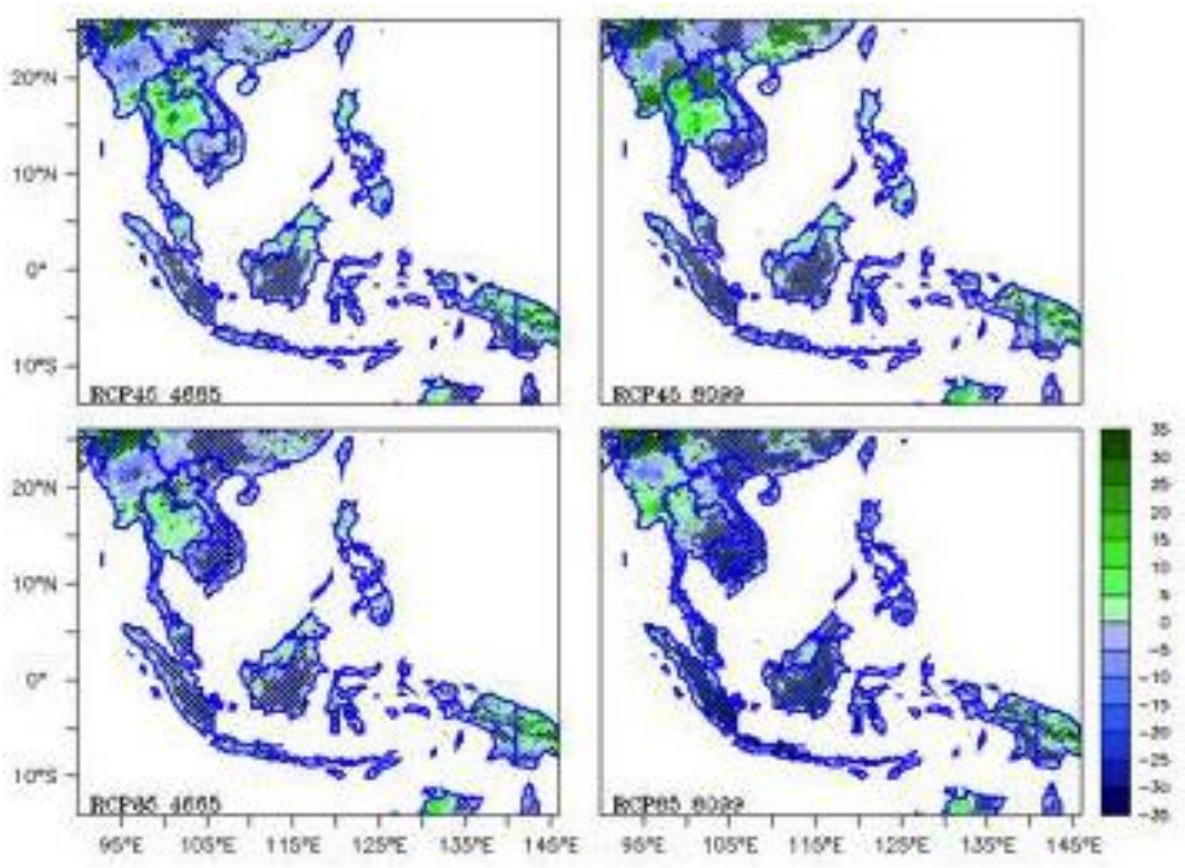

Figure 4.4. Relative rainfall change (%) simulated by ENS in SEA under the RCP4.5 and RCP8.5 scenarios for the period 2046-2065 and 2080-2099 compared to the baseline 1986-2005. Cross hatching denotes the agreement of at least two thirds of the individual RCM experiments.

baseline period while those ratios are smaller for three other cases (RCP4.5 2046-2065, RCP4.5 2080-2099, RCP8.5 2046-2065).

Figure 4.4 displays the precipitation relative change over the SEA region with crossing hatching showing the agreement of at least 4 out of 6 experiments. The most agreement is found under RCP8.5 at the end of the century while the least agreement goes with RCP4.5 in the middle of the century. The regions with the high uncertainty locate in Myanmar, Thailand and eastern Malaysia. These results are very compatible with those in Figure 4.3, which means that the RCP, the period and the regions with high agreeme-

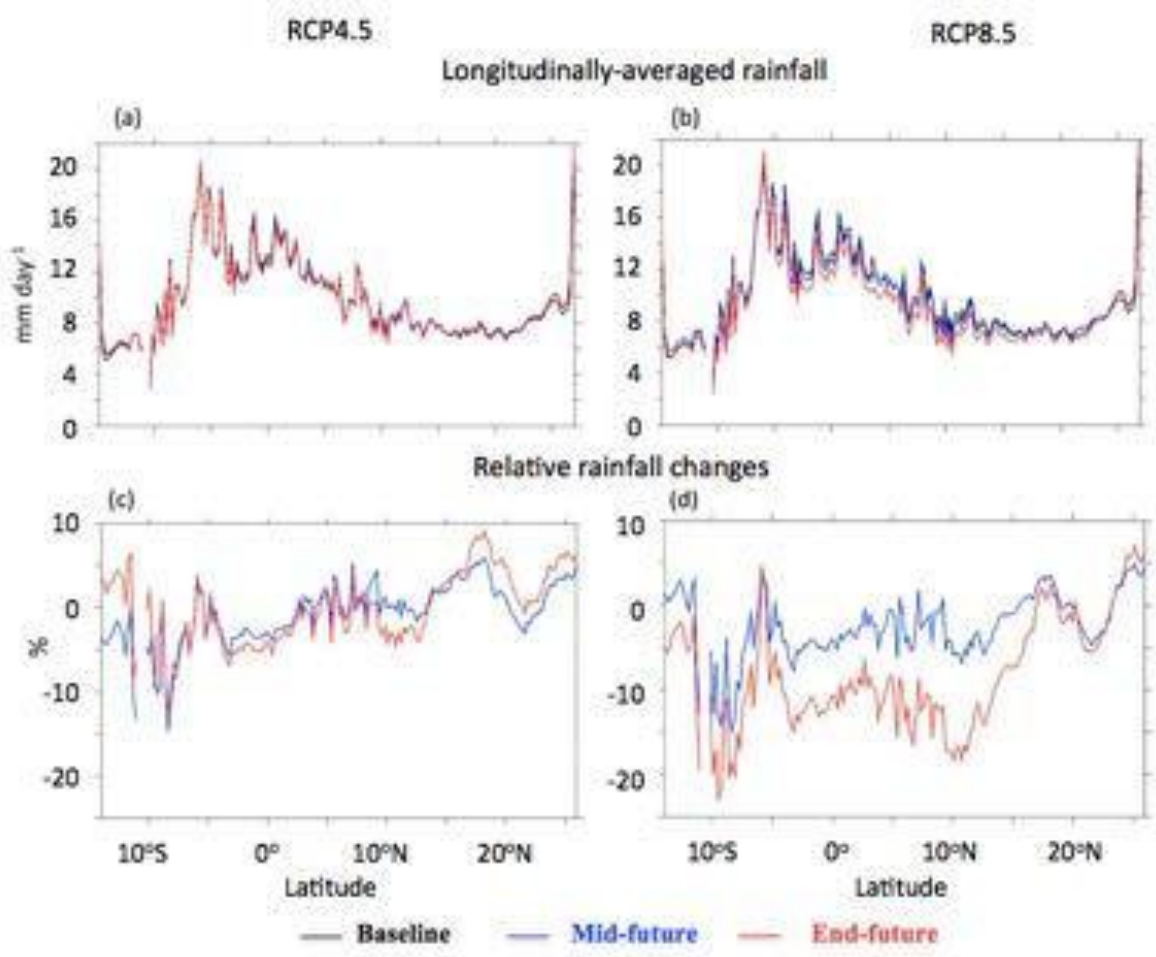

Figure 4.5. Longitudinally averaged rainfall (a, b) and rainfall change (c, d) for each latitude in the SEA region for the baseline period (black line), the mid-future (blue) and the far-future (red) under the RCP4.5 (left column) and the RCP8.5 (right column).

-nt among experiments are generally those having much significant rainfall difference at 95% confidence level compared to the baseline period.

Figure 4.5 displays the longitudinally averaged rainfall and its changes for each latitude in the SEA region. It can be seen that the projected rainfall by the mid- and far-future periods under the RCP4.5 seems to be very similar to that of the baseline period 1986-2005, which varies from 3 to 22 mm day^{-1}. The projected rainfall under the RCP4.5 can both increase (by 10%, e.g. in the Indochina peninsula) and decrease (by -15%, e.g. over the Maritime

continent) compared to the baseline rainfall. Under the RCP8.5, the drier tendency (-23%) is more pronounced, especially over the Maritime continent by the far-future period.

4.2. Relocation of cities' climate and climate analog in SEA

Figure 4.6 and Table 4.1 display the analog locations of six specific cities in the SEA region including Ha Noi, Bangkok, Manila, Jakarta, Kuala Lumpur and Hinthada based on the minimum climate distance for the R_ENS and G_ENS experiments. The selection of the six cities in six countries in SEA aims to indicate the locations with present climate similar to the future climate of these six cities. The thesis does not intend to analyse climate analog in either megacities or capital cities in SEA. This selection of the cities only means relatively geographic and climatic representation. In the Indochina region, Ha Noi is highly influenced by winter monsoon while Bangkok is strongly affected by summer monsoon. Manila locates in the Philippine archipelago in the northern hemisphere while Jakarta is at about 6.2^{o}S in the southern hemisphere. Kuala Lumpur is about 3^{o}N distant from the equator. Thus, added selection of other cities for illustration does not improve scientific and practical values of the thesis.

The results of both GCM and RCM analysed facilitate general assessment and comparison between these two kinds of models' performance. It can be noted that there is a remarkable difference between the RCM and the GCM locations. For example, under RCP8.5, future climate of Ha Noi is most similar to the present climate of the point with coordinate ~110.125E, 20.375N (Guangdong, China) according to the R_ENS. However if we consider the result of G_ENS, the analog location of Ha Noi is located in the far northwestern region of the SEA domain (~90.125E, 22.875N) – Jambari, Bangladesh which is about 100 km far from sea. In general, when the original

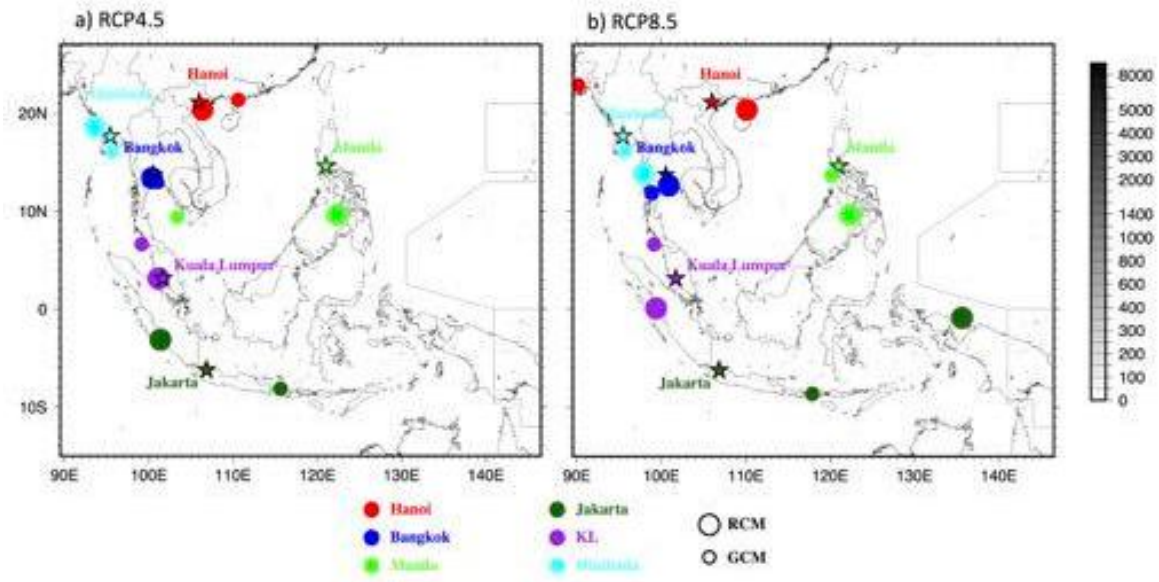

Figure 4.6. Relocation of six cities' climate in SEA at the end of the 21st century under the a) RCP4.5, and b) RCP8.5 scenario. The locations of the six cities are marked with the star symbols. The best analog locations were found with the R_ENS (bigger circles) and G_ENS (smaller circles) experiments.

cities lie in the northern hemisphere, their best analogs with the R_ENS are usually located southwards, i.e. towards warmer regions. This is as climate tends to be warmer in the future due to increasing GHG contrentration. For Jakarta in the southern hemisphere, its best analog is located northwards, in the Supiori island of Indonesia (~135.625E, 0.875S) for RCP8.5; and in the Bengkulu province (~101.375E, 3.125S) in the southwest coast of Sumatra for RCP4.5. The R_ENS analogs of some cities remain almost at the same locations such as the cases of Ha Noi and Kuala Lumpur under RCP4.5, and of Bangkok under both RCP4.5 and RCP8.5. In the future, Manila's climate is closest to the present climate of the Negros Occidental province (~122.375E, 9.625N) under both scenarios. Kuala Lumpur's future climate under RCP8.5 is similar to the present climate of the West Pasaman Regency (~99.375E,0.125N) located in West Sumatra, Indonesia. The G_ENS analog -

Table 4.1. Best analog locations with the R_ENS and G_ENS experiments of the six cities and their respective climate distances (ClimD) for the RCP4.5 and the RCP8.5 scenario.

Reference city	**Best Analog RCP4.5**			**Best Analog RCP8.5**		
RCM	Lon	Lat	ClimD	Lon	Lat	ClimD
Ha Noi	106.375	20.375	1.1	110.125	20.375	1.66
Bangkok	100.375	13.375	1.16	100.875	12.625	2.06
Manila	122.375	9.625	1.21	122.375	9.625	2.03
Kuala Lumpur	101.125	3.125	0.62	99.375	0.125	1.4
Jakarta	101.375	-3.125	0.87	135.625	-0.875	2.07
Hinthada	93.625	18.625	0.69	97.875	13.875	1.68
GCM						
Ha Noi	110.625	21.375	0.62	90.125	22.875	0.86
Bangkok	101.125	12.875	0.95	98.875	11.875	1.88
Manila	103.375	9.375	0.89	120.125	13.625	1.98
Kuala Lumpur	99.125	6.625	0.72	99.125	6.625	1.73
Jakarta	115.625	-8.125	1.14	117.875	-8.625	2.01
Hinthada	95.625	16.125	0.96	95.625	16.125	1.71

of Hinthada are identical under both RCP4.5 and RCP8.5 (Figure 4.6, Table 4.1). The R_ENS analog location of Hinthada under RCP8.5 situates towards the equation while it moves a bit norwards under RCP4.5.

The climate distance estimated from the R_ENS is smaller than that estimated from the G_ENS for Kuala Lumpur and Hinthada under both RCPs, and for Jakarta under the RCP4.5, while it is greater for the other three cities -

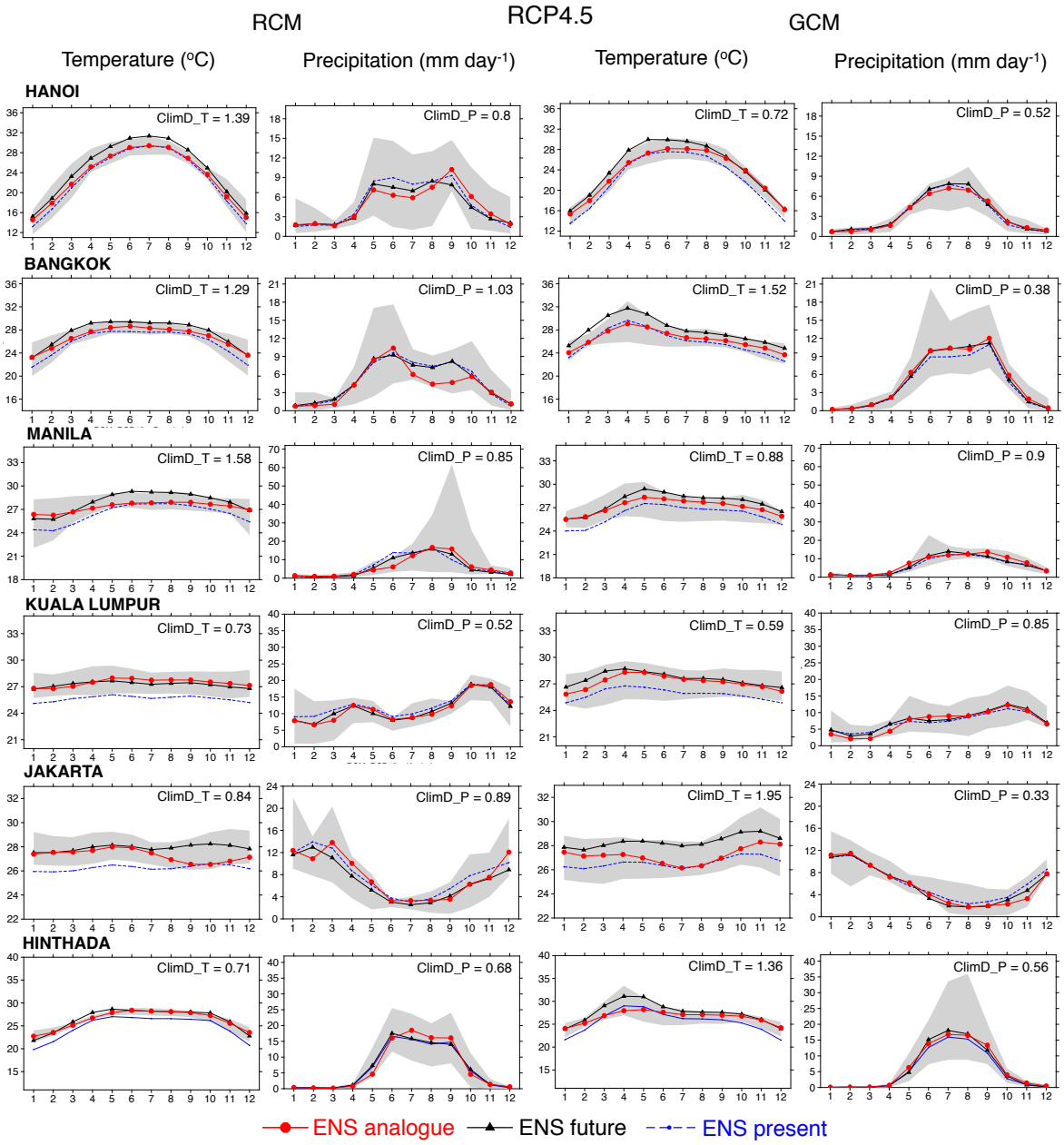

Figure 4.7. Seasonal cycles of temperature (1st and 3rd columns) and precipitation (2nd and 4th columns) by the R_ENS (1st and 2nd columns) and G_ENS (3rd and 4th columns) at the six big cities. Blue point-symboled dashed lines and black triangle-symboled lines indicate the present and RCP4.5 projected cycles of a reference site, respectively, while red octagol-symboled lines indicate the present cycles of the respective best analog location. The grey shading denotes the range of 6 RCM or 6 GCM at the best analog location.

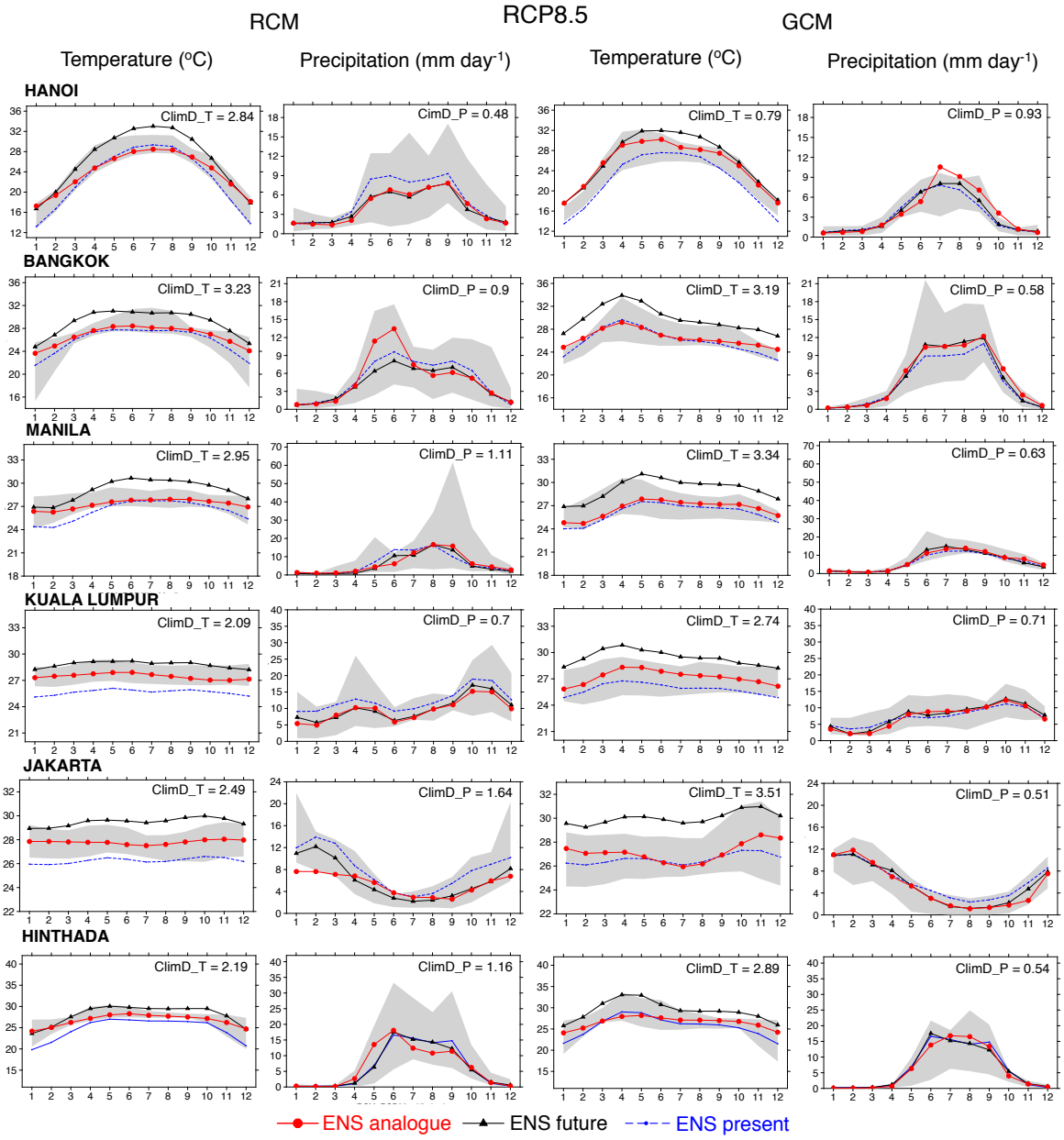

Figure 4.8. As in Figure 4.7 but for RCP8.5.

(Table 4.1). The climate distance is also much greater (approximately twice or more) for the RCP8.5 compared to the RCP4.5, except for Ha Noi where the climate distance increases only ~1.5 times. The increase in climate distance is mainly due to the increase in the distance of temperature, which is a direct consequence of the increase in greenhouse gas concentration; while there is no systematic increase in the distance of rainfall (Figure 4.7**,** Figure 4.8).

The current seasonal rainfall cycles at the TP-best analog sites are quite close to the future rainfall cycles at the reference points, resulting in a relatively small rainfall distance (usually less than 1). At these TP-best analog sites, the values of temperature distance are often much greater than those of precipitation, especially for the RCP8.5 scenario. The determination of a large or small ClimD value, i.e. whether a reference point has a good-, poor- analog or novel climate in the future within the SEA region, thus depends a lot on the distance of temperature, ClimD_T. In Ha Noi, the future temperature simulated by RCM is 4^{o}C higher than the present temperature at its best analog location in summer time. The future precipitation and present precipitation at Ha Noi's best analog location by RCM under RCP8.5 are almost similar. In Kuala Lumpur, while the future temperature under RCP8.5 by GCM is about 3^{o}C higher than the present temperature at its best analog location, the future precipitation and present precipitation at its best analog location are fairly similar.

Good-analog, poor-analog and novel climate over SEA

Figure 4.9 displays the distribution of poor-, good-analog and novel climate locations at the end of the 21st century under the RCP4.5 and RCP8.5 for both the G_ENS and R_ENS experiments. For the RCP4.5 scenario, most of SEA showed good-analogs with coverage of 65% and 69% corresponding to the R_ENS and the G_ENS, respectively (**Table 4.2**). The detailed table of the fractions of novel climate in SEA according to each experiment, period and type of model (RCM/GCM) is shown in **Annex 3**. Only 2% of the SEA area in some islands and near-equatorial coastal areas is defined as novel climate locations with the R_ENS while this number is 0% for the G_ENS.

Poor-analog areas are concentrated mainly in low topographical regions, coastal regions and islands, with an area of 33% for the R_ENS and

31% for the G_ENS, respectively. It is shown that some of these poor-analog areas under the RCP4.5 become novel climate locations under the RCP8.5. In general, the results of the R_ENS and the G_ENS are quite similar for RCP4.5. Most ENS good-analog areas have good agreements with the individual experiments (shown as cross hatching in **Figure 4.9**, if at least 2/3 -

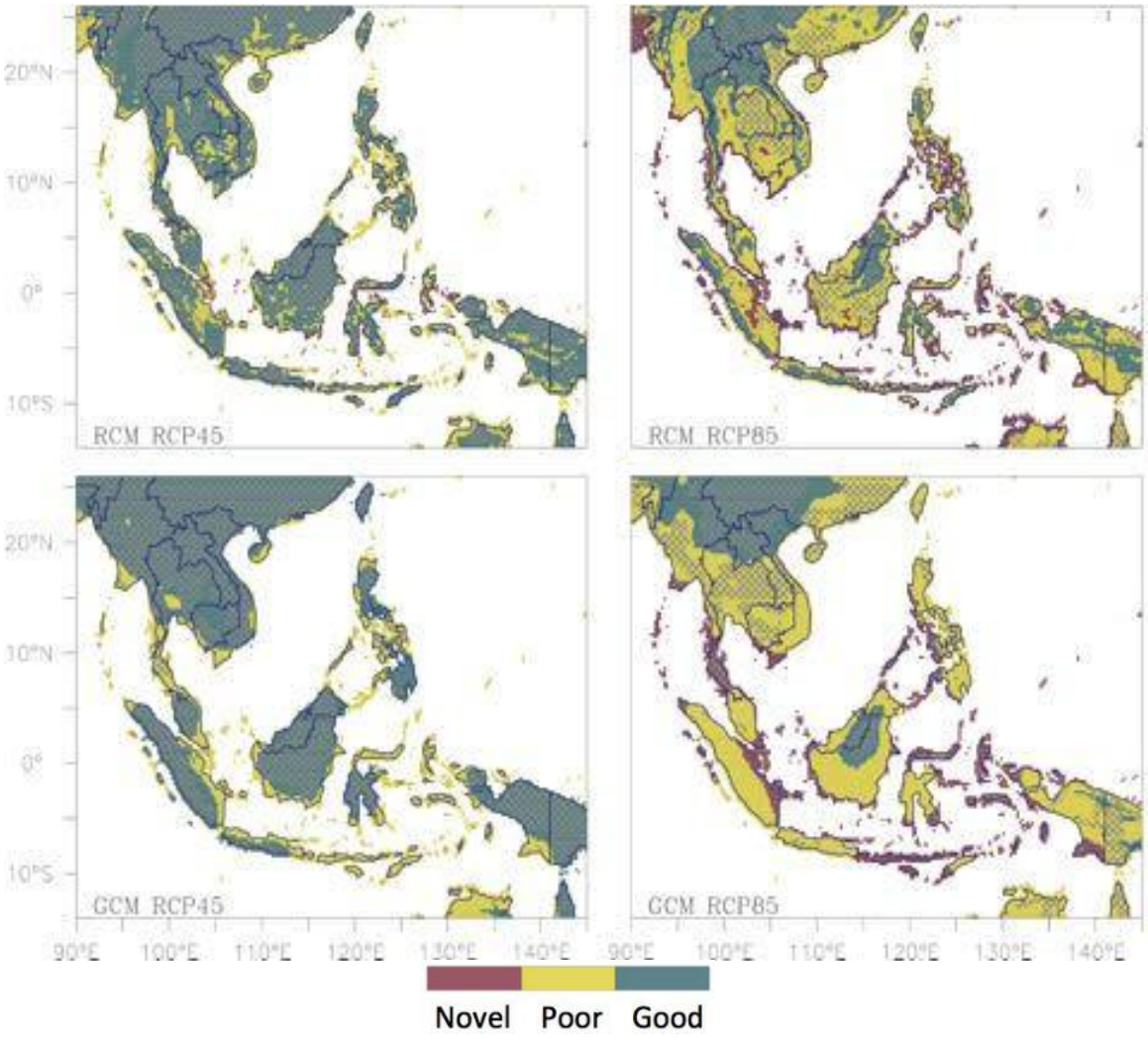

Figure 4.9. Locations of good-analog (green), poor-analog (yellow), and novel climate (red). Results are obtained from the R_ENS (upper) and G_ENS (lower) in the RCP4.5 and RCP8.5 scenario at the end of the 21st century and based on both temperature and precipitation. Cross hatching denotes the agreement of at least two thirds of the individual RCM or GCM experiments.

Table 4.2. Land ratio (%) in Southeast Asia for *TP*-, *T*- and *P*-novel climate, poor- and good- analogs resulted from the R_ENS and the G_ENS for the RCP4.5 and RCP8.5 at the end of the 21st century.

Scenario	Analog type	R_ENS			G_ENS		
		Novel	Poor	Good	Novel	Poor	Good
RCP4.5	TP_analog	2	33	65	0	31	69
	T_analog	5	15	80	2	33	65
	P_analog	0	1	99	0	0	100
RCP8.5	TP_analog	24	49	27	21	60	19
	T_analog	29	22	50	50	24	26
	P_analog	0	7	93	0	2	98

of the experiments show the same analog characteristic with the ENS), but very few ENS poor-analog areas have a high consistency among the models. It can be seen that the results in good-, poor-analog or novel climate are quite similar to the case of T-analog (**Figure 4.10**). With RCP4.5, the ratio of T-novel climate (T-poor analog) area is 5% (15%) and 2% (33%) for the R_ENS and the G_ENS, respectively. For precipitation, 0% of SEA has P-novel climate, and 93% to 100% of Southeast Asia has P-good analog for both the RCP4.5 and the RCP8.5 (Table 4.2). It means that future projected seasonal cycle of precipitation at most locations in SEA can be found in the present climate within the region, due to the substantial internal variability of precipitation and its non-significant climate change signal [37], [103].

For the RCP8.5 scenario, the ratio of areas with novel climate and poor-analog significantly increased compared to the RCP4.5. Twenty-four percent (21%) of Southeast Asia is defined as novel climate by the R_ENS (G_ENS). These areas are mainly located in low coastal areas and islands,

especially near equatorial areas, and overlap quite a lot with poor-analog areas defined in the RCP4.5 scenario. **Figure 4.9** shows that the member experiments are in good agreement in presenting the analog patterns in these areas. The precipitation distance values (S_P) are still much smaller than the temperature ones (S_T). With the G_ENS, fifty percent of the SEA

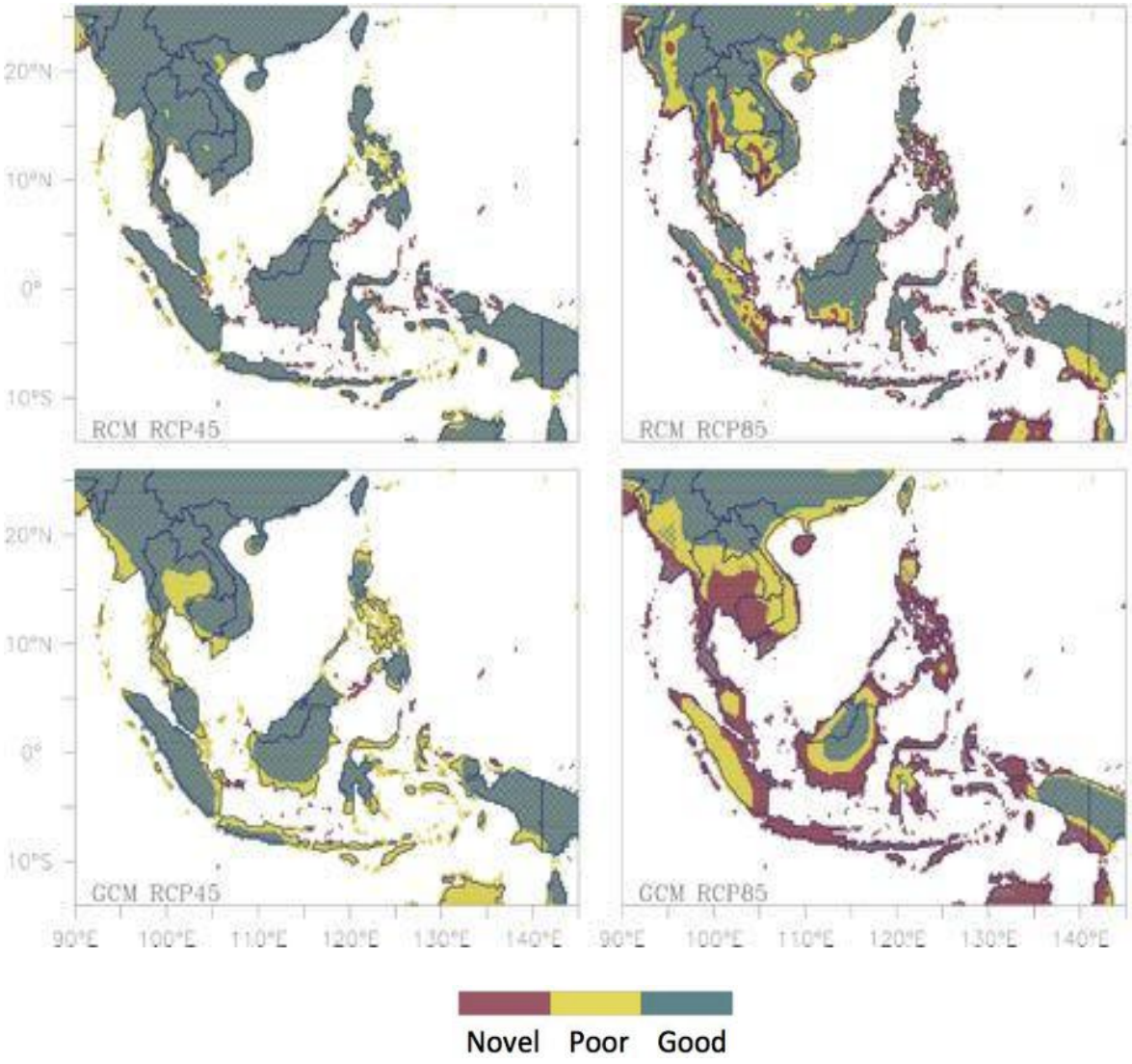

Figure 4.10. Locations of good-analog (green), poor-analog (yellow), and novel climate (red). Results are obtained from the R_ENS (upper) and G_ENS (lower) in the RCP4.5 and RCP8.5 scenario at the end of the 21st century and based on temperature only (i.e. $1/\beta \times T_{dis}$, according to Eq. 2.12). Cross hatching denotes the agreement of at least two thirds of the individual RCM or GCM experiments.

region has T-novel climate while this number is 29% for the R_ENS (**Table 4.2**). At the end of the 21st century, forty nine percent (27%) of SEA has poor-analog (good-analog) according to the R_ENS, while this ratio is 60% (19%) for the G_ENS. The RCM experiments show higher agreements than the GCM ones, especially over the Maritime Continent. The much lower percentage of novel climate under RCP4.5 compared to RCP8.5 can be resulted from lower temperature increase under RCP4.5 (over 1.5°C [79]) than under RCP8.5 (over 2°C [79]) at the end of the 21st century. This is also the reason why the percentage of poor analog under RCP4.5 is smaller than under RCP8.5 as temperature has a major role in identifying the percentage of novel and poor climate. As a result, the rest that is the percentage of good analog under RCP4.5 is bigger than under RCP8.5. Among the results on TP_analog under the two RCPs, the highest percentage of novel climate and the lowest percentage of good analog are under RCP8.5. The underlying values of **Figure 4.9** (i.e. the standard values S_{TP} are not classified into the three type of values) are shown in **Annex 4**.

The area of novel climate increases significantly under the RCP8.5 compared with that under the RCP4.5. Figure 4.9 – Figure 4.11 show that the future novel climate areas are strongly determined by the T-novel ones with some differences between the results of the R_ENS and the G_ENS. The underlying values of Figure 4.10 (Figure 4.11). It should be noted that Figure 3.5 showed the advantages of the RCM experiments compared to the GCMs when simulating temperature, particular for R_ENS. Thus, the novel climate results obtained with the R_ENS have certain advantages over the results from the GCMs. 100% of SEA land display significant differences between the projected temperature and baseline temperature with 95% confidence level for all the periods and the scenarios (analyzed in Section 4.1). For the case of precipitation, the ratios of land having rainfall differences with 95%

confidence level are lower compared to the case of temperature, especially under RCP4.5. The lower radiative forcing leads to a lower GHG concentration, making less significant differences between the future and the baseline period (for both temeperature and rainfall) under RCP4.5 compared to the case under RCP8.5. Therefore, the percentage of novel climate under RCP4.5 (5% when applying only temperature, and 2% when applying both te-

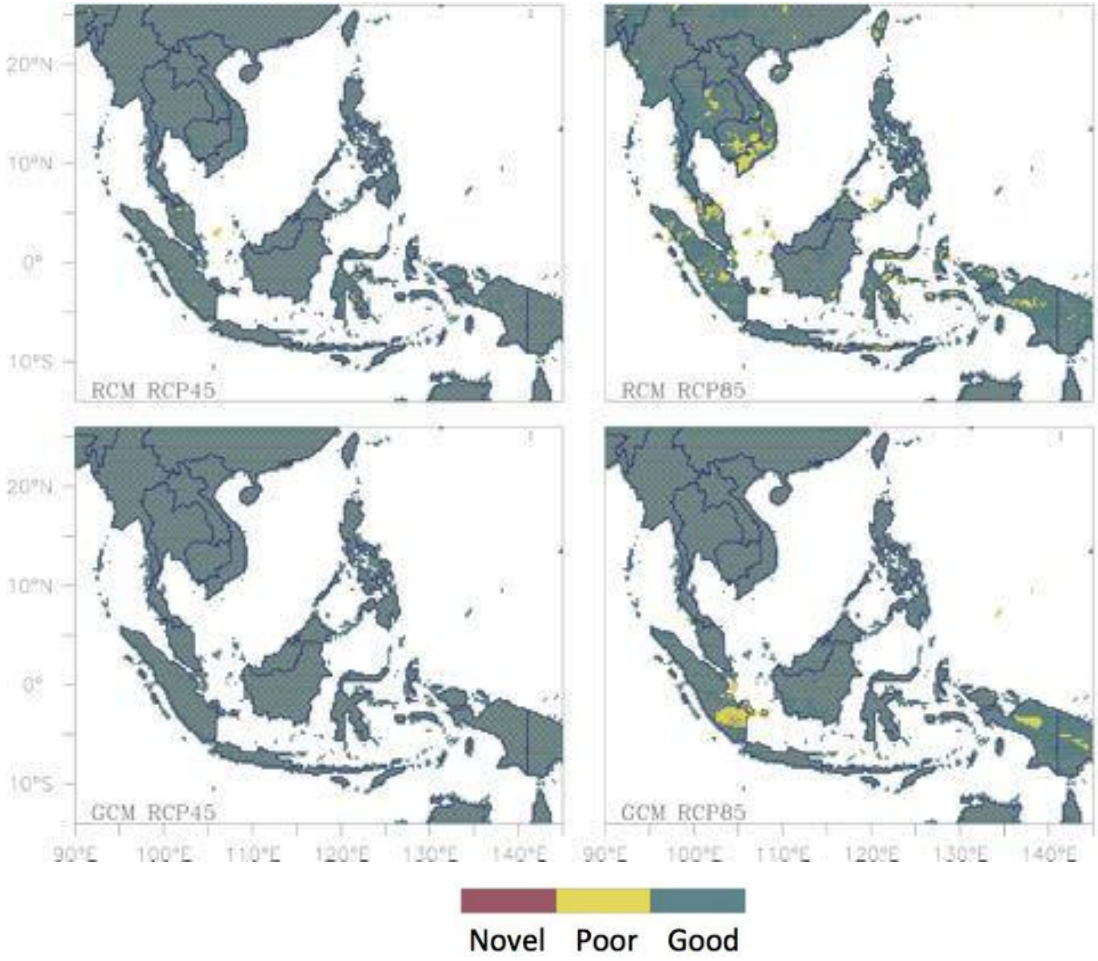

Figure 4.11. Locations of good-analog (green), poor-analog (yellow), and novel climate (red). Results are obtained from the R_ENS (upper) and G_ENS (lower) in the RCP4.5 and RCP8.5 scenario at the end of the 21st century and based on precipitation only (i.e. $\mathbf{1/\beta \times \alpha_{ENS} \times P_{dis}}$, according to Eq. 2.13). Cross hatching denotes the agreement of at least two thirds of the individual RCM or GCM experiments.

-mperature and precipitation, (Table 4.2)) is generally lower than that under RCP8.5. This result is presented in the study of Nguyen-Thi et al. [127].

4.3. Projected changes of temperature and rainfall in Viet Nam

Figure 4.12 depicts the projected temperature change in Viet Nam. Under the RCP4.5 for the mid-century period, the temperature changes in the whole country range from 1.2 to 1.8^{o}C, while this change in the CC Scenario is 1.3 – 1.7^{o}C. The temperature in the Northwest (NW), Northeast (NE), Red River Delta (RRD) regions generally increases by 1.6 – 1.8^{o}C. In the CC Scenario, the corresponding rise in these three regions was 1.6-1.7^{o}C. For the North Central (NC) region, the CC Scenario showed a projected change from 1.5-1.6^{o}C, while an increase of 1.4-1.6^{o}C is exhibited in the present study. The changes of 1.4-1.6^{o}C (1.3-1.4^{o}C) are also notable in the South Central (SC), Central Highlands (CH) and Southern Viet Nam (SV) regions based on the results of the current study (CC Scenario). Under the RCP4.5 for the period 2080-2099, the changes range from 1.8 to 2.2^{o}C (1.9-2.4^{o}C) in the northern and 1.6-1.8^{o}C (1.7-1.9^{o}C) in the southern Viet Nam according to the study (CC Scenario). In terms of significance test, the difference at a 5% significance level under the two RCPs and two periods are all 100%.

Under the RCP8.5 scenario during the 2046-2065 period, the temperature in the whole country rises by 1.8-2.4^{o}C (1.8-2.3^{o}C) by the present study (CC Scenario). For the northern and southern parts, the temperature increases by 2.0-2.4^{o}C and 1.8-2.0^{o}C, respectively. By the end of the century under the RCP8.5, the changes of 3.4 – 4.2^{o}C (3.0-3.4^{o}C) are found in the northern (southern) part. It can be indicated that the projected T2m changes by the CC Scenario and the present study are particularly similar under both the scenarios and periods (**Table 4.3**). Figure 4.13 shows the longitudinally --

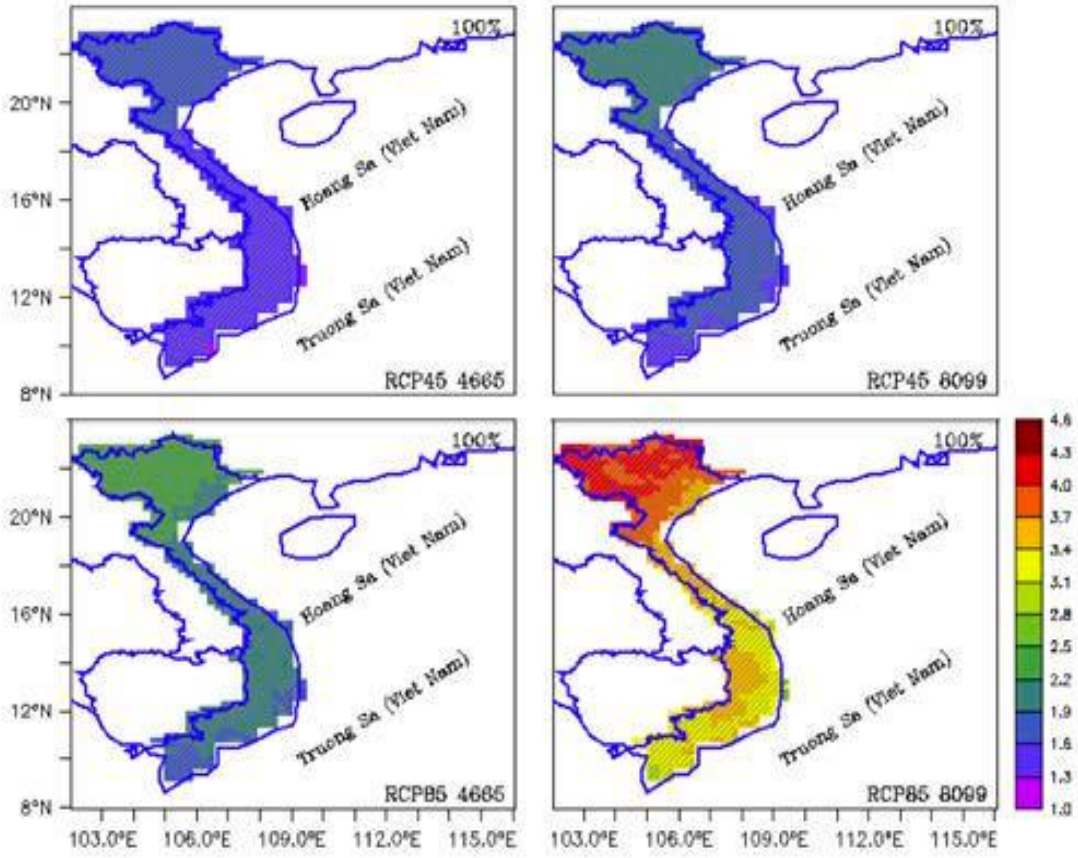

Figure 4.12. Projected temperature changes (ºC) in Viet Nam under the RCP4.5 and RCP8.5 scenarios for the periods 2046-2065 and 2080-2099 compared to the baseline period 1986-2005. Difference at 5% significance level under t-test indicated by diagonal lines and the number in the upper-right corner of each panel shows the percentage of grid points with significant differences.

averaged temperature and the temperature changes at each latitude by the mid- and far-future periods under the two scenarios in Viet Nam. The projected changes increase by 1.3 – 1.8^{o}C (1.7 – 2.4^{o}C) and 1.5 – 2.1^{o}C (2.9 – 4.1^{o}C) by the mid- and far-future periods under the RCP4.5 (RCP8.5), which are relatively similar to those shown in Figure 4.12.

Figure 4.14 depicts the relative rainfall changes in Viet Nam with the 10 to 5% (5-15%) range in the whole country under the RCP4.5 for the period

2046-2065 based on the present study (CC Scenario). The changes range from -10 to 5% and -10 to 0% in the present study by the far-future under the RCP4.5 and by the mid-future under the RCP8.5. By the end of the 21st century under the RCP8.5, the rainfall in most of the country changes from 25 to 5% (Table 4.4). The differences at 5% significance level is very high under RCP8.5, which are 89% and 98% in the middle and at the end of the century, respectively. This is due to more apparent rainfall change under RCP8.5 than under RCP4.5.

Similar to **Figure 4.14**, Figure 4.15 indicates relative rainfall changes in Viet Nam but with cross hatching denoting the agreement of at least four o-

Table 4.3. Temperature change (ºC) projected by the CC Scenario and by the present study in the regions of Viet Nam, compared to the reference period 1986-2005.

Scenario	Period	Region	Temperature change (ºC)	
			The CC Scenario	The present study
RCP4.5	2046-2065	Whole country	1.3-1.7	1.2-1.8
		NW, NE, RRD	1.6 – 1.7	1.6-1.8
		NC	1.5-1.6	1.4-1.6
		SC, CH, SV	1.3-1.4	1.2-1.6
	2080-2099	Northern part	1.9-2.4	1.8-2.2
		Southern part	1.7-1.9	1.6-1.8
RCP8.5	2046-2065	Whole country	1.8-2.3	1.8-2.4
		Northern part	2.0-2.3	2.0-2.4
		Southern part	1.8-1.9	1.8-2.0
	2080-2099	Northern part	3.3-4.0	3.4-4.2
		Southern part	3.0-3.5	3.0-3.4

-ut of the six individual RCM experiments. The highest agreement is found under RCP8.5 at the end of the century with the almost coverage of the Viet Nam land while only under 50% Viet Nam is with the model agreement under

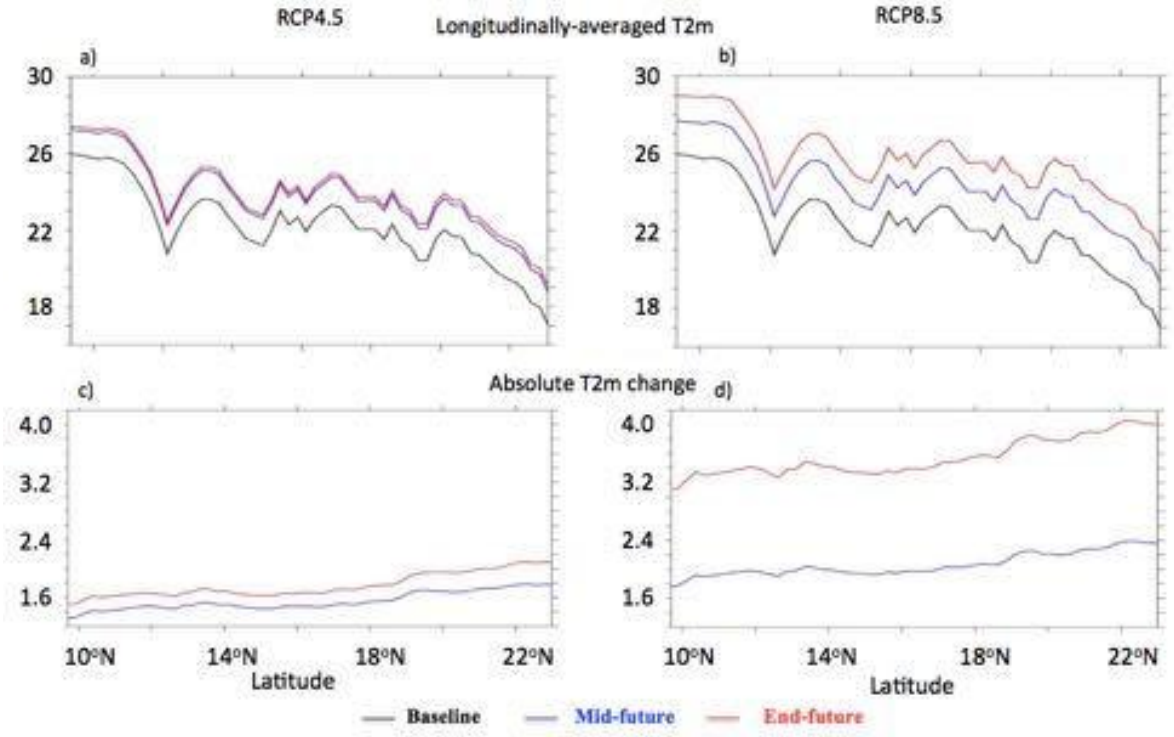

Figure 4.13. Longitudinally averaged temperature (a, b) and T2m change (c, d) for each latitude over Vietnam for the baseline period (black line), the mid-future (blue) and the far-future (red) under the RCP4.5 (left column) and the RCP8.5 (right column).

Table 4.4. As in Table 4.3 but for relative rainfall change (%).

Scenario	**Period**	**Rainfall (%)**	
		The CC scenario	**The present study**
RCP4.5	2046-2065	5-15	-5 to 5
	2080-2099	5-15	-10 to 5
RCP8.5	2046-2065	5-15	-10 to 0
	2080-2099	most > 20	-25 to 5

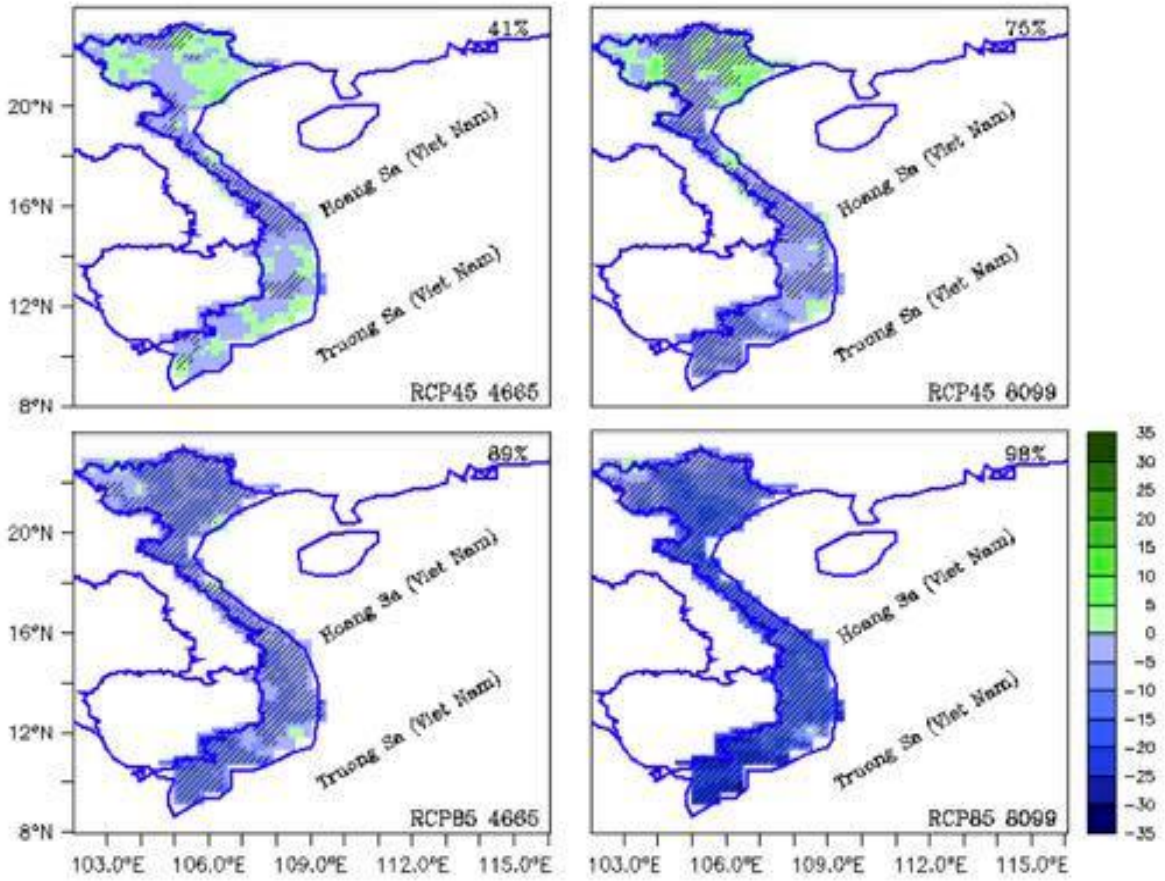

Figure 4.14. Projected relative rainfall change (%) in Viet Nam under the RCP4.5 and RCP8.5 scenarios for the periods 2046-2065 and 2080-2099 compared to the baseline period 1986-2005. Difference at 5% significance level under t-test indicated by diagonal lines and the number in the upper-right corner of each panel shows the percentage of grid points with significant differences.

RCP4.5 in the middle of the century. The region with the highest projection uncertainty under both RCP and two periods locates in the Northwest and North Central of Viet Nam.

In general, the projected rainfall under the RCP4.5 for both the periods is rather similar to that in the baseline with a slight decrease in the future. This decreasing trend is more significant under the RCP8.5, which is down to 10%

(mid-future) and -25% (far-future) (Figure 4.15). This indicates a drier tendency projected at the end of the century in Viet Nam, leading to more drought events possibly occurring in the future. It should be noted that the results from the CC scenario suggested an overall increasing rainfall trend over the whole country. The differences in the projected results between our present study and the CC scenario can be attributed to the methodology and the different downscaling experiments used. The conclusion on the various downscaled precipitation patterns by RCMs was shown in the previous studies (e.g. [74], [83], [162]). It is worth to mention that a number of previo--

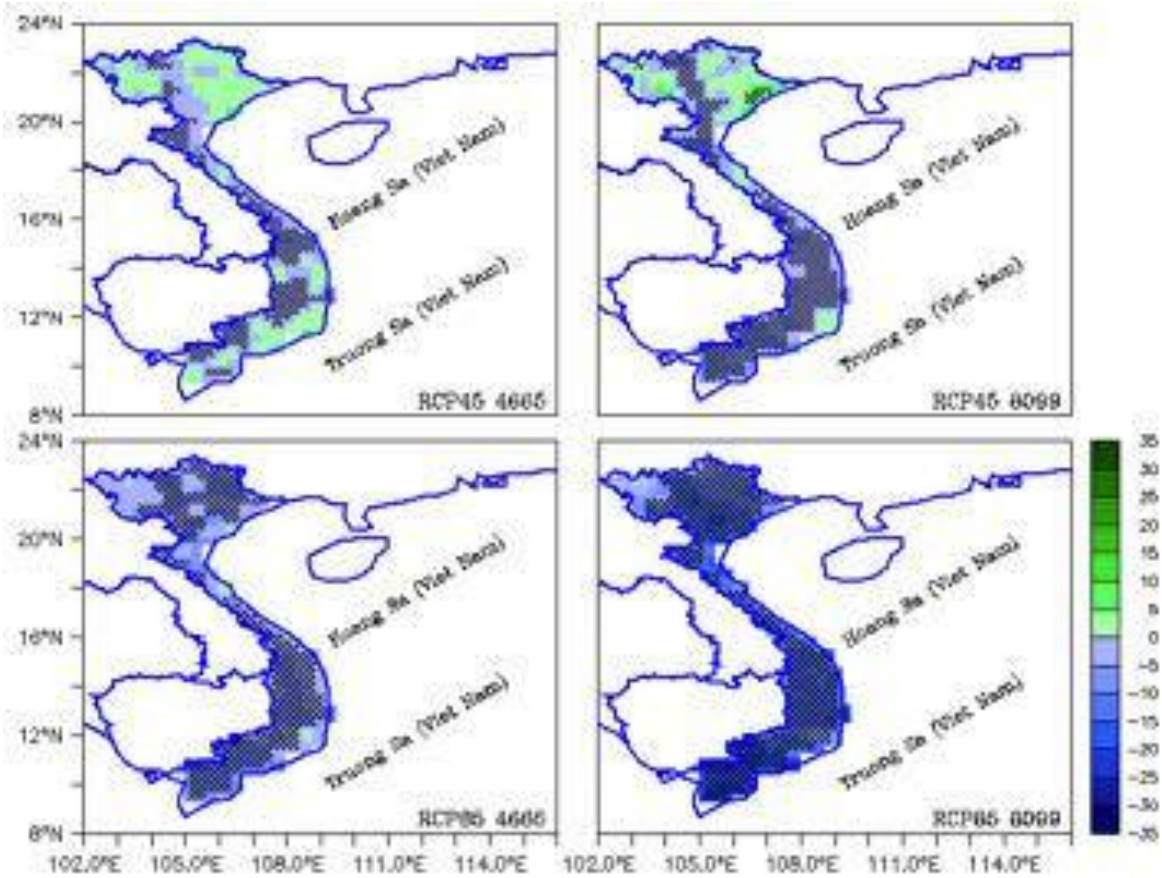

Figure 4.15. Projected relative rainfall change (%) in Viet Nam under the RCP4.5 and RCP8.5 scenarios for the periods 2046-2065 and 2080-2099 compared to the baseline period 1986-2005. Cross hatching denotes the agreement of at least two thirds of the individual RCM experiments.

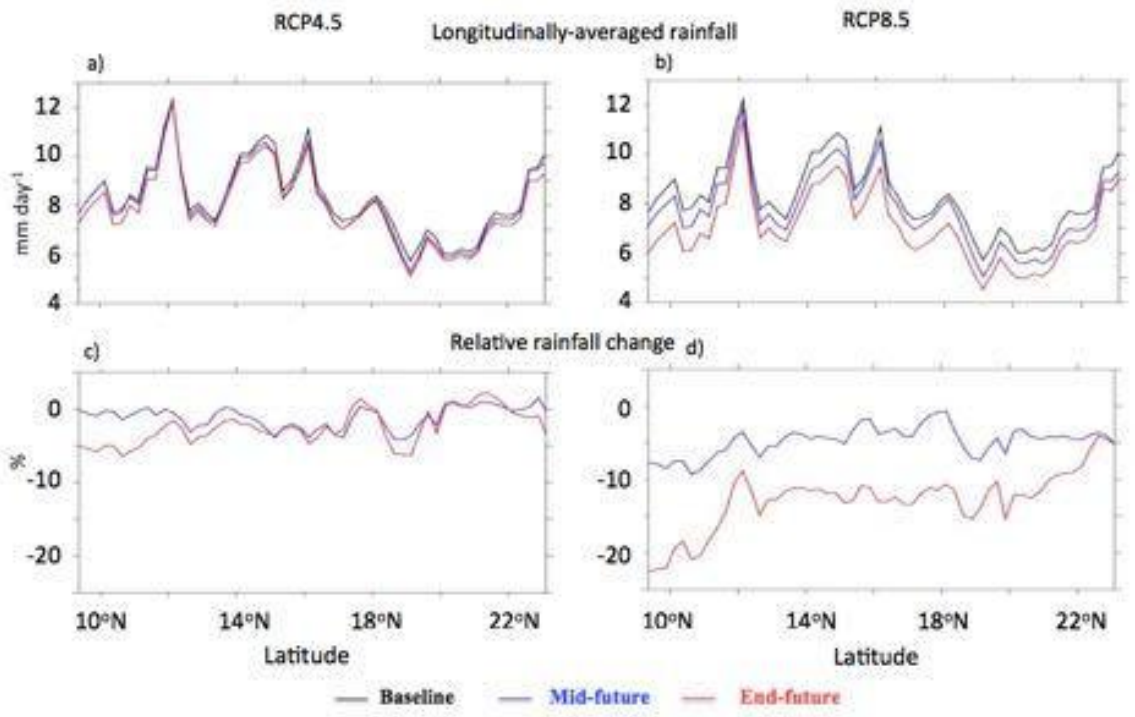

Figure 4.16. Longitudinally averaged rainfall (a, b) and rainfall change (c, d) for each latitude over Vietnam for the baseline period (black line), the mid-future (blue) and the far-future (red) under the RCP4.5 (left column) and the RCP8.5 (right column).

-us studies also showed the drier tendency of future projected rainfall over some locations of Viet Nam and SEA at specific time points in the year (e.g. [105], [124], [138], [155], [156]). Ho et al. [72] and Manomaiphiboon et al. [105] attributed the decreasing trend of summer precipitation to both the relationship between the projected rainfall and sea surface temperature (SST) and weakening of summer monsoon from the West.

4.4. Relocation of cities' climate and climate analog in Viet Nam

This section identifies best analog locations of 78 cities in Viet Nam within the domain of SEA and disappearing climate in the future in Viet Nam with regional climate experiments resulted from the SEACLID/CORDEX-SEA project.

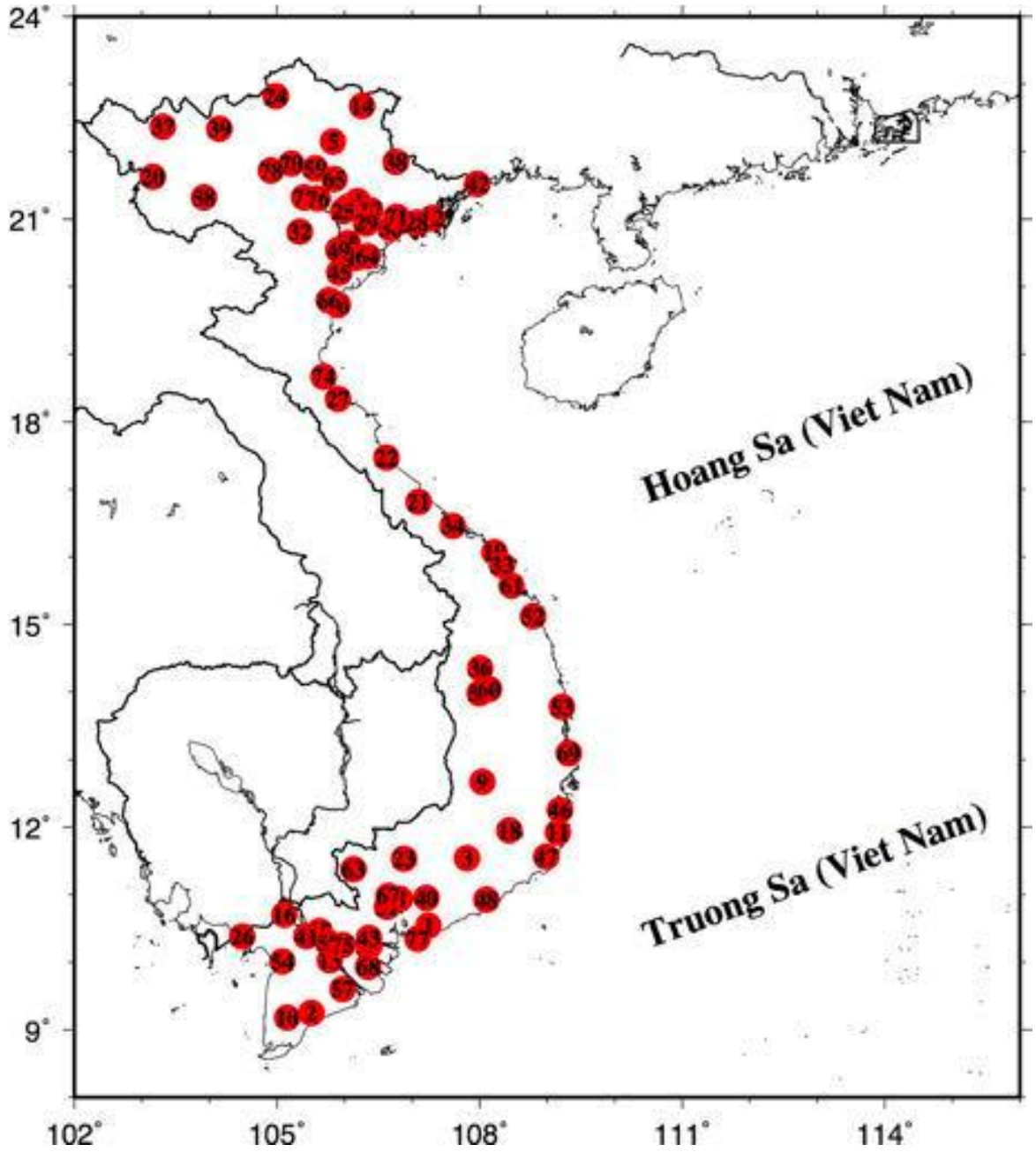

Figure 4.17. The locations of 78 cities (displayed with red circles and numbered from 1 to 78 according to the respective order of cities in the **Table 4.5**) in Viet Nam used in this study.

The best analog location of the target grid point is the point at which the climate distance *ClimD* is defined to be the minimum. Based on this, the best analog locations of 78 cities in Viet Nam (Figure 4.17, Table 4.5) are identified. For illustrative purposes, only analyses for five central cities

including Ha Noi, Hai Phong, Da Nang, Ho Chi Minh and Can Tho are conducted in the following part.

Climatic relocation of five central cities in Viet Nam

Based on the ranking of the experiments in the previous part, ENS and CNRM are proved to be the best and ECEA to be the worst. These three experiments are chosen for analyzing the climate analog in the following sections, so the performances of the best and the worst experiments are shown.

Figure 4.18 shows the locations of the best climate analog (with minimum climate distance) of the five central cities in Viet Nam projected by the CNRM, ECEA and ENS experiments. The best analog locations tend to be located southward from the reference cities. Those of Ha Noi, Hai Phong and Da Nang are close to their original cities except for the RCP8.5 scenario with the ENS experiment while those of Ho Chi Minh and Can Tho are at far distances from their origins. The ECEA future climates of both Ho Chi Minh and Can Tho under the RCP8.5 are similar to the present climate of Illoning, Maluku, Indonesia (131.375E, 4.125S). The ENS future climate of Can Tho for both the scenarios and of Ho Chi Minh under RCP4.5 are analogous to the present climate of Penang island, Malaysia (100.125E, 6.125N). The climate distances under the RCP8.5 are greater than those under the RCP4.5 (Table 4.5).

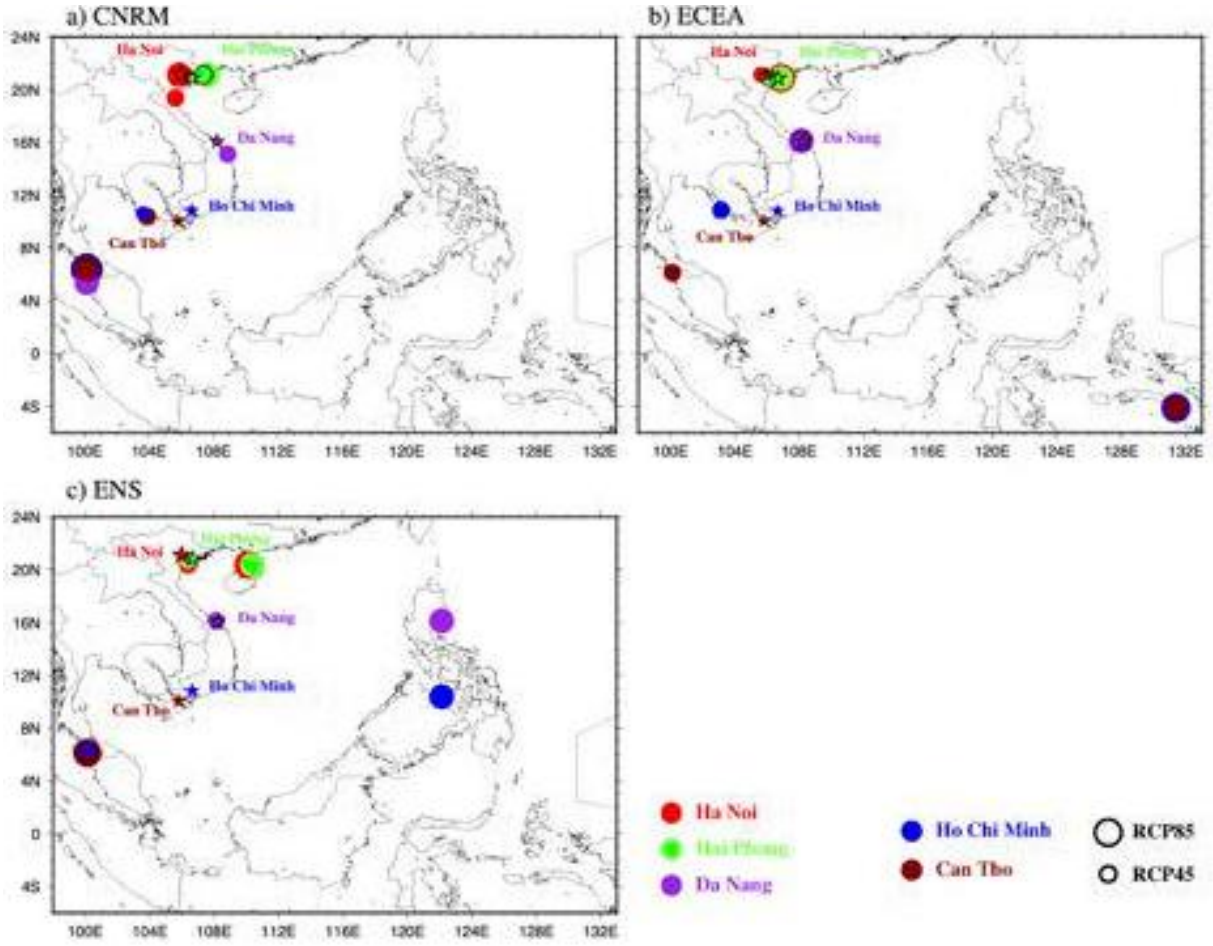

Figure 4.18. Climatic relocation of 5 central cities (Ha Noi – red, Hai Phong – green, Da Nang – purple, Ho Chi Minh – blue, and Can Tho – darkred circles) in Viet Nam at the end of the 21st century under the RCP4.5 (smaller circles) and the RCP8.5 scenario (larger circles) with the a) CNRM, b) ECEA and c) ENS experiment. The original locations of the 5 cities are marked with star symbols.

Table 4.5. The original and best analog locations within the SEA domain of 78 cities in Viet Nam and their respective climate distances (CD) under the RCP4.5 and RCP8.5 scenarios, obtained with the ENS experiment.

No.	Reference city	Original locations		Best Analog RCP4.5			Best Analog RCP8.5		
		Lon	Lat	Lon	Lat	ClimD	Lon	Lat	ClimD
1	Ba Ria	107.243	10.542	99.625	7.125	0.758	122.125	10.375	1.763
2	Bac Lieu	105.510	9.250	99.375	6.625	1.570	124.125	6.125	2.469
3	Bao Loc	107.812	11.542	107.125	12.375	0.581	99.375	11.375	0.768
4	Bac Giang	106.190	21.270	105.875	21.125	0.859	110.125	20.375	1.567
5	Bac Kan	105.830	22.150	108.625	21.875	0.419	110.375	21.375	0.817
6	Bac Ninh	106.050	21.180	106.375	20.625	1.058	110.125	20.375	1.667
7	Ben Tre	106.370	10.240	100.125	6.375	1.011	100.125	6.375	1.737
8	Bien Hoa	106.820	10.940	100.125	6.375	0.852	100.125	6.375	1.691
9	Buon Ma Thuot	108.040	12.670	107.375	12.875	0.944	99.875	12.875	1.255
10	Ca Mau	105.150	9.180	99.875	6.375	1.010	99.875	6.375	1.780
11	Cam Ranh	109.160	11.920	97.625	5.125	1.234	108.125	4.125	1.551
12	Cam Pha	107.300	21.020	109.375	19.875	1.096	110.375	20.875	1.770
13	Can Tho	105.780	10.030	100.125	6.125	0.760	100.125	6.125	1.890
14	Cao Bang	106.260	22.680	109.375	21.875	0.450	111.625	21.625	0.890
15	Cao Lanh	105.630	10.460	100.125	6.125	0.803	100.125	6.375	1.870
16	Chau Doc	105.108	10.702	100.125	6.375	0.776	100.125	6.375	1.759
17	Chi Linh	106.383	21.133	106.375	20.625	0.953	106.375	20.375	1.632
18	Da Lat	108.440	11.950	108.375	14.125	0.800	107.625	12.625	0.870
19	Da Nang	108.220	16.068	108.125	16.125	1.430	122.125	16.125	2.370
20	Dien Bien Phu	103.160	21.630	105.375	22.375	0.750	106.875	21.375	0.820
21	Dong Ha	107.100	16.816	107.625	16.625	1.076	109.125	14.625	1.777

22	Dong Hoi	106.620	17.469	106.875	17.125	1.070	108.375	15.875	1.812
23	Dong Xoai	106.880	11.530	98.875	8.125	0.959	123.875	7.625	1.557
24	Ha Giang	104.980	22.823	104.875	22.625	0.391	114.125	22.875	0.977
25	Ha Noi	105.980	21.120	106.375	20.375	1.100	110.125	20.375	1.660
26	Ha Tien	104.487	10.380	99.625	7.125	1.284	98.375	9.625	2.459
27	Ha Tinh	105.905	18.340	105.875	18.375	1.084	106.875	17.375	1.699
28	Ha Long	107.070	20.950	110.125	18.375	1.403	106.875	20.625	2.049
29	Hai Duong	106.320	20.938	105.625	20.875	1.007	106.375	20.375	1.737
30	Hai Phong	106.680	20.860	106.375	20.625	1.170	110.375	20.375	1.710
31	Ho Chi Minh	106.630	10.820	100.125	6.375	0.780	122.125	10.375	1.780
32	Hoa Binh	105.337	20.817	105.625	20.875	1.007	110.375	20.375	1.621
33	Hoi An	108.335	15.879	108.375	15.875	1.380	122.375	18.125	2.236
34	Hue	107.600	16.460	108.875	15.125	1.050	108.625	15.625	1.540
35	Hung Yen	106.050	20.646	106.375	20.375	0.998	106.375	20.375	1.758
36	Kon Tum	108.008	14.350	106.375	15.375	0.718	107.875	12.875	0.809
37	Lai Chau	103.310	22.368	105.375	22.375	0.746	109.625	21.875	0.826
38	Lang Son	106.760	21.850	105.375	20.875	0.523	106.125	20.375	0.934
39	Lao Cai	104.148	22.338	107.875	22.125	0.501	105.125	21.375	0.822
40	Long Khanh	107.211	10.951	98.875	8.125	0.838	122.125	10.375	1.646
41	Long Xuyen	105.435	10.386	100.125	6.125	0.789	100.125	6.375	1.797
42	Mong Cai	107.966	21.524	110.125	21.375	1.003	110.625	19.625	1.442
43	My Tho	106.360	10.360	98.875	8.125	0.984	100.125	6.375	1.538
44	Nam Dinh	106.177	20.430	106.375	20.375	1.040	106.125	20.125	1.801
45	Ninh Binh	105.920	20.210	106.375	20.375	1.006	106.125	20.125	1.722
46	Nha Trang	109.190	12.250	108.625	15.625	1.160	118.375	9.125	1.610
47	Phan Rang – Thap Cham	108.988	11.560	109.125	14.125	0.982	122.375	18.375	1.195

48	Phan Thiet	108.100	10.928	104.875	9.625	0.541	123.625	9.625	1.390
49	Phu Ly	105.910	20.545	106.125	20.375	0.983	110.375	20.375	1.596
50	Phuc Yen (Vinh Phuc)	105.705	21.237	105.625	21.125	1.115	110.125	20.375	1.797
51	Pleiku	108.000	13.983	107.625	13.625	0.277	120.125	15.125	0.907
52	Quang Ngai	108.790	15.120	108.875	15.125	1.440	118.625	9.375	2.117
53	Quy Nhon	109.220	13.780	108.625	15.625	1.220	122.375	18.125	1.640
54	Rach Gia	105.080	10.012	100.125	6.375	0.913	99.875	6.375	1.907
55	Sa Dec	105.756	10.290	100.125	6.125	0.803	100.125	6.375	1.936
56	Sam Son	105.899	19.733	105.875	19.375	1.154	110.625	20.375	1.808
57	Soc Trang	105.970	9.600	100.125	6.125	0.750	100.125	6.375	1.810
58	Son La	103.918	21.325	101.375	20.875	0.829	95.875	23.875	0.848
59	Song Cong	105.565	21.749	105.625	21.125	0.844	111.375	21.375	1.479
60	Tam Diep	108.138	14.041	106.125	15.375	0.872	105.125	14.375	0.806
61	Tam Ky	108.474	15.573	108.875	15.125	1.224	108.625	15.625	1.910
62	Tan An (Long An)	106.405	10.538	100.125	6.375	0.793	100.125	6.375	1.739
63	Tay Ninh	106.131	11.375	99.625	7.125	0.814	99.625	7.125	1.852
64	Thai Binh	106.340	20.450	105.875	19.625	1.171	110.625	20.375	1.872
65	Thai Nguyen	105.848	21.594	105.625	21.125	0.820	111.375	21.375	1.473
66	Thanh Hoa	105.770	19.800	106.875	20.625	1.090	110.625	20.375	1.700
67	Thu Dau Mot	106.650	10.980	100.125	6.375	0.776	122.125	10.375	1.783
68	Tra Vinh	106.349	9.933	100.125	6.375	0.763	123.875	7.625	1.976
69	Tuy Hoa	109.320	13.095	101.625	6.875	1.403	104.125	2.875	1.864
70	Tuyen Quang	105.214	21.823	105.375	21.125	0.723	109.875	21.125	1.421
71	Uong Bi	106.770	21.034	105.625	19.625	0.905	110.375	20.375	1.387
72	Vi Thanh (Hau Giang)	105.470	9.784	100.125	6.125	0.805	100.125	6.125	1.721
73	Viet Tri	105.401	21.322	105.625	21.125	1.041	110.375	20.375	1.619

74	Vinh	105.690	18.670	106.875	17.375	0.880	106.875	17.375	1.470
75	Vinh Long	105.972	10.253	100.125	6.125	0.803	100.125	6.375	1.936
76	Vinh Yen (Vinh Phuc)	105.604	21.308	105.625	21.125	1.065	107.875	20.875	1.648
77	Vung Tau	107.080	10.345	99.625	6.875	0.948	122.375	9.625	2.167
78	Yen Bai	104.911	21.723	105.125	21.375	0.914	110.125	20.625	1.700

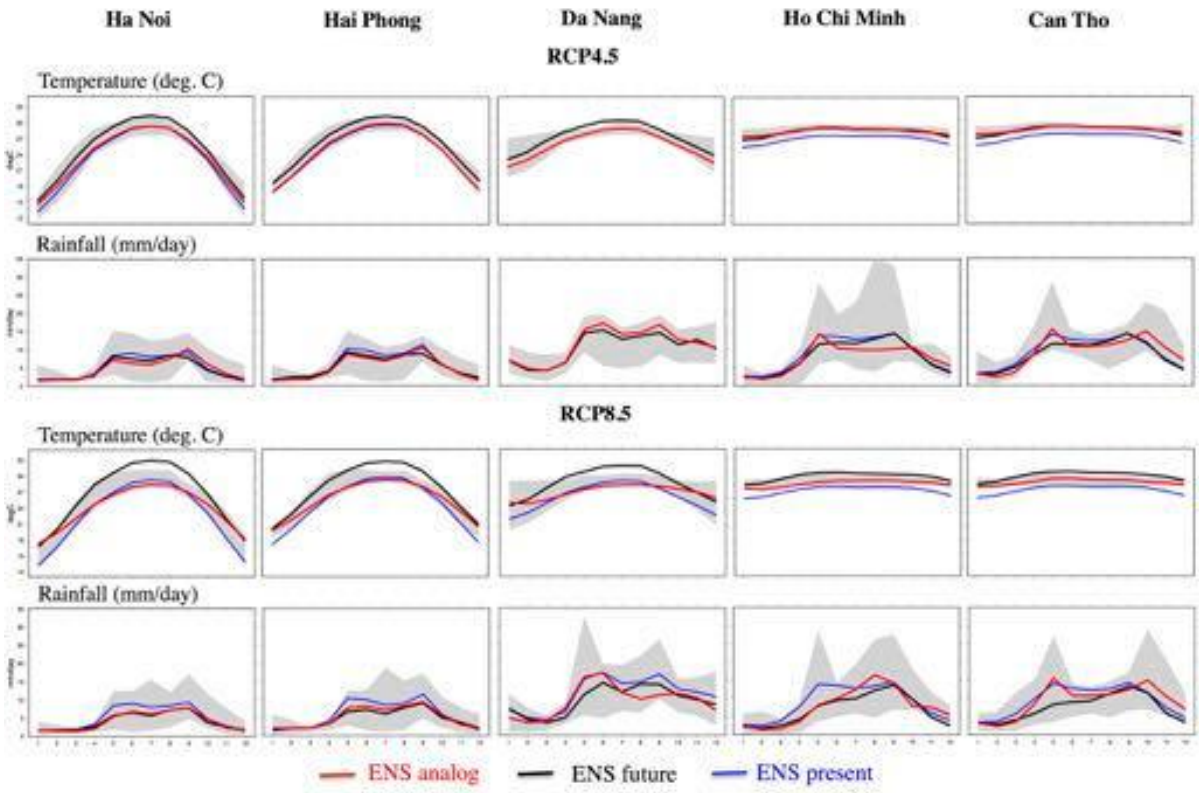

Figure 4.19. Seasonal cycles of temperature and precipitation of the five central cities (Ha Noi, Hai Phong, Da Nang, Ho Chi Minh and Can Tho) in Viet Nam. Blue and black lines show the present and future projected cycles of a reference site, respectively. Red lines represent the present cycles of the respective best analog location with the ENS experiment. Grey shading displays the range of 6 RCMs at the best analog location.

Figure 4.19 describes the future seasonal cycles of temperature and precipitation of the five central cities (black lines), which generally fit well with the present cycles of the analog locations (red lines). There is a better similarity for temperature than for precipitation, and for the RCP4.5 than for the RCP8.5. The future precipitation in Ho Chi Minh and Can Tho is not in good agreement with the present one at the analog locations under both the scenarios. This is also appropriate for Da Nang under the RCP8.5. The results shown in Figure 4.19 are in line with those shown in Figure 4.18c, i.e. the

distances between Ho Chi Minh and Can Tho and their analog locations are large for both the RCP4.5 and the RCP8.5. For the case of Hai Phong, the present temperature at the best analog location is 4^{o}C lower in summer time compared to the future temperature in Hai Phong under RCP8.5. In Da Nang, the precipitation at the bes analog location is a little higher than the projected future precipitation under RCP4.5. In Can Tho, the temperature at the best analog location is almost similar to the projected future temperature under RCP4.5 but about 1.5^{o}C lower under RCP8.5.

Disappearing climate in Viet Nam

The land fractions of disappearing climate in Viet Nam are 0.66%, 1.75% and 2.39% for the CNRM, ECEA and ENS experiments under the RC-

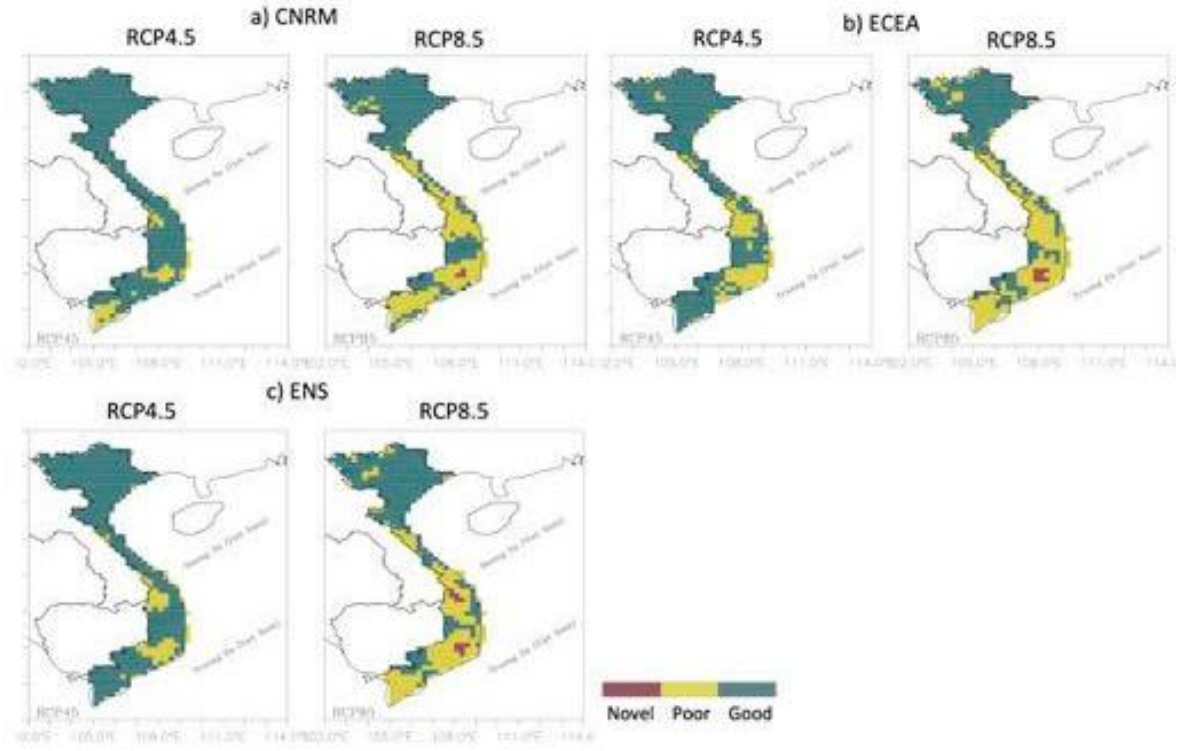

Figure 4.20. Locations of good analog (green), poor analog (yellow), and disappearing climate (red) in Viet Nam. Results are obtained under the RCP4.5 and RCP8.5 scenario at the end of the 21st century with the a) CNRM, b) ECEA and c) ENS experiment.

Table 4.6. Land ratio (%) of disappearing climate, poor- and good-analogs within the Viet Nam domain projected from the CNRM, ECEA and ENS experiments for the RCP4.5 and RCP8.5 scenarios at the end of the 21st century.

Experiment	RCP	Disappearing	Poor-analog	Good-analog
CNRM	RCP45	0.00	8.47	91.53
	RCP85	0.21	27.59	72.19
ECEA	RCP45	0.00	21.19	78.81
	RCP85	0.79	42.70	56.51
ENS	RCP45	0.00	10.72	89.28
	RCP85	0.85	35.15	64.00

-P8.5, respectively (**Table 4.6**). This means that we can almost find a location within the SEA region at which the projected future climate is close to the present climate of a given place in Viet Nam. The present climate in only a few small parts in the Northern and Southern Central Highlands of Viet Nam (red parts in **Figure 4.20**) will disappear in SEA in the future. This is in agreement with the results of Williams et al. [175], which showed that disappearing climate was located in mountainous tropical areas. The good-analog percentage is high (~80% - 90%) under the RCP4.5 and lower (~53% - 62%) under the RCP8.5. The poor-analog percentage accounts for 37% - 44% of the Viet Nam land under the RCP8.5, which mainly lies in the Central and Southern Viet Nam (**Figure 4.20**). This indicates that the warmer regions tend to be poor analog or disappearing climate locations in the future while the cooler ones (e.g. the Northern Viet Nam) show good-analog characteristics.

4.5. Chapter 4 summary

Chapter 4 presented the projected temperature and rainfall changes in the SEA region in the mid- (2046-2065) and far- (2080-2099) future periods

under the RCP4.5 and RCP8.5 scenarios. The projected temperature changes range from 1 to 2.2^{o}C (1.3 to 2.8^{o}C) for the period 2046-2065 and from 1 to 2.5^{o}C (2.5 to 4.6^{o}C) for the period 2080-2099 under the RCP4.5 (RCP8.5). The northern areas of SEA have higher temperature increases. By the end of the century under the RCP8.5, the rainfall was projected to decrease by -30% while it ranges from -25 to 30% under the RCP4.5. T-test was applied to define the difference between the means of baseline and future data. With 5% significance level, 100% land area in SEA had difference in temperature. For precipitation, the highest percentage (89%) was for the period 2080-2099 under RCP8.5 and the lowest fraction (49%) was for the period 2046-2065 under RCP4.5.

Climate analog and novel climate analysis in the SEA region were implemented using a modified version of the formulation presented by Fabienne et al. [51] to estimate climate distance. A common tendency of climatic relocation for the six selected cities in SEA towards warmer regions was prominent with the regional ENS experiment. Under the RCP8.5 at the end of the century, the future climate of Ha Noi is most similar to the present climate of the location with grid point ~110.125E, 20.375N; Jakarta – the Supiori island of Indonesia (~135.625E, 0.875S); Manila – the Negros Occidental province (~122.375E, 9.625N); Kuala Lumpur – the West Pasaman Regency (~99.375E,0.125N) in West Sumatra, Indonesia; and Bangkok – very close to its origin.

Under the RCP4.5, the percentages of novel climate areas in SEA at the end of the 21st century were projected to be 2% and 0% for the regional and global ENS experiments, respectively. These percentages remarkably increased under the RCP8.5, to respectively 24% and 21%. The novel climate areas, strongly determined by the future temperature change, mainly located

in low elevation, coastal, equatorial regions and islands. With the advantages of the RCM experiments compared to the GCMs when simulating temperature, the novel climate results obtained with the regional ENS experiment could be more robust compared to those obtained with the global one. The results of this study on climate analog and future appearance of novel climate would provide valuable information for climate change communication, impact assessments and adaptation strategies in the SEA region.

In Viet Nam

It generally showed similar temperature changes with the results presented in the CC Scenario. Under the RCP8.5 (RCP4.5), the mean temperature changes in the whole country were projected to increase by up to 4.2^{o}C (2.4ºC) at the end of the 21st century compared to the reference period 1986-2005. Regarding rainfall, a drier tendency was projected, particularly down to -25% in the far-future under the RCP8.5. It should be taken into account the different results from the CC scenario, in which an overall increasing rainfall trend over the whole Vietnam was projected. Thus, it would be of great importance to conduct a further study to investigate the reliability of different projected rainfall results, as this information is particularly essential for stakeholders, decision makers and other societal entities in preparing adaptation and mitigation strategies for climate change.

Chapter 4 also showed the climatic relocations of 78 cities in Viet Nam in the future under the RCP4.5 and RCP8.5 scenarios, which generally exhibited a southward tendency. The climate distance under the RCP8.5 was larger than that under the RCP4.5. The climate analog locations of Ha Noi, Hai Phong and Da Nang were closer to their original cities than those of Ho Chi Minh and Can Tho. In the future, about 2.39% of Viet Nam land, mainly

located in the Central Highlands and Southern Viet Nam, was projected to experience disappearing climate by the ENS experiment under the RCP8.5. It should be noted that the climate distance threshold for identifying disappering climate was a subjective threshold, thus the information about the disappearing area of 2.39% should be used with caution. The poor-analog locations are prominent in the Central and Southern Viet Nam while the good-analog areas are mainly in the Northern Viet Nam.

CONCLUSIONS AND RECOMMENDATIONS

1. Conclusions

In the thesis, the 2-m temperature and rainfall variables were evaluated and projected over SEA and Viet Nam. Climate analog, disappearing and novel climate analysis over SEA and Viet Nam were also implemented. The RegCM4.3 model was used to downscale six the CMIP5 GCMs under the framework of SEACLID/CORDEX-SEA project. The results showed that:

i. Regional downscaling allowed a more accurate representation of temperature but displayed a higher variability of rainfall over SEA compared to the results of the GCMs.

ii. The ENS had advantages in reproducing temperature and rainfall variations compared to individual GCM and RCM experiments in SEA and Viet Nam.

iii. A modified version of the existing formulation to estimate climate distance was introduced with weighting factors for temperature and precipitation, and for the ensemble.

iv. A common tendency of climatic relocation for the six big cities in SEA including Ha Noi, Manila, Kuala Lumpur, Bangkok, Jakarta and HinthadaHinthada towards warmer regions is prominent with the regional ENS experiment.

v. The percentages of novel climate areas in SEA at the end of the 21st century were projected to be 24% (RCM ENS) and 21% (GCM ENS) under the RCP8.5.

vi. Novel climate are mainly located in coastal areas and islands, especially near equatorial areas and disappearing climate are found in mountainous areas.

vii. In Viet Nam, the projection results of this study were also compared to those in the previous study. The results showed a high agreement in the temperature changes but remarkably uncertainty in rainfall trend.

viii. 2.39% of Viet Nam land, mainly located in the Northern and Southern Central Highlands, was projected to experience disappearing climate by the ENS experiment under the RCP8.5.

The results of the present study would provide worthwhile inputs for climate change impact assessment, adaptation and mitigation research. When conducting climate-related research using multi-models, it is necessary to evaluate their performance before implementing the following analyses. The results of novel climate and disappearing climate in Southeast Asia and Viet Nam could be linked to various sectors such as agriculture, infrastructure, urban, health, immigration, etc. to help people better adapt to and mitigate climate change.

2. Recommendations

Based on the results and findings presented in the thesis, the following issues could be implemented in futher studies:

i. The uncertainty of models should be considered. Thus, bias correction could be applied before implementing the projection over SEA and Viet Nam.

ii. More efforts on understanding the mechanism of future rainfall changes should be made, that could help to better understand the different wetter/drier signals between the results of the previous study and of the thesis.

LIST OF PUBLICATIONS

1. **Nguyen‐Thi, T,** Ngo‐Duc, T, Tangang, FT, *et al.* Climate analogue and future appearance of novel climate in Southeast Asia. *Int J Climatol*. 2020; 1–18. https://doi.org/10.1002/joc.6693
2. **Nguyen-Thi, T**, Ngo-Duc, T., Phan-Van, T. (2019), Climate Analog Locations of Cities and Disappearing Climate in Viet Nam. *VNU Journal of Science: Earth and Environmental Sciences*, [S.l.], v. 35, n. 4, dec. 2019. ISSN 2588-1094. doi: https://doi.org/10.25073/2588-1094/vnuees.4409.
3. **Nguyen-Thi, T**, Ngo-Duc, T., Phan-Van, T. (2019), Performance of SEACLID/CORDEX-SEA multi-model experiments in simulating temperature and rainfall in Vietnam. *Vietnam Journal Of Earth Sciences*, [S.l.], v. 41, n. 4, p. 374-387, aug. 2019. ISSN 0866-7187. doi:https://doi.org/10.15625/0866-7187/41/4/14259.
4. **Nguyễn Thị Tuyết**, Ngô Đức Thành, Phan Văn Tân (2019), Biến đổi nhiệt độ và lượng mưa trong thế kỷ 21 trên khu vực Đông Nam Á theo dự tính đa mô hình SEACLID/CORDEX-SEA, *Tạp chí Khoa học Biến đổi khí hậu*, số 11 – Tháng 9/2019. ISSN 2525-2496.
5. **Nguyen-Thi, T.**, Ngo-Duc, T., Phan-Van, T. (2017), Sensitivity evaluation of climate analog patterns with varying weighting factor values of rainfall of some capital cities over the Southeast-Asia. The International Conference on Research Development and Cooperation in Geophysics (Viet-Geophys-2017), Viet Nam, *Proceedings*.

REFERENCE

Vietnamese References

1. Bộ Tài nguyên và Môi trường (2003), *Thông báo Quốc gia lần thứ nhất cho Công ước khung Liên hợp quốc về Biến đổi khí hậu*, Hà Nội.

2. Bộ Tài nguyên và Môi trường (2008), *Chương trình Mục tiêu Quốc gia Ứng phó với Biến đổi khí hậu*, Hà Nội.

3. Bộ Tài nguyên và Môi trường (2009), *Kịch bản Biến đổi khí hậu, Nước biển dâng cho Việt Nam*, Hà Nội.

4. Bộ Tài nguyên và Môi trường (2012), *Kịch bản Biến đổi khí hậu, Nước biển dâng cho Việt Nam*, Nhà xuất bản Tài nguyên – Môi trường và bản đồ Việt Nam, Hà Nội.

5. Bộ Tài nguyên và Môi trường (2016), *Kịch bản Biến đổi khí hậu và Nước biển dâng cho Việt Nam*, Nhà xuất bản Tài nguyên môi trường và bản đồ Việt Nam, Hà Nội.

6. Nguyễn Văn Hiệp và nnk (2015): *Nghiên cứu luận cứ khoa học cập nhật kịch bản biến đổi khí hậu và nước biển dâng cho ViệtNam*, BĐKH-43, Báo cáo tổng kết đề tài nghiên cứu KHCN cấp Nhà nước.

7. Mai Văn Khiêm (2018), "Xây dựng kịch bản Biến đổi khí hậu cho TP. HCM", *Tạp chí Khoa học ĐHQGHN: Các Khoa học Trái đất và Môi trường*, Tập 34, số 1S (2018) 26-32, doi: 10.25073/2588-1094/vnuees.4332.

8. Trần Việt Liễn, Hoàng Đức Cường, Trương Anh Sơn (2007), "Xây dựng các kịch bản khí hậu cho các vùng khí hậu ở Việt Nam giai đoạn 2010-2100", Tạp chí KTTV, Tháng 1.

9. Nguyễn Đức Ngữ, Nguyễn Trọng Hiệu (1991), *Biến đổi khí hậu và tác động của chúng ở Việt Nam trong khoảng 100 năm qua – Thiên nhiên và con người*, Nhà XB Sự thật, Hà Nội.

10. Nguyễn Đức Ngữ, Nguyễn Trọng Hiệu (2004), *Khí hậu và tài nguyên khí hậu Việt Nam*, Nhà xuất bản Nông nghiệp, Hà Nội.

11. Nguyễn Đức Ngữ (2008), *Biến đổi khí hậu*, Nhà xuất bản Khoa học và Kỹ thuật.

12. Phan Văn Tân và nnk (2010), *Nghiên cứu tác động của BĐKH toàn cầu đến các yếu tố và hiện tượng khí hậu cực đoan ở Việt Nam, khả năng dự báo và giải pháp chiến lược ứng phó*, Báo cáo tổng kết đề tài nghiên cứu KHCN cấp Nhà nước.

13. Nguyễn Văn Thắng và nnk (2010), *Biến đổi khí hậu và Tác động ở Việt Nam,* Viện Khoa học Khí tượng Thuỷ văn và Môi trường.

English References

14. Ackerly, D. D., S. R. Loarie, W. K. Cornwell, S. B. Weiss, H. Hamilton, R. Branciforte, and N. J. B. Kraft (2010), The geography of climate change: implications for conservation biogeography, *Diversity and Distributions*, 16(3), 476-487.

15. ADB (2009), *The Economics of Climate Change in Southeast Asia*: *A Regional Review.*

16. Aldrian, E., L. Dümenil-Gates, D. Jacob, R. Podzun, and D. Gunawan (2004), Long-term simulation of Indonesian rainfall with the MPI regional model, *Climate Dynamics*, 22(8), 795-814.

17. Arnbjerg-Nielsen, K. (2012), Quantification of climate change effects on extreme precipitation used for high resolution hydrologic design, *Urban Water Journal*, 9(2), 57-65.

18. Arnbjerg-Nielsen K, Funder SG, Madsen H (2015) Identifying climate analogues for precipitation extremes for Denmark based on RCM simulations from the ENSEMBLES database, *Water Science and Technology* 71(3): 418-425.

19. Arora, V. K., and Coauthors, 2013: Carbon–concentration and carbon–climate feedbacks in CMIP5 Earth system models, *J. Climate*, 26, 5289–5314, doi:10.1175/JCLI-D-12-00494.1.

20. Artale, V., et al. (2010), An atmosphere–ocean regional climate model for the Mediterranean area: assessment of a present climate simulation, *Climate Dynamics*, 35(5), 721-740.

21. Billa, L., S.B. Mansor, A.R. Mahmud (2004), Spatial information technology in flood early warning system: an overview of theory, application and latest development in Malaysia, *Disaster Prevention and Management*, 13(5), pp. 356-363.

22. Bos, S. P. M., T. Pagella, R. Kindt, A. J. M. Russell, and E. Luedeling (2015), Climate analogs for agricultural impact projection and adaptation—a reliability test, *Frontiers in Environmental Science*, 3(65).

23. Bowden, J. H., Otte, T. L., Nolte, C. G., & Otte, M. J. (2011). Examining interior grid nudging techniques using two-way nesting in the wrf model for regional climate modeling, *Journal of Climate*, 25, 2805–2823.

24. Braconnot, P., S. P. Harrison, M. Kageyama, P. J. Bartlein, V. Masson-Delmotte, A. Abe-Ouchi, B. Otto-Bliesner, and Y. Zhao, 2012: Evaluation of climate models using palaeoclimatic data, *Nat. Climate Change*, 2, 417–424, doi: 10.1038/nclimate1456.

25. Chan, S. C., Kendon, E. J., Fowler, H. J., Blenkinsop, S., Ferro, C. A. T., & Stephenson, D. B. (2013). Does increasing the spatial resolution of a regional climate model improve the simulated daily precipitation?, *Climate Dynamics*, 41, 1475–1495.

26. Chhin, R., Hoang-Hai, B., Shigeo, Y. (2017), Characterization of monthly precipitation over Indochina region to evaluate CMIP5 historical

runs, DPRI Annuals, 60B, 502-522.

27. Chotamonsak, C., E. P. Salathé, J. Kreasuwan, S. Chantara, and K. Siriwitayakorn (2011), Projected climate change over Southeast Asia simulated using a WRF regional climate model, *Atmospheric Science Letters*, 12(2), 213-219.

28. Chou, S. C., et al. (2012), Downscaling of South America present climate driven by 4-member HadCM3 runs, *Climate Dynamics*, 38(3), 635-653.

29. Christensen, J., K. K. K, E. Aldrian, and A. SI (2013), *Climate phenomena and their relevance for future regional climate change*, In: Stocker TF, Qin D, Plattner GK, Tignor M and others (eds) Climate change 2013: the physical science basis. Contribution of Working Group I to the Fifth Assessment Report of the Intergovernmental Panel on Climate Change. Cambridge University Press, Cambridge, 1217-1308.

30. Christensen, J., E. Kjellström, F. Giorgi, G. Lenderink, and M. Rummukainen (2010), Weight Assignment in Regional Climate Models, *Climate Research*, 44, 179-194 pp.

31. Covey, C., K. M. AchutaRao, U. Cubasch, P. Jones, S. J. Lambert, M. E. Mann, T. J. Phillips, and K. E. Taylor (2003), An overview of results from the Coupled Model Intercomparison Project, *Global Planet. Change*, 37, 103–133.

32. Cruz FT, Narisma GT, Dado JB, Singhruck P, Tangang F et al (2017), Sensitivity of temperature to physical parameterization schemes of RegCM4 over the CORDEX-Southeast Asia region, *International Journal of Climatology* 37(15): 5139-5153.

33. Daniel S.W. (2006), *Statistical methods in the atmospheric sciences,* International Geophysics Series, Elsevier.

34. De Elía, R., S. Biner, and A. Frigon (2013), Interannual variability and expected regional climate change over North America, *Climate Dynamics*, 41(5), 1245-1267.

35. Dee DP, Uppala SM, Simmons AJ, Berrisford P, Poli P, Kobayashi S et al (2011), The ERA-Interim reanalysis: configuration and performance of the data assimilation system, *Quarterly Journal of the Royal Meteorological Society* 137(656): 553-597

36. Dennis, L. H. (1994), *Global Physical Climatology*, Volume 56 in the International Geophysics Series.

37. Déqué M., Rowell D., Lüthi D., Giorgi F., Christensen J., Rockel B., Jacob D., Kjellström E., De Castro M., and van den Hurk B. (2007), An intercomparison of regional climate simulations for Europe: Assessing uncertainties in model projections, *Clim. Change*, 81(1), 53–70.

38. Dickinson, R. E., Errico, R. M., Giorgi, F., and Bates, G. T. (1989). A regional climate model for the western United States, *Climatic Change*, 15, 383–422.

39. Diffenbaugh Noah, S., M. Ashfaq, and M. Scherer (2011), Transient regional climate change: Analysis of the summer climate response in a high-resolution, century-scale ensemble experiment over the continental United States, *Journal of Geophysical Research: Atmospheres*, 116(D24).

40. Dobrowski SZ, Parks SA (2016), Climate change velocity underestimates climate change exposure in mountainous regions, *Nature Communications,* 7, 12349.

41. Dorn, W., K. Dethloff, and A. Rinke (2009), Improved simulation of feedbacks between atmosphere and sea ice over the Arctic Ocean in a coupled regional climate model, *Ocean Modelling*, 29(2), 103-114.

42. Döscher, R., K. Wyser, H. E. M. Meier, M. Qian, and R. Redler

(2010), Quantifying Arctic contributions to climate predictability in a regional coupled ocean-ice-atmosphere model, *Climate Dynamics*, 34(7), 1157-1176.

43. Druyan, L. M., et al. (2010), The WAMME regional model intercomparison study, *Climate Dynamics*, 35(1), 175-192.

44. Dunne, J. P., John, J., Adcroft, A., Griffies, S., Hallberg, R., Shevliakova, E. et al. (2012), GFDL's ESM2 Global Coupled Climate–Carbon Earth System Models. Part I: Physical Formulation and Baseline Simulation Characteristics, *Journal of Climate*, 25(19), 6646-6665.

45. Dunne, J. P., John, J., Shevliakova, E., Stouffer, R., Krasting, J., Malyshev, S. Milly, P. et al. (2013), GFDL's ESM2 Global Coupled Climate–Carbon Earth System Models. Part II: Carbon System Formulation and Baseline Simulation Characteristics, *Journal of Climate*, 26(7), 2247-2267.

46. Ehhalt, D. H. (1980), In situ Observations, Philosophical Transactions of the Royal Society of London. Series A, *Mathematical and Physical Sciences*, 296(1418), 175-189.

47. Ellingson R. G., Ellis J., and Fels S. (1991), The intercomparison of radiation codes used in climate models: Long wave results, *J. Geophys. Res.*, 96(D5), 8929–8953.

48. Emanuel KA, Živković-Rothman M (1999) Development and Evaluation of a Convection Scheme for Use in Climate Models. Journal of the Atmospheric Sciences 56(11): 1766-1782.

49. Eyring, V., and Coauthors (2013), Long-term ozone changes and associated climate impacts in CMIP5 simulations, *J. Geophys. Res. Atmos.*, 118, 5029–5060, doi:10.1002/jgrd.50316.

50. Eyring, V., Bony, S., Meehl, G. A., Senior, C. A., Stevens, B.,

Stouffer, R. J., and Taylor, K. E. (2016), Overview of the Coupled Model Intercomparison Project Phase 6 (CMIP6) experimental design and organization, *Geosci. Model Dev.*, 9, 1937-1958, doi:10.5194/gmd-9-1937-2016.

51. Fabienne, D., Erich, M. F., and Reto, K. (2017), Future local climate unlike currently observed anywhere, *Environmental Reseach Letters*, 12 (2017) 084004.

52. Feng, J., and C. Fu (2006), Inter-comparison of 10-year precipitation simulated by several RCMs for Asia, *Advances in Atmospheric Sciences*, 23(4), 531-542.

53. Feng, J., D.-K. Lee, C. Fu, J. Tang, Y. Sato, H. Kato, J. L. McGregor, and K. Mabuchi (2011), Comparison of four ensemble methods combining regional climate simulations over Asia, *Meteorology and Atmospheric Physics,* 111(1), 41-53.

54. Fisher B, Nakicenovic N, Alfsen K, Corfee Morlot J, de la Chesnaye F, Hourcade J-C, Jiang K, Kainuma M, La Rovere E, Matysek A et al (2007), *Issues related to mitigation in the long-term context*. In: Metz B, Davidson O, Bosch P, Dave R, Meyer L (eds) Climate change 2007. Mitigation of climate change. Contribution of Working Group III to the Fourth Assessment Report of the Intergovernmental Panel on Climate Change. Cambridge University Press, New York, pp 169–250.

55. Fitzpatrick, M. C., and R. R. Dunn (2019), Contemporary climatic analogs for 540 North American urban areas in the late 21st century, *Nature Communications*, 10(1), 614.

56. Foley, A. M. (2010), Uncertainty in regional climate modelling: A review, *Progress in Physical Geography*, 34, 647–670.

57. Ford, J. D., E. C. H. Keskitalo, T. Smith, T. Pearce, L. Berrang-Ford,

F. Duerden, and B. Smit (2010), Case study and analog methodologies in climate change vulnerability research, *Wiley Interdisciplinary Reviews: Climate Change*, 1(3), 374-392.

58. Francisco, R. V., J. Argete, F. Giorgi, J. Pal, X. Bi, and W. J. Gutowski (2006), Regional model simulation of summer rainfall over the Philippines: Effect of choice of driving fields and ocean flux schemes, *Theoretical and Applied Climatology*, 86(1), 215-227.

59. Friedlingstein, P., M. Meinshausen, V. K. Arora, C. D. Jones, A. Anav, S. K. Liddicoat, and R. Knutti (2014), Uncertainties in CMIP5 climate projections due to carbon cycle feedbacks, *J. Climate*, 27, 511–526, doi:10.1175/JCLI-D-12-00579.1.

60. Funtowicz and Ravetz (1990), *Uncertainty and Quality in Science for Policy,* Series A: Philosophy and Methodology of the Social Sciences, Volume 15, Springer Netherlands, doi/10.1007/978-94-009-0621-1.

61. GCOS (2010a), Implementation plan for the global observing system for climate in support of the UNFCCC (2010 update). GCOS Rep. 138, 186 pp. [Available online at www.wmo.int/pages/prog/gcos /Publications/gcos-138.pdf.].

62. Giorgi, F., C. Jones, and G. Asrar (2009), *Addressing climate information needs at the regional level: The CORDEX framework*, WMO Bulletin, 58(3), 175-183.

63. Giorgi, F., et al. (2012), RegCM4: model description and preliminary tests over multiple CORDEX domains, *Climate Research*, 52, 7-29.

64. Glisan, JM, Jones, R, Lennard, C, *et al* . A metrics‐based analysis of seasonal daily precipitation and near‐surface temperature within seven Coordinated Regional Climate Downscaling Experiment domains. *Atmos Sci*

Lett. 2019; 20:e897. https://doi.org/10.1002/asl.897

65. Gu, H., Yu, Z., Yang, C., Ju, Q., Yang, T., and Zhang, D.: High-resolution ensemble projections and uncertainty assessment of regional climate change over China in CORDEX East Asia, Hydrol. Earth Syst. Sci., 22, 3087–3103, https://doi.org/10.5194/hess-22-3087-2018, 2018.

66. Guo, D.-L., J.-Q. Sun, and E.-T. Yu (2018), Evaluation of CORDEX regional climate models in simulating temperature and precipitation over the Tibetan Plateau, *Atmospheric and Oceanic Science Letters*, *11*(3), 219-227.

67. Gutowski, W. J. (2010), Regional extreme monthly precipitation simulated by NARCCAP RCMs, *J. Hydrometeorol.*, 11, 1373–1379.

68. Hallegatte, S., J.-C. Hourcade, and P. Ambrosi (2007), Using climate analogs for assessing climate change economic impacts in urban areas, *Climatic Change*, 82(1), 47-60.

69. Henderson-Sellers A., Yang Z., and Dickinson R. (1993), The project for intercomparison of land-surface parameterization schemes, *Bull. Am. Meteorol. Soc.*, 74(7), 1335–1349.

70. Hibino K, Takayabu I, Nakaegawa T (2015), Objective estimate of future climate analogues projected by an ensemble AGCM experiment under the SRES A1B scenario, *Climatic Change,* 131(4): 677-689.

71. Hijioka, Y., L. E, P. JJ, C. RT, and a. others (2014), Asia. In: Barros VR, Field CB, Dokken DJ, Mastrandrea MD and others (eds), *Climate change 2014: impacts, adaptation, and vulnerability. Part B: regional aspects*. Contribution of Working Group II to the Fifth Assessment Report of the Intergovernmental Panel on Climate Change. Cambridge University Press, Cambridge, 1327−1370.

72. Ho, T., V. Phan, N. Le, and Q. Nguyen (2011), Extreme climatic events over Viet Nam from -observational data and RegCM3 projections,

Climate Research, 49(2), 87-100.

73. Iizumi, T., M. Nishimori, K. Dairaku, S. A. Adachi, and M. Yokozawa, 2011: Evaluation and intercomparison of downscaled daily precipitation indices over Japan in present-day climate: Strengths and weaknesses of dynamical and bias correction-type statistical downscaling methods. J. Geophys. Res., 116, doi:10.1029/2010JD014513.

74. Im, E.-S., J.-B. Ahn, A. R. Remedio, and W.-T. Kwon (2008), Sensitivity of the regional climate of East/Southeast Asia to convective parameterizations in the RegCM3 modelling system. Part 1: Focus on the Korean peninsula, *International Journal of Climatology*, 28(14), 1861-1877.

75. IMHEN and UNDP (2015), *Viet Nam Special Report on Managing the Risks of Extreme Events and Disasters to Advance Climate Change Adaptation* [Tran Thuc, Koos Neefjes, Ta Thi Thanh Huong, Nguyen Van Thang, Mai Trong Nhuan, Le Quang Tri, Le Dinh Thanh, Huynh Thi Lan Huong, Vo Thanh Son, Nguyen Thi Hien Thuan, Le Nguyen Tuong], Viet Nam Publishing House of Natural Resources, Environment and Cartography, Ha Noi, Viet Nam.

76. Inoue, J., J. Liu, J. O. Pinto, and J. A. Curry (2006), Intercomparison of Arctic Regional Climate Models: Modeling Clouds and Radiation for SHEBA in May 1998, *Journal of Climate*, 19(17), 4167-4178.

77. IPCC (2000), *Emissions Scenarios*, Cambridge University Press, UK.

78. IPCC (2007), *Report of the 26th session of the IPCC*, Bangkok. April 30–May 4 2007, Intergovernmental Panel on Climate Change, Geneva, Switzerland.

79. IPCC (2013), *Climate Change 2013: The Scientific Basis,* Contribution of Working Group I to the Fifth Assessment Report of the

Intergovernmental Panel on Climate Change, Cambridge University Press, Cambridge, United Kingdom and New York, NY, USA.

80. IPCC (2013), *Climate Change 2013: Mitigation of Climate Change*, Contribution of Working Group III to the Fifth Assessment Report of the Intergovernmental Panel on Climate Change Cambridge University Press, Cambridge, United Kingdom and New York, NY, USA.

81. Ishizaki NN, Shiogama H, Takahashi K, Emori S, Dairaku K, Kusaka H, Nakaegawa T, Takayabu I (2012), An Attempt to Estimate of Probabilistic Regional Climate Analogue in a Warmer Japan, *Journal of the Meteorological Society of Japan*, Ser. II, 90B: 65-74.

82. Ishizaki, N. N., I. Takayabu, M. Oh'izumi, H. Sasaki, K. Dairaku, S. Iizuka, F. Kimura, H. Kusaka, S. A. Adachi, K. Kurihara, K. Murazaki, and K. Tanaka, 2012: Improved performance of simulated Japanese climate with a multi-model ensemble. J. Meteor. Soc. Japan, 90, 235−254.

83. Juneng, L., et al. (2016), Sensitivity of Southeast Asia rainfall simulations to cumulus and air-sea flux parameterizations in RegCM4, *Climate Research*, 69(1), 59-77.

84. Katzfey, JJ, McGregor, JL and Suppiah, R (2014), *High-resolution climate projections for Vietnam,* Technical Report, CSIRO, Australia. 266 pp.

85. Katzfey J, Nguyen K, McGregor J, Hoffmann P, Ramasamy S, Nguyen HV et al (2016) High-resolution simulations for Vietnam - methodology and evaluation of current climate. Asia-Pacific J. Atmos. Sci. 52: 91–106, doi:10.1007/s13143-016-0011-2.

86. Kendon, E. J., N. M. Roberts, C. A. Senior, and M. J. Roberts (2012), Realism of Rainfall in a Very High-Resolution Regional Climate Model, *Journal of Climate*, 25(17), 5791-5806.

87. Kieu-Thi, X., H. Vu-Thanh, T. Nguyen-Minh, D. Le, L. Nguyen-Manh, I. Takayabu, H. Sasaki, and A. Kitoh (2016), Rainfall and Tropical Cyclone Activity over Viet Nam Simulated and Projected by the Non-Hydrostatic Regional Climate Model - NHRCM, *Journal of the Meteorological Society of Japan*. Ser. II, 94A, 135-150.

88. Kim, G., Cha, D., Park, C. *et al.* Evaluation and Projection of Regional Climate over East Asia in CORDEX-East Asia Phase I Experiment. *Asia-Pacific J Atmos Sci* (2020). https://doi.org/10.1007/s13143-020-00180-8.

89. Kjellstro, E., G. Nikulin, U. Hansson, G. Strandberg, and A. Ullerstig (2011), 21st century changes in the European climate: uncertainties derived from an ensemble of regional climate model simulations, Tellus A, *Dynamic Meteorology and Oceanography*, 63(1), 24-40.

90. Kopf, S., M. Ha-Duong, and S. Hallegatte (2008), Using maps of city analogs to display and interpret climate change scenarios and their uncertainty, *Nat. Hazards Earth Syst. Sci.*, 8(4), 905-918.

91. Krüger, L., R. da Rocha, M. Reboita, and T. Ambrizzi (2012), RegCM3 nested in HadAM3 scenarios A2 and B2: Projected changes in extratropical cyclogenesis, temperature and precipitation over the South Atlantic Ocean, *Clim. Change*, 113, 599–621.

92. Lamarque, J.-F., and Coauthors (2013), The Atmospheric Chemistry and Climate Model Intercomparison Project (ACCMIP): Overview and description of models, simulations and climate diagnostics, *Geosci. Model Dev.*, 6, 179–206, doi:10.5194/gmd-6-179-2013.

93. Laprise, R. (2008), Regional climate modelling, *Journal of Computational Physics*, 227(7), 3641-3666.

94. Laprise, R., L. Hernández-Díaz, K. Tete, L. Sushama, L. Šeparović,

A. Martynov, K. Winger, and M. Valin (2013), Climate projections over CORDEX Africa domain using the fifth-generation Canadian Regional Climate Model (CRCM5), *Climate Dynamics*, 41(11), 3219-3246.

95. Leggett J, Pepper W, Swart RJ (1992), *Emissions Scenarios for the IPCC: an Update*. In: Houghton JT, Callander BA, Varney SK (eds) Climate change 1992. The Supplementary Report to the IPCC Scientific Assessment. Cambridge University Press, Cambridge, pp 71–95

96. Li, D., B. Yin, J. Feng, A. Dosio, B. Geyer, J. Qi, H. Shi, and Z. Xu, 2018: Present Climate Evaluation and Added Value Analysis of Dynamically Downscaled Simulations of CORDEX—East Asia. *J. Appl. Meteor. Climatol.*, **57**, 2317–2341, https://doi.org/10.1175/JAMC-D-18-0008.1.

97. Loh, J. L., F. Tangang, L. Juneng, D. Hein, and D.-I. Lee (2016), Projected rainfall and temperature changes over Malaysia by the end ofthe 21st century based on PRECIS modelling system, *Asia-Pacific Journal of Atmospheric Sciences*, 52(2), 191-208.

98. Lorenz, P., & Jacob, D. (2005), Influence of regional scale information on the global circulation: A two-way nesting climate simulation, *Geophysical Research Letters*, 32, L18706.

99. Luedeling (2011), *Climate change impacts on crop production in Busia and Homa Bay Counties*, *Kenya,* World Agroforestry Centre, Kenya.

100. Luedeling, and H. Neufeldt (2012), Carbon sequestration potential of parkland agroforestry in the Sahel, *Climatic Change*, 115(3), 443-461.

101. Luedeling, C. Muthuri, and R. Kindt (2013), *Ecosystem vulnerability to climate change: A literature review*, 56p, World Agroforestry Centre, Nairobi, Kenya.

102. Luedeling, E., R. Kindt, N. I. Huth, and K. Koenig (2014),

Agroforestry systems in a changing climate-challenges in projecting future performance, *Current Opinion in Environmental Sustainability*, 6, 1-7.

103. Mahlstein I, Portmann RW, Daniel JS, Solomon S, Knutti R (2012), Perceptible changes in regional precipitation in a future climate, *Geophys Res Lett,* 39(5)

104. Mahony CR, Cannon AJ, Wang T, Aitken SN (2017), A closer look at novel climates: new methods and insights at continental to landscape scales, *Global Change Biology*, 23(9): 3934-3955

105. Manomaiphiboon, K., M. Octaviani, K. Torsri, and S. Towprayoon (2013), Projected changes in means and extremes of temperature and precipitation over Thailand under three future emissions scenarios, *Climate Research*, 97-115 pp.

106. Matsumoto, J. (1997), Seasonal transition of summer rainy season over Indochina and adjacent monsoon region. *Adv. Atmos. Sci.*, **14**, 231−245.

107. Mearns LO, Hulme M, Carter TR, Leemans R, Lal M, Whetton P (2001), *Climate Scenario Development*. In: Houghton JT et al (ed) Climate Change 2001: The Physical Science Basis. Contribution of Working Group I to the Third Assessment Report of the Intergovernmental Panel on Climate Change, pp 739-768.

108. Mearns, L. O., Giorgi, F., Whetton, P., Pabon, D., Hulme, M., and Lal, M. (2003), *Guidelines for use of climate scenarios developed from Regional Climate Model experiments*, Data Distribution Centre of the Intergovernmental Panel on Climate Change.

109. Mearns, L. O., et al. (2012), The North American Regional Climate Change Assessment Program: Overview of Phase I Results, *Bulletin of the American Meteorological Society*, 93(9), 1337-1362.

110. Meehl, G.A., G.J. Boer, C. Covey, M. Latif, and R.J. Stouffer (1997), Intercomparison makes for a better climate model. *Eos*, 78, 445--446, 451.

111. Meehl, G.A., G.J. Boer, C. Covey, M. Latif, and R.J. Stouffer (2000), The Coupled Model Intercomparison Project (CMIP), *Bull. Amer. Meteorol. Soc.*, 81, 313--318.

112. Meehl, G.A., C. Covey, M. Latif, B. McAvaney, J. F. B. Mitchell, and R. Stouffer (2004), Soliciting participation in climate model analyses leading to IPCC Fourth Assessment Report, *Eos, Trans. Amer. Geophys. Union*, 85, 274.

113. Meehl, G.A., C. Covey, B. McAvaney, M. Latif, and R. J. Stouffer (2005b), Overview of the Coupled Model Intercomparison Project, *Bull. Amer. Meteor. Soc.*, 86, 89–93.

114. Meehl, G. A., R. Moss, K. E. Taylor, V. Eyring, R. J. Stouffer, S. Bony, and B. Stevens (2014), Climate Model Intercomparisons: Preparing for the Next Phase, *Eos, Transactions American Geophysical Union*, 95(9), 77-78.

115. Menendez, C., M. de Castro, A. Sorensson, J. Boulanger, and C. M. Grp (2010), CLARIS Project: Towards climate downscaling in South America, *Meteorol. Z.*, 19, 357–362.

116. Michael, J. P., V. Misra, and E. P. Chassignet (2013), The El Niño and Southern Oscillation in the historical centennial integrations of the new generation of climate models, *Regional Environmental Change*, 13(1), 121-130.

117. Morgan, and Henrion (1990), *Uncertainty: A Guide to Dealing with Uncertainty In Quantitative Risk and Policy Analysis*, Cambridge University Press, New York. ISBN 0-521-36542-2.

118. Moss, R., Edmonds, J., hibbard, K., Manning, M., Rose, S., van Vuuren, D., Carter, T., Emori, S., Kainuma, M. et al. (2010), The next generation of scenarios for climate change research and assessment, *Nature*, 463, 747.

119. Nakaegawa, T., K. Hibino, and I. Takayabu (2017), Identifying climate analogs for cities in Australia by a non-parametric approach using multi-ensemble, high-horizontal-resolution future climate projections by an atmospheric general circulation model, MRI-AGCM3.2H, *Hydrological Research Letters*, 11(1), 72-78.

120. Nakicenovic, N. and R. Swart (2000), *Special Report on Emissions Scenarios (SRES)* – A Special Report of Working Group III of the Intergovernmental Panel on Climate Change.

121. NASA-Earth Observation (2011), *Unseasonably heavy rain floods in Thailand*, Retrieved January 29, 2014 from http://earthobservatory.nasa.gov/IOTD/view.php?id=49929

122. Ngo-Duc, T., T. Nguyen Quang, L. Trinh, T. H. Vu, T. Phan-Van, and P. Van Cu (2012), Near Future Climate Projections over the Red River Delta of Vietnam using the Regional Climate Model Version 3, *Sains Malaysiana*, 41, 1325-1334.

123. Ngo-Duc, C. Kieu, M. Thatcher, D. Nguyen-Le, and T. Phan-Van (2014), Climate projections for Viet Nam based on regional climate models, *Climate Research*, 60(3), 199-213.

124. Ngo-Duc, et al. (2016), Performance evaluation of RegCM4 in simulating extreme rainfall and temperature indices over the CORDEX-Southeast Asia region, *International Journal of Climatology*, 37(3), 1634-1647.

125. Ngo-Thanh, H., T. Ngo-Duc, H. Nguyen-Hong, P. Baker, and T.

Phan-Van (2017), A distinction between summer rainy season and summer monsoon season over the Central Highlands of Viet Nam, *Theoretical and Applied Climatology*.

126. Nguyen, D.-Q., J. Renwick, and J. McGregor (2014), Variations of surface temperature and rainfall in Viet Nam from 1971 to 2010, *International Journal of Climatology*, 34(1), 249-264.

127. Nguyen‐Thi, T, Ngo‐Duc, T, Tangang, FT, *et al*. Climate analogue and future appearance of novel climate in Southeast Asia. *Int J Climatol*. 2020; 1– 18. https://doi.org/10.1002/joc.6693.

128. Nikulin, G., et al. (2012), Precipitation Climatology in an Ensemble of CORDEX-Africa Regional Climate Simulations, *Journal of Climate*, 25(18), 6057-6078.

129. Nyairo, R., R. Onwonga, K. Cherogony, and E. Luedeling (2014), Applicability of Climate Analogs for Climate Change Adaptation Planning in Bugabira Commune of Burundi, *Sustainable Agriculture Research*, 3(4).

130. Octaviani M, Manomaiphiboon K (2011), Performance of Regional Climate Model RegCM3 over Thailand, *Climate Research,* 47(3): 171-186

131. Ozturk, T., H. Altinsoy, M. Türkeş, and L. Kurnaz (2012), Simulation of temperature and precipitation climatology for the Central Asia CORDEX domain using RegCM 4.0, *Climate Research*, 52(1) 63-76 pp.

132. Paeth, H., et al. (2011), Progress in regional downscaling of west African precipitation, *Atmospheric Science Letters*, 12(1), 75-82.

133. Pedersen C. A., and Winther J.-G. (2005), Intercomparison and validation of snow albedo parameterization schemes in climate models, *Clim. Dyn.*, 25(4), 351–362.

134. Phan-Van, T. Ngo-Duc, and T. M. H. Ho (2009), Seasonal and interannual variations of surface climate elements over Viet Nam, *Climate*

Research, 40(1), 49-60.

135. Phan-Van, H. Van Nguyen, L. Trinh Tuan, T. Nguyen Quang, T. Ngo-Duc, P. Laux, and T. Nguyen Xuan (2014), Seasonal Prediction of Surface Air Temperature across Viet Nam Using the Regional Climate Model Version 4.2 (RegCM4.2), *Advances in Meteorology*, 1-13.

136. Pugh, T. A. M., C. Müller, J. Elliott, D. Deryng, C. Folberth, S. Olin, E. Schmid, and A. Arneth (2016), Climate analogs suggest limited potential for intensification of production on current croplands under climate change, *Nature Communications,* 7, 7, 12608.

137. Raghavan, S. V., M. T. Vu, and S. Y. Liong (2016), Regional climate simulations over Viet Nam using the WRF model, *Theoretical and Applied Climatology*, 126(1), 161-182.

138. Raghavan, S. V., M. T. Vu, and S. Y. Liong (2017), Ensemble climate projections of mean and extreme rainfall over Vietnam, *Global Planet. Change*, 148, 96−104, doi:10.1016/j.gloplacha.2016.12.003.

139. Rahmat, R., Boonlert A., P. Chai et al. (2014), *A regional climate modelling experiment for Southeast Asia Report*, Meterological Service Singapore.

140. Raktham, C., C. Bruyère, J. Kreasuwun, J. Done, C. Thongbai, and W. Promnopas (2015), Simulation sensitivities of the major weather regimes of the Southeast Asia region, *Climate Dynamics*, 44(5), 1403-1417.

141. Ramírez-Villegas, J., C. Lau, A. Kohler, A. Jarvis, N. Arnell, T. M. Osborne, and J. Hooker (2011), *Climate analogs: finding tomorrow's agriculture today,* Research Program on Climate Change, Agriculture and Food Security.

142. Rana, A., Nikulin, G., Kjellström, E. *et al.* Contrasting regional and global climate simulations over South Asia. *Clim Dyn* **54,** 2883–2901

(2020). https://doi.org/10.1007/s00382-020-05146-0.

143. Ratna, S. B., J. V. Ratnam, S. K. Behera, F. T. Tangang, and T. Yamagata (2017), Validation of the WRF regional climate model over the subregions of Southeast Asia: climatology and interannual variability, *Climate Research*, 71(3), 263-280.

144. Rotstayn Rotstayn, L. D., S. J. Jeffrey, M. A. Collier, S. M. Dravitzki, A. C. Hirst, J. I. Syktus, and K. K. Wong (2012), Aerosol- and greenhouse gas-induced changes in summer rainfall and circulation in the Australasian region: a study using single-forcing climate simulations, *Atmos. Chem. Phys.*, 12(14), 6377-6404.

145. Rummukainen, M. (2010), State-of-the-art with regional climate models, *Wiley Interdisciplinary Reviews: Climate Change*, 1(1), 82-96.

146. Ruti, P. M., et al. (2011), The West African climate system: a review of the AMMA model inter-comparison initiatives, *Atmospheric Science Letters*, 12(1), 116-122.

147. Serreze, M.C., R.G. Barry, R.J. Chorley (Eds.) (2010), *Climate Change*. Atmosphere, Weather and Climate, Routledge, Oxon.

148. Shkolnik, I. M., V. P. Meleshko, and V. M. Kattsov (2007), The MGO climate model for Siberia, *Russian Meteorology and Hydrology*, 32(6), 351-359.

149. Siew, J.H., Tangang, F.T. and Juneng, L. (2014), Evaluation of CMIP5 coupled atmosphere–ocean general circulation models and projection of the Southeast Asian winter monsoon in the 21st century. Int. J. Climatol., 34: 2872-2884. doi:10.1002/joc.3880.

150. Smith, B., P. Samuelsson, A. Wramneby, and M. Rummukainen (2011a), A model of the coupled dynamics of climate, vegetation and terrestrial ecosystem biogeochemistry for regional applications, *Tellus A*,

63(1), 87-106.

151. Solomon S et al (2007), *Global climate projections*, Cambridge University Press, Cambridge, UK.

152. Stevens, B. and S. Bony (2013), What are climate models missing? *Science*, 340, 1053–1054, doi:10.1126/science.1237554.

153. Stouffer, R. J., V. Eyring, G. A. Meehl, S. Bony, C. Senior, B. Stevens, and K. E. Taylor (2016), CMIP5 Scientific Gaps and Recommendations for CMIP6, *Bulletin of the American Meteorological Society*, 98(1), 95-105.

154. Supari, et al. (2020), Multi-model projections of precipitation extremes in Southeast Asia based on CORDEX-Southeast Asia simulations, *Environmental Research*, *184*, 109350.

155. Tangang F, Supari S, Chung JX, Cruz F, Salimun E, Ngai ST et al (2018), Future changes in annual precipitation extremes over Southeast Asia under global warming of 2°C, *APN Science Bulletin*, 8(1).

156. Tangang, F., Je. Santisirisomboon, L. Juneng, E. Salimun, J. Chung, Supari, F. Cruz, T. Ngo-Duc, P. Singhruck, Ja. Santisirisomboon, W. Wongsaree, K. Promjirapawat, Y. Sukamongkol, R. Srisawadwong, D. Setsirichok, G. Narisma, S. T. Ngai, T. Phan-Van, E. Aldrian, D. Gunawan, G. Nikulin, H. Yang (2019), Projected future changes in mean precipitation over Thailand based on multi-model regional climate simulations of CORDEX Southeast Asia, *International Journal of Climatology*, 124. https://doi.org/10.1002/joc.6163.

157. Tangang, F., Chung, J.X., Juneng, L. *et al.* Projected future changes in rainfall in Southeast Asia based on CORDEX–SEA multi-model simulations. *Clim Dyn* (2020). https://doi.org/10.1007/s00382-020-05322-2.

158. Taylor KE (2001), Summarizing multiple aspects of model

performance in a single diagram, *Journal of Geophysical Research: Atmospheres,* 106(D7): 7183-7192.

159. Taylor , KE, R. J. Stouffer, and G. A. Meehl (2011), An Overview of CMIP5 and the Experiment Design, *Bulletin of the American Meteorological Society*, 93(4), 485-498.

160. Taylor, K. E., R. J. Stouffer, and G. A. Meehl (2012), An overview of CMIP5 and the experiment design, *Bull. Amer. Meteor. Soc.*, 93, 485–498, doi:10.1175/BAMS-D-11-00094.1.

161. Torsri, K., M. Octaviani, K. Manomaiphiboon, and S. Towprayoon (2013), Regional mean and variability characteristics of temperature and precipitation over Thailand in 1961–2000 by a regional climate model and their evaluation, *Theoretical and Applied Climatology*, 113(1), 289-304.

162. Trinh-Tuan L, Matsumoto J, Tangang FT, Juneng L, Cruz F, Narisma G et al (2019), Application of Quantile Mapping Bias Correction for Mid-Future Precipitation Projections over Viet Nam, *SOLA* 15: 1-6

163. Tsunematsu, U., K. Dairaku, and J. Hirano, 2013: Future changes in summertime precipitation amounts associated with topography in the Japanese islands. J. Geophys. Res. Atmos., 118, 4142−4153.

164. United Nations, Department of Economic and Social Affairs (2019), *World Population Prospects 2019*, Data Booklet.

165. van den Besselaar, E.J., G. van der Schrier, R.C. Cornes, A.S. Iqbal, and A.M. Klein Tank (2017), SA-OBS: A Daily Gridded Surface Temperature and Precipitation Dataset for Southeast Asia. *J. Climate,* 30, 5151–5165, https://doi.org/10.1175/JCLI-D-16-0575.1

166. Van Khiem, M., G. Redmond, C. McSweeney, and T. Thuc (2014), Evaluation of dynamically downscaled ensemble climate simulations for Viet Nam, *International Journal of Climatology*, 34(7), 2450-2463.

167. Van Vuuren, D. P., J. A. Edmonds, M. Kainuma, K. Riahi, and J. Weyant (2011), A special issue on the RCPs, *Climatic Change*, 109(1), 1.

168. Van Vuuren, D. P., J. A. Edmonds, M. Kainuma, K. Riahi, A. Thomson, K. Hibbard, G. Hurtt, T. Kram, V. Krey, J.F. Lamarque, T. Masui et al. (2011), The representative concentration pathways: an overview, *Climatic Change*, 109(1), 5.

169. Van Vuuren DP, Riahi K (2011), The relationship between short-term emissions and long-term concentration targets: a letter, *Climatic Change,* 104, Issue 3–4, 793–801.

170. Vautard, R., et al. (2013), The simulation of European heat waves from an ensemble of regional climate models within the EURO-CORDEX project, *Climate Dynamics*, 41(9), 2555-2575.

171. Veloz, S., J. W. Williams, D. Lorenz, M. Notaro, S. Vavrus, and D. J. Vimont (2012), Identifying climatic analogs for Wisconsin under 21st-century climate-change scenarios, *Climatic Change*, 112(3), 1037-1058.

172. Voldoire, A., et al. (2013), The CNRM-CM5.1 global climate model: description and basic evaluation, *Climate Dynamics*, 40(9), 2091-2121.

173. Wakazuki, Y., M. Nakamura, S. Kanada, and C. Muroi (2008), Climatological Reproducibility Evaluation and Future Climate Projection of Extreme Precipitation Events in the Baiu Season Using a High-Resolution Non-Hydrostatic RCM in Comparison with an AGCM, *Journal of the Meteorological Society of Japan*, Ser. II, 86(6), 951-967.

174. Williams JW, Jackson ST (2007), Novel climates, no-analog communities, and ecological surprises, *Frontiers in Ecology and the Environment,* 5(9): 475-482.

175. Williams, S. T. Jackson, and J. E. Kutzbach (2007), Projected distributions of novel and disappearing climates by 2100 AD, *Proceedings of the National Academy of Sciences*, 104(14), 5738-5742.

176. Yasutomi N, Hamada A, Yatagai A. (2011), Development of a long-term daily gridded temperature dataset and its application to rain/snow discrimination of daily precipitation, *Global Environmental Research,* V15N2: 165 – 172.

ANNEX

Annex 1. List of coordinates of observation stations in SEA.

No.	Stations	Longitude	Latitude
	VIET NAM		
1	PHUHO	105.14	21.27
2	VIETTRI	105.25	21.18
3	TAMDAO	105.39	21.28
4	BAVI	105.26	21.06
5	HUNGYEN	106.03	20.4
6	CHILINH	106.23	21.07
7	NHOQUAN	105.45	20.19
8	VANLY	106.18	20.07
9	YENCHAU	104.283	21.05
10	SONLA	103.9	21.333
11	DIENBIEN	103	21.35
12	LAICHAU	103.15	22.05
13	BAICHAY	107.067	20.967
14	COTO	107.767	20.983
15	YENBAI	104.52	21.42
16	TUYENQUANG	105.13	21.49
17	LANGSON	106.767	21.833
18	SAPA	103.833	22.333
19	BACQUANG	104.083	22.483
20	HAGIANG	104.983	22.817
21	THAINGUYEN	105.833	21.583
22	THANHHOA	105.767	19.817
23	BACHLONGVI	107.717	20.133
24	NINHBINH	105.983	20.267
25	HOIXUAN	105.117	20.367
26	NAMDINH	106.09	20.26
27	THAIBINH	106.23	20.25
28	PHULIEN	106.38	20.48
29	HOABINH	105.333	20.817
30	HAIDUONG	106.18	20.57
31	HA NOI	105.85	21.017
32	SONTAY	105.3	21.08
33	VINHYEN	105.36	21.19

34	HUE	107.683	16.4
35	DONGHA	107.083	16.85
36	DONGHOI	106.617	17.467
37	TUYENHOA	106.133	17.833
38	KYANH	106.283	18.083
39	HUONGKHE	105.7	18.183
40	HATINH	105.9	18.35
41	VINH	105.667	18.667
42	TUONGDUONG	104.433	19.283
43	NAMDONG	107.717	16.15
44	PHANRANG	108.93	11.57
45	NHATRANG	109.2	12.25
46	TUYHOA	109.283	13.083
47	QUYNHON	109.217	13.767
48	BATO	108.717	14.767
49	QUANGNGAI	108.783	15.133
50	TRAMY	108.217	15.35
51	DANANG	108.183	16.033
52	ALUOI	107.417	16.2
53	BAOLOC	107.8	11.467
54	DALAT	108.433	11.95
55	DAKNONG	107.683	12
56	BMTHUOT	108.05	12.683
57	AYUNPA	108.26	13.25
58	PLEIKU	108	13.983
59	KONTUM	107.617	14.333
60	PHANTHIET	108.1	10.933
61	CONDAO	106.6	8.233
62	TRUONGSA	111.917	8.65
63	CAMAU	105.283	9.167
64	RACHGIA	105.083	10
65	CANTHO	105.783	10.033
66	PHUQUOC	103.967	10.217
67	VUNGTAU	107.083	10.333
68	PHUQUY	108.933	10.517
69	TUANGIAO	103.417	21.583
70	MOCCHAU	104.633	20.85
	INDONESIA		

71	ADISUMARMO	110.9167	-7.8667
72	AMAHAI	128.8833	-3.35
73	BALIKPAPAN	116.9	-1.2667
74	BANDUNGGEOSTA	107.6	-6.9167
75	BANJARBARUCLIMSTA	114.8833	-3.9333
76	BANJARMASIN	114.75	-3.4333
77	BANYUWANGI	114.3833	-8.2167
78	BAU-BAU	122.6167	-5.4667
79	BAWEAN	112.6333	-5.85
80	BENGKULU	102.3333	-3.8833
81	BIAK	136.1167	-1.1833
82	BIMA	118.7	-8.55
83	BITUNG	125.1833	1.4333
84	BLANGBINTANG	95.4167	5.5167
85	BULUHTUMBANG	107.75	-2.75
86	CILACAP	109.0167	-7.7333
87	CITEKO	106.9333	-6.7
88	CURUG	106.65	-6.2333
89	DENPASAR	115.1667	-8.75
90	DEPATIPARBO	101.3667	-2.7667
91	DRAMAGA	106.7498	-6.5536
92	GESER	130.8333	-3.8
93	GORONTALO	123.0667	0.5167
94	HALIMPERDANAKUSUMA	106.9	-6.25
95	JAKARTAOBS	106.8333	-6.1833
96	JAMBI	103.65	-1.6333
97	JATIWANGI	108.2667	-6.75
98	KAIRATUCLIMSTA	128.4	-3.25
99	KALIANGET	113.9667	-7.05
100	KENTENCLIMSTA	104.9	-2.52
101	KEPAHIANGGEOSTA	102.5891	-3.6706
102	KOTABARU	116.2167	-3.4
103	KUPANG	123.6667	-10.1667
104	LAMPUNG	105.1833	-5.2667
105	LHOKSEUMAWE	97.2	5.2333
106	LUWUK	122.7833	-0.9
107	MAJENE	119	-2.5
108	MAKASAR	119.55	-5.0667

109	MANADO	124.9167	1.5333
110	MANADOCLIMSTA	124.61	1.24
111	MATARAM	116.0667	-8.5333
112	MEDANCLIMSTA	98.7933	3.62
113	MEDANMARINESTA	98.7	3.8
114	MEULABOH	96.1167	4.25
115	MUARATEWEH	114.9	-0.95
116	NAHA	125.4667	3.5833
117	NAMLEA	127.0833	-3.25
118	NANGAPINOH	111.7833	-0.35
119	PADANG	100.35	-0.8833
120	PALANGKARAYA	114	-1
121	PALEMBANG	104.7	-2.9
122	PALOH	109.3	1.7
123	PALU	119.7333	-0.6833
124	PANGKALANBUN	111.7	-2.7
125	PANGKALPINANG	106.1333	-2.1667
126	PEKANBARU	101.45	0.4667
127	PERAKI	112.7167	-7.2167
128	PERAKII	113.7167	-7.2167
129	PINANGSORI	98.8833	1.55
130	POLONIA	98.6833	3.5667
131	PONDOKBETUNGCLIMSTA	106.75	-6.2558
132	PONTIANAK	109.4	-0.15
133	PONTIANAKCLIMSTA	109.1833	0.25
134	POSO	120.7333	-1.3833
135	RAHADIOSMAN	109.9667	-1.85
136	RENGAT	102.3167	-0.4667
137	SABANG	95.3167	5.8667
138	SAUMLAKI	131.3	-7.9833
139	SEMARANG	110.3833	-6.9833
140	SEMARANGCLIMSTA	110.3833	-6.9833
141	SEMARANGMARINESTA	110.4167	-6.9667
142	SENTANI	140.4833	-2.5667
143	SERANG	106.1333	-6.1167
144	SITOLI	97.6333	1.5
145	SOEKARNO-HATTA	106.65	-6.1167
146	SUMBAWABESAR	117.4167	-8.4333

147	SURABAYA	112.7667	-7.3667
148	SUSILOSINTANG	111.5333	0.1167
149	TANJUNGPINANG	104.5333	0.9167
150	TANJUNGPRIOKMARINESTA	106.8667	-6.1
151	TANJUNGREDEP	117.45	2.1167
152	TARAKAN	117.5667	3.3333
153	TEGAL	109.15	-6.85
154	TERNATE	127.3833	0.7833
155	TOLI-TOLI	120.8	1.0167
156	TRETESGEOSTA	112.635	-7.704
157	TUAL	132.75	-5.6833
158	WAINGAPU	120.3333	-9.6667
	THAILAND		
159	ARANYAPRATHET	99.83334	19.91667
160	BANGKOKMETROPOLIS	99.16666	18.18333
161	BANGNA	99.23333	17.63333
162	BHUMIBOLDAM	100.45	18.51667
163	BUACHUM	99	18.55
164	CHAINAT	99.83334	19.91667
165	CHAIYAPHUM	99	18.55
166	CHANTHABURI	98.98333	18.78333
167	CHIANGMAI	99.46667	19.51667
168	CHIANGRAIAGROMET	99.46667	19.51667
169	CHIANGRAI	99.83334	19.91667
170	CHOKCHAI	100.1	17.61667
171	CHONBURI	99.46667	19.51667
172	CHUMPHON	99.83334	19.91667
173	DONMUANG	100.1667	18.16667
174	HATYAIAIRPORT	100.45	18.51667
175	HUAHIN	97.93333	18.16667
176	HUAIPONGAGROMET	99	18.55
177	KABINBURI	97.93333	18.16667
178	KAMPHAENGPHET	98.88333	16.01667
179	KAMPHAENGSAENAGROMET	99.16666	18.18333
180	KANCHANABURI	98.98333	18.78333
181	KHLONGYAI	99.16666	18.18333
182	KHOHONGAGROMET	100.1667	18.16667
183	KHONKAEN	99.9	19.13333

184	KOLANTA	100.8	19.11667
185	KOSAMUI	98.98333	18.78333
186	KOSICHANG	99.9	19.13333
187	KOSUMPHISAI	99.23333	17.63333
188	LAMPANGAGROMET	99.51667	18.28333
189	LAMPANG	99.9	19.13333
190	LAMPHUN	99.16666	18.18333
191	LOEIAGROMET	99.83334	19.91667
192	LOEI	97.83334	19.3
193	LOMSAK	100.1	17.61667
194	LOPBURI	99.03333	19.91667
195	MAEHONGSON	97.83334	19.3
196	MAEJO	99.46667	19.51667
197	MAESARIANG	97.93333	18.16667
198	MAESOT	99.16666	18.18333
199	MUKDAHAN	99.03333	19.91667
200	NAKHONPHANOMAGROMET	98.98333	18.78333
201	NAKHONPHANOM	99.46667	19.51667
202	NAKHONRATCHASIMA	99.16666	18.18333
203	NAKHONSAWAN	97.83334	19.3
204	NAKHONSITHAMMARAT	99.03333	19.91667
205	NAKHORNSRITHAMMARATAGROMET	99.23333	17.63333
206	NANAGROMET	99.51667	18.28333
207	NANGRONG	98.55	16.66667
208	NAN	99	18.55
209	NARATHIWAT	99.03333	18.56667
210	NONGKHAI	97.83334	19.3
211	NONGPHLUPAGROMET	99.83334	19.91667
212	PAKCHONGAGROMET	100.8833	19.4
213	PATTANIAIRPORT	99.23333	17.63333
214	PHATTHALUNGAGROMET	99.03333	18.56667
215	PHATTHAYA	99.03333	19.91667
216	PHAYAO	99.9	19.13333
217	PHETCHABUN	99.03333	18.56667
218	PHETCHABURI	97.83334	19.3
219	PHITSANULOK	99.23333	17.63333
220	PHRAE	99.03333	19.91667
221	PHRIUAGROMET	99.51667	18.28333

222	PHUKETAIRPORT	98.98333	18.78333
223	PHUKET	99	18.55
224	PHUNPHINAIRPORT	99.51667	18.28333
225	PILOTSTATION	98.98333	18.78333
226	PRACHINBURI	97.83334	19.3
227	PRACHUAPKHIRIKHAN	97.83334	19.3
228	RANONG	99.46667	19.51667
229	RAYONG	98.98333	18.78333
230	ROIETAGROMET	100.45	18.51667
231	ROIET	98.98333	18.78333
232	SAKONNAKHONAGROMET	99.03333	19.91667
233	SAKONNAKHON	99.83334	19.91667
234	SATTAHIP	99.03333	19.91667
235	SATUN	99.11667	15.88333
236	SAWIAGROMET	99.9	19.13333
237	SISAKETAGROMET	100.1	17.61667
238	SISAMRONGAGROMET	99.03333	18.56667
239	SONGKHLA	99.16666	18.18333
240	SUPHANBURI	99.46667	19.51667
241	SURATTHANI	99.9	19.13333
242	SURINAGROMET	99.51667	17.1
243	SURIN	99.23333	17.63333
244	TAKFAAGROMET	97.93333	18.16667
245	TAK	99.51667	18.28333
246	TAKUAPA	100.1667	18.16667
247	THAPHRAAGROMET	99.51667	18.28333
248	THATUM	99.11667	15.88333
249	THAWANGPHA	99.16666	18.18333
250	THONGPHAPHUM	99.51667	18.28333
251	TRANGAIRPORT	99.51667	18.28333
252	UBONRATCHATHANIAGROMET	100.7833	18.78333
253	UBONRATCHATHANI	99.51667	18.28333
254	UDONTHANI	97.93333	18.16667
255	UMPHANG	100.8833	19.4
256	UTHONGAGROMET	99.9	19.13333
257	UTTARADIT	98.98333	18.78333
258	WICHIANBURI	99.1	17.78333
259	YALAAGROMET	99.05	17.23333

260	BANGKOK	100.56	13.7264
261	SAKON-NAKHON	104.133	17.15
262	KHORAT	102.079	14.935
263	SURIN	103.5	14.883
264	BANGKOK-INTL	100.607	13.913
265	ARANYAPRATHET	102.504	13.7
266	HUA-HIN	99.952	12.636
267	SATTAHIP	100.983	12.683
268	CHANTHABURI	102.117	12.6
269	PRACHUAP	99.805	11.788
270	CHUMPHON	99.362	10.711
271	RANONG	98.585	9.778
272	SURAT-THANI	99.136	9.133
273	PHUKET-INTL	98.317	8.113
274	TRANG	99.617	7.509
275	HAT-YAI-INTL	100.393	6.933
276	NARATHIWAT	101.743	6.52
	MALAYSIA		
277	ALORSETAR	100.4008	6.2004
278	BATUEMBUN	102.3507	3.9686
279	BAYANLEPAS	100.2672	5.3006
280	BINTULU	113.0334	3.2004
281	BUTTERWORTH	100.3841	5.4676
282	CAMERONHIGHLANDS	101.3674	4.4676
283	CHUPING	100.2672	6.4843
284	IPOH	101.1002	4.5678
285	K.K.TERENGGANU	103.1336	5.334
286	KLUANG	103.3173	2.0167
287	KOTABHARU	102.2839	6.167
288	KOTAKINABALU	116.0501	5.9352
289	K.TANAHRATA	101.3841	4.4676
290	KUALAKRAI	102.2004	5.5344
291	KUALATERENGGANUAIRPORT(SULTANMAHMUD)	103.1002	5.3841
292	KUANTAN	103.2171	3.7849
293	KUCHING	110.334	1.4843
294	KUDAT	116.835	6.9185
295	LABUAN	115.2505	5.3006
296	MALACCA	102.2505	2.2672

297	MERSING	103.835	2.4509
298	MIRI	113.9853	4.334
299	MUADZAMSHAH	103.0835	3.0501
300	PETALINGJAYA	101.6513	3.1002
301	SANDAKAN	118.0668	5.9018
302	SENAI	103.668	1.6346
303	SIBU	111.9686	2.2505
304	SITIAWAN	100.7014	4.2171
305	SRIAMAN	111.4509	1.2171
306	SUBANG	101.5511	3.1169
307	TAWAU	118.1169	4.3006
308	TEMERLOH	102.3841	3.4676
309	U.MALAYA	101.6513	3.1169
	PHILIPPINES		
310	ALABAT	122.01	14.103
311	AMBULONG	121.055	14.092
312	BAGUIO	120.6	16.41
313	CABANATUAN	120.962	15.488
314	CALAPAN	121.17	13.413
315	CASIGURAN	122.123	16.28
316	CATARMAN	124.638	12.5
317	CATBALOGAN	124.88	11.778
318	CORON	120.203	11.998
319	CUYO	121.007	10.853
320	DAET	122.953	14.113
321	DAGUPAN	120.333	16.043
322	DAVAO	125.833	7.3
323	DIPOLOG	123.338	8.592
324	DUMAGUETE	123.307	9.302
325	GENERALSANTOS	125.183	6.117
326	HINATUAN	126.337	8.37
327	INFANTA	121.647	14.75
328	LAOAG	120.592	18.2
329	LEGASPI	123.733	13.138
330	MALAYBALAY	125.077	8.153
331	MASBATE	123.618	12.37
332	PUERTOPRINCESA	118.733	9.742
333	ROMBLON	122.268	12.577

334	ROXAS	122.75	11.583
335	SCIENCEGARDEN	121.042	14.645
336	SURIGAO	125.492	9.792
337	TACLOBAN	125	11.245
338	TAGBILARAN	123.855	9.643
339	TAYABAS	121.588	14.028
340	VIRAC	124.23	13.585
341	ZAMBOANGA	122.075	6.905
	MYANMAR		
342	BHAMO	97.2	24.27
343	DAWEI	98.22	14.1
344	GWA	94.58	17.58
345	HINTHADA	95.42	17.67
346	HKAMTI	95.7	26
347	HOMALIN	94.92	24.87
348	HPA-AN	97.67	16.75
349	KATHA	96.33	24.17
350	KAWTHONG	98.58	9.97
351	KENGTUNG	99.62	21.3
352	KYAUKPYU	93.55	19.42
353	KYAUKTAW	92.63	20.85
354	LASHIO	97.75	22.93
355	LOIKAW	97.22	19.68
356	MEIKTILA	95.83	20.83
357	MONYWA	95.13	22.1
358	MYEIK	98.6	12.43
359	MYITKYINA	97.4	25.37
360	PYINMANA	96.22	19.72
361	TAUNGGYI	97.05	20.78
362	TAUNGOO	96.47	18.92
363	THANDWE	94.35	18.47
364	YAY	97.87	15.25
	LAOS		
365	WATTAY INTL	102.563	17.988

Annex 2. Mean dissimilarities of temperature (Tdis) and precipitation (Pdis) over all reference grid points computed with six GCMs and six RCMs and their ensemble (ENS) values for the RCP4.5 and the RCP8.5 and for two periods (mid-, and far-future). **α** is the ratio between mean Tdis and mean Pdis. **β** is the ratio between the mean $\mathbf{T_{dis}}$ of the ENS experiment and the average values of the mean $\mathbf{T_{dis}}$ of the six RCM experiments.

Model	RCM				GCM		
	Mean T-diss	**Mean P-diss**	**α**		**Mean T-diss**	**Mean P-diss**	**α**
RCP85; 2080 - 2099							
CNRM	5.9	1.4	**4.2**		4.8	1.1	**4.2**
CSIR	6.4	1.4	**4.6**		5.3	1.5	**3.6**
ECEA	6.1	1.4	**4.3**		5.2	1.4	**3.6**
GFDL	4.7	1.3	**3.6**		3.7	1.2	**3.1**
HadG	7.7	1.6	**4.9**		6.3	1.7	**3.8**
MPI	5.4	1.4	**4.0**		4.0	1.2	**3.4**
ENS	11.0	2.9	**3.8**		9.1	2.8	**3.3**
Average without ENS	**6.0**	**1.4**	**4.3**		**4.9**	**1.4**	**3.6**
β	***1.8***				***1.9***		
RCP85; 2046 - 2065							
CNRM	5.2	1.4	**3.7**		4.1	1.1	**3.7**
CSIR	5.3	1.4	**3.8**		4.1	1.4	**2.9**
ECEA	5.4	1.5	**3.7**		4.2	1.5	**2.8**
GFDL	4.3	1.2	**3.6**		2.9	1.1	**2.6**
HadG	5.9	1.6	**3.8**		4.4	1.7	**2.6**
MPI	4.6	1.4	**3.4**		3.2	1.2	**2.6**

Model	RCM				GCM		
	Mean T-diss	**Mean P-diss**	**α**		**Mean T-diss**	**Mean P-diss**	**α**
ENS	9.3	2.9	**3.2**		7.0	2.7	**2.6**
Average without ENS	**5.1**	**1.4**	**3.7**		**3.8**	**1.3**	**2.9**
β	***1.8***				***1.8***		
RCP45; 2080 - 2099							
CNRM	5.4	1.4	**3.9**		4.2	1.1	**3.8**
CSIR	6.1	1.4	**4.2**		4.6	1.5	**3.1**
ECEA	6.1	1.5	**4.1**		4.5	1.5	**2.9**
GFDL	4.3	1.2	**3.5**		2.8	1.1	**2.5**
HadG	6.7	1.5	**4.3**		5.1	1.8	**2.9**
MPI	5.0	1.3	**3.7**		3.2	1.2	**2.7**
ENS	11.2	2.9	**3.8**		8.1	2.7	**3.0**
Average without ENS	**5.6**	**1.4**	**4.0**		**4.1**	**1.4**	**3.0**
β	***2.0***				***2.0***		
RCP45; 2046 - 2065							
CNRM	5.4	1.4	**3.7**		4.1	1.2	**3.6**
CSIR	5.3	1.4	**3.9**		3.9	1.4	**2.9**
ECEA	6.1	1.5	**4.1**		4.3	1.5	**2.9**
GFDL	4.4	1.3	**3.5**		2.9	1.2	**2.5**
HadG	6.2	1.6	**4.0**		4.7	1.7	**2.7**
MPI	5.0	1.4	**3.7**		3.2	1.2	**2.7**
ENS	10.8	3.0	**3.6**		7.7	2.7	**2.8**

Model	RCM				GCM		
	Mean T-diss	Mean P-diss	α		Mean T-diss	Mean P-diss	α
Average without ENS	**5.4**	**1.4**	**3.8**		**3.9**	**1.4**	**2.9**
β	***2.0***				***2.0***		

Annex 3. Land ratio (%) in Southeast Asia for novel climate resulted from each RCM and GCM experiment for the RCP4.5 and RCP8.5 for two periods (2046-2065, 2080-2099).

Experiment	RCM	GCM	Experiment	RCM	GCM
RCP8.5			**RCP4.5**		
2080 - 2099					
ENS	23.99	21.14	ENS	1.90	0.00
CNRM	17.32	11.07	CNRM	0.45	0.00
CSIR	48.89	62.96	CSIR	16.03	18.06
ECEA	32.83	40.73	ECEA	5.54	4.08
GFDL	0.99	3.29	GFDL	0.00	0.00
HADG	52.95	65.91	HADG	17.36	8.36
MPI	20.37	19.55	MPI	0.17	0.00
2046 - 2065					
ENS	0.01	0.00	ENS	0.02	0.00
CNRM	0.06	0.00	CNRM	0.00	0.00
CSIR	3.11	0.16	CSIR	1.05	0.00
ECEA	3.00	2.96	ECEA	1.69	0.23
GFDL	0.00	0.00	GFDL	0.00	0.00
HADG	12.17	2.62	HADG	6.36	0.80
MPI	0.10	0.00	MPI	0.03	0.00

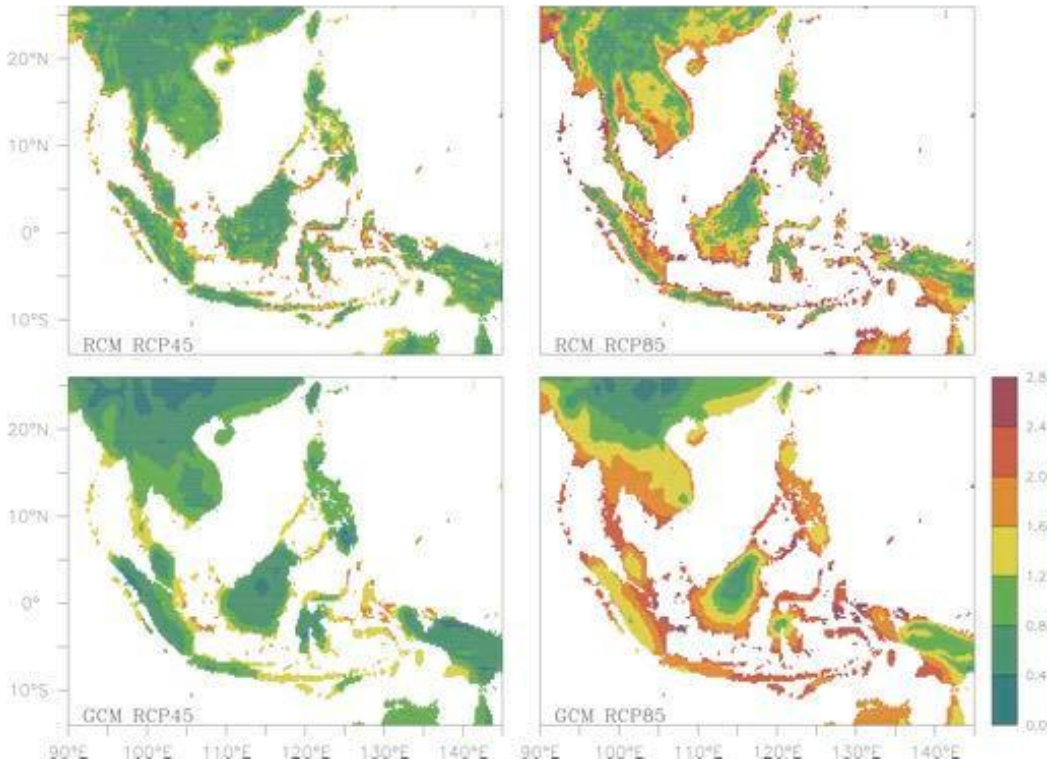

Annex 4. Underlying values of **Figure 4.9** in the main text.

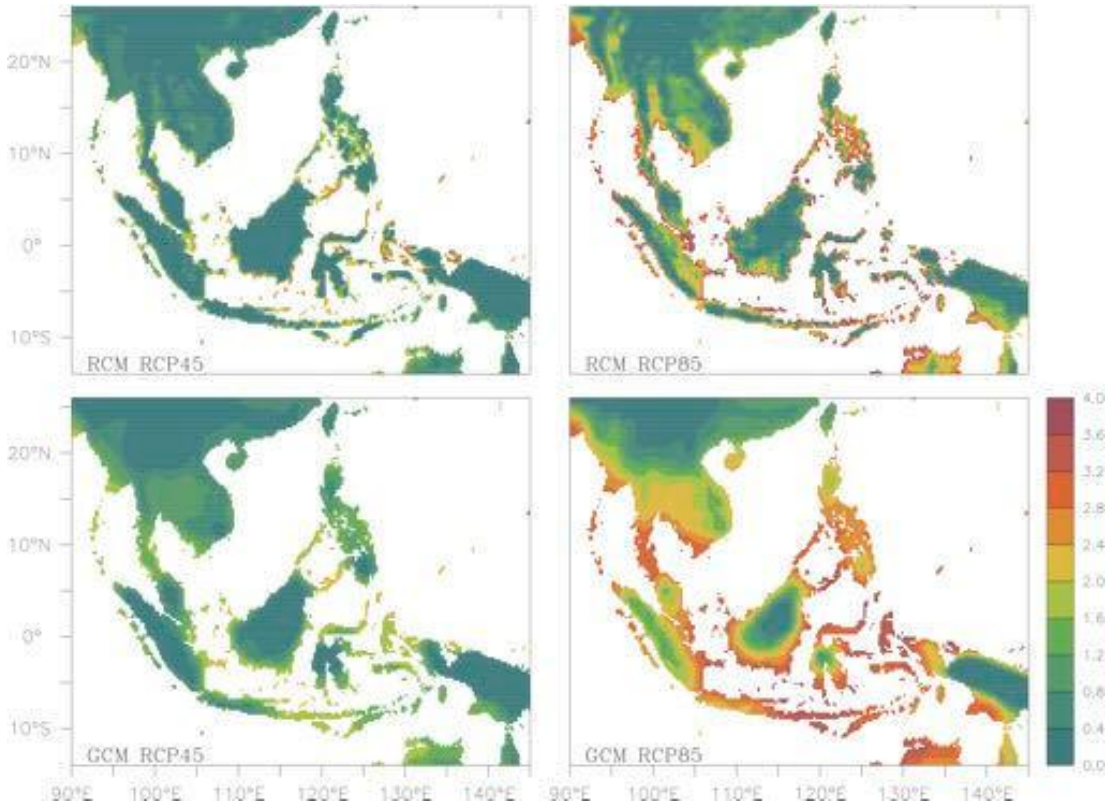

Annex 5. Underlying values of **Figure 4.10** in the main text.

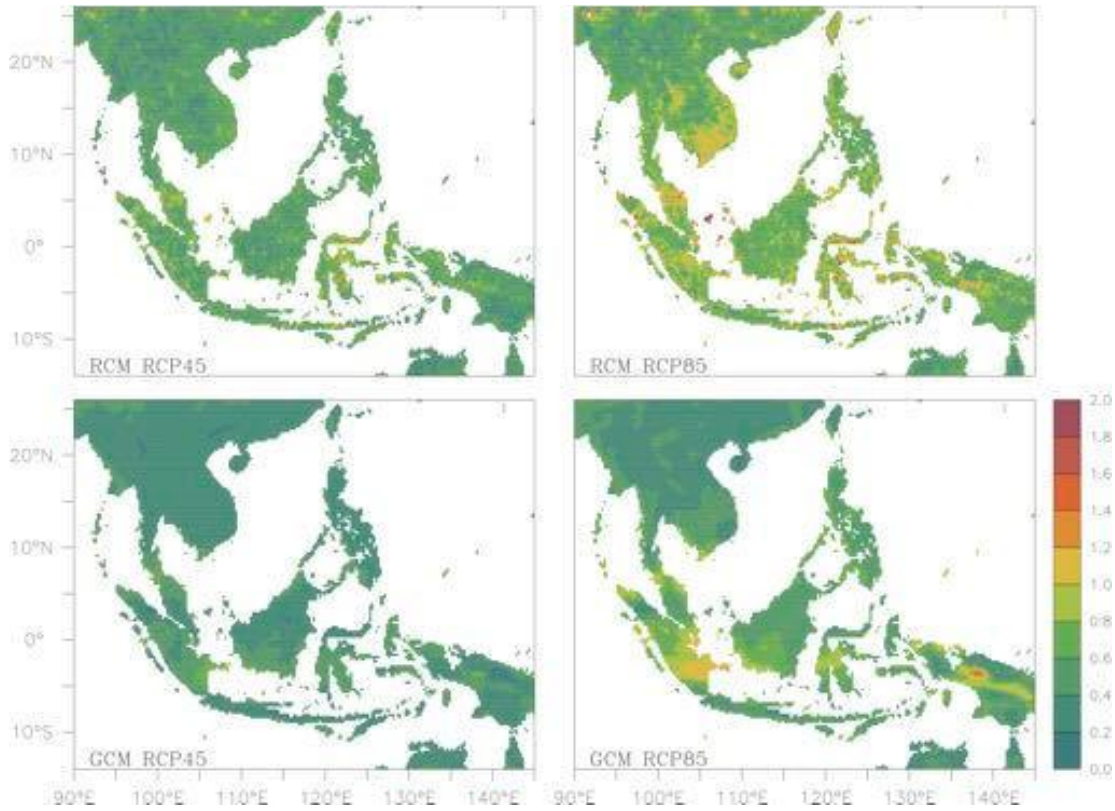

Annex 6. Underlying values of Figure 4.11 in the main text.